



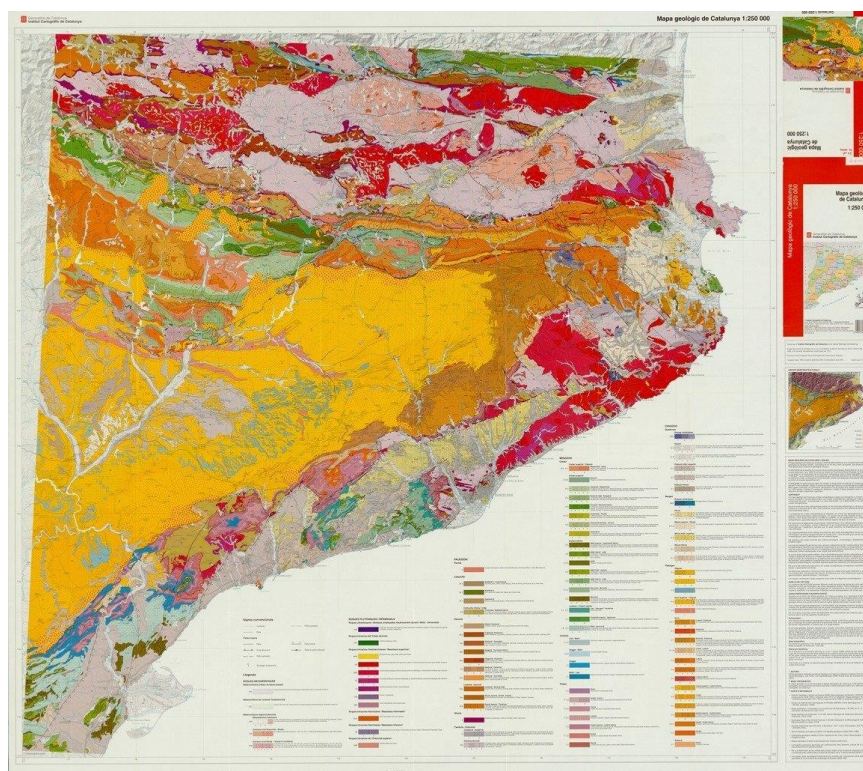
UNIVERSITAT DE
BARCELONA



Geology and Metallogeny of Catalonia

Field trip guide

September 5th – September 9th, 2017



Editors:

Eva Agut

Marc Campeny

Diego Domínguez Carretero

Júlia Farré de Pablo

Lisard Torró

Cristina Villanova de Benavent

English translation by:

Damià Benet

Arnau Blasco

Sandra Baurier

Ariana Carrazana

Daniel Garcia

Miquel Garcia

Anna Giralt Mirón

Joan Gutiérrez

Núria Pujol Solà

Index

Program of the field trip	5
List of participants.....	6
1. Field trip to Cap de Creus.....	7
1.1 The trip to Cap de Creus.....	7
1.2 Geological setting	8
1.3 Pegmatite typology.....	9
1.4 Age of pegmatites	19
1.5 Conclusions.....	19
References.....	19
2. Introduction to the geology of SW Catalonia	21
2.1 Geographical situation.....	21
2.2 Geological setting	21
2.3 Pre-hercynian cycle.....	21
2.4 Hercynian cycle	23
2.4.1 The pre-carboniferous hercynian series	23
2.4.2 The Carboniferous series	26
2.4.3 Hercynian deformation and metamorphism.....	28
2.4.4 The Tardi-Hercynian granite intrusions and associated porphyry.....	28
2.4.5 Contact metamorphism	30
2.5 Preorogenic alpine cycle stage: the Mesozoic megasequence.....	30
2.5.1 Buntsandstein.....	31
2.5.2 Muschelkalk.....	32
2.5.3 Keuper.....	32
2.5.4 Jurassic.....	32
2.6 The synorogenic state from the Alpine cycle (Paleogene)	32
2.6.1 The Palocene series.....	32
2.6.2 The Eocene series	33
2.6.3 The Oligocene series.....	33
2.6.4 The Alpine compressive structures	33
2.6.5 Late-orogenic stage of the Alpine Cycle (Neogene).....	34
2.6.6 Quaternary.....	34
References.....	34
3. Mineral deposit types of the SW of Catalonia	38
3.1 Introduction.....	38
3.2 Stratabound mineralizations (Pb- Zn- Cu- W) in pre-Hercynian series.....	38
3.3 Mineralizations associated with the dynamics of Hercynian basins.....	39
3.4 Mineralization related to late-hercynian tectonic and magmatic activity	41

3.5 Mineralizations related to the Alpine cycle	43
References	51
4. Gavà mineralizations: Phosphate mineralization types	55
4.1 Origin of phosphate mineralizations	57
References	58
5. Cardona salt diapir	59
5.1 Geological setting	59
5.2 Mineralization	61
References	62
6. Field trip to the Western Pyrenees	64
6.1 Catalonia geological units	64
6.2 Eureka uranium mine	64
6.3 Cierco lead and zinc mine	67
6.4 Victoria Mine	70
6.5 Silurian secondary minerals	78
References	78

Program of the field trip

Mon. 04/09: Arrival to Barcelona

Night: Center Ramblas Hostel, Carrer de l'Hospital, 63, 08001 Barcelona (+34 934 12 40 69)

Tue. 05/09: Visit to Cap de Creus

Night: Center Ramblas Hostel, Carrer de l'Hospital, 63, 08001 Barcelona (+34 934 12 40 69)

Wed. 06/09: Visit to Bellmunt del Priorat

Night: Center Ramblas Hostel, Carrer de l'Hospital, 63, 08001 Barcelona (+34 934 12 40 69)

Thu. 07/09: Visit to Gavà and Cardona mines

Night: Center Ramblas Hostel, Carrer de l'Hospital, 63, 08001 Barcelona (+34 934 12 40 69)

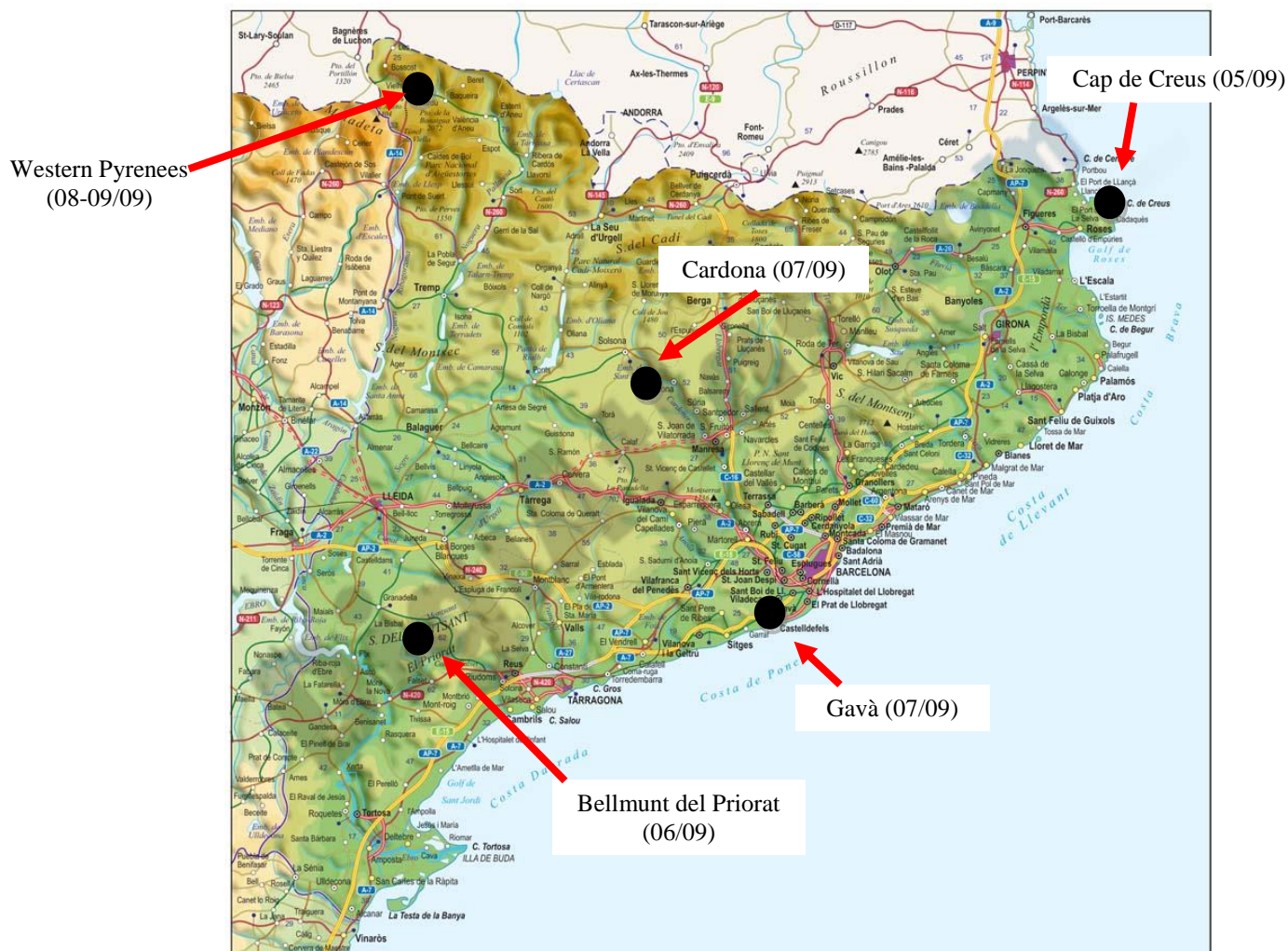
Fri. 08/09: Visit to Vall Fosca mines (Western Pyrenees)

Night: Era Garona, Carretera de Vielha, s/n, 25598 Salardú, Lleida (+34 973 64 52 71)

Sat. 09/09 Visit to Val d'Aran mines (Western Pyrenees)

Night: Center Ramblas Hostel, Carrer de l'Hospital, 63, 08001 Barcelona (+34 934 12 40 69)

Sun. 10/09: Departure



Field trip visits. Modified from <http://www.digiatlas.com>

List of participants

Participants from Barcelona student chapter

Miquel Garcia, 4th year of BSc
Alvaro Martinez, 4th year of BSc
Júlia Farré de Pablo, 1st year PhD Student
Joan Gutierrez, 4th year of BSc
Dani Rodriguez, Graduate
Diego Domínguez Carretero, 4th year of BSc
Malena Cazorla, 2nd year of BSc
Javier Casado, UB Geology lecturer
Berta Sagués, 2nd year of BSc
Eva Agut, 4th year of BSc
Arnau Blasco, 4th year of BSc
Oriol Vilanova, 2nd year of BSc
Núria Pujol Solà, 1st year PhD Student

Field supervisors

Joan Carles Melgarejo
Marc Campeny
Sandra Amores
Lisard Torró
Cristina Villanova de Benavent

Participants from Russia student chapter

Maria Cherdantseva, 3 rd year of PhD
Ivan Chaika, 4 th year of BSc
Alexey Kotov, 1 st year of MSc
Maria Shapovalova, 1 st year of PhD
Dmitriy Chebotarev, 3 rd year of PhD
Anna Nekipelova, 1 st year of MSc
Alina Lapega, 1 st year of MSc

Participants from Czech Republic student chapter

Jan Kulhánek, MSc
Dominik Brém, BSc
Daniil Belokopytov, MSc
Karolína Hladíková, BSc
Šárka Matoušková, Employee of Czech Academy of
Science
Marek Tuhý, PhD
Matěj Němec, PhD
Ivan Petrov, BSc

1. Field trip to Cap de Creus

J.C. Melgarejo¹, P. Alfonso²

1. *Departament de Cristal·lografia, Mineralogia i Dipòsits Minerals. Facultat de Geologia, Universitat de Barcelona*

2. *Departament d'Enginyeria Minera i Recursos Naturals, Universitat Politècnica de Catalunya, Manresa.*

1.1 The trip to Cap de Creus

We leave Barcelona by bus following the highway in NE direction, passing along the cities of Girona and Figueres (the last one being famous for hosting the Dalí Museum). From Figueres we head towards the Cap de Creus. The bus will arrive until the lighthouse there (Fig. 1.1). From the lighthouse we will be able walking along some trails in order to visit different types of barren and fertile pegmatites.



Figure 1.1 Access to Cap de Creus area from Barcelona.

IMPORTANT RULES

We are visiting a national park. The access to many areas of the park is extremely restricted. Use of hammers or collecting rocks without authorization is strictly forbidden, and only the professors can exceptionnally collect rocks from the ground. Hence, **NO HAMMERS PLEASE**. Penalties for leaving trash are severe. Please follow all the rules of the park.

1.2 Geological setting

The Cap de Creus area of NE Spain constitutes the Hercynian basement at the E end of the Pyrenees (Fig. 1.2).

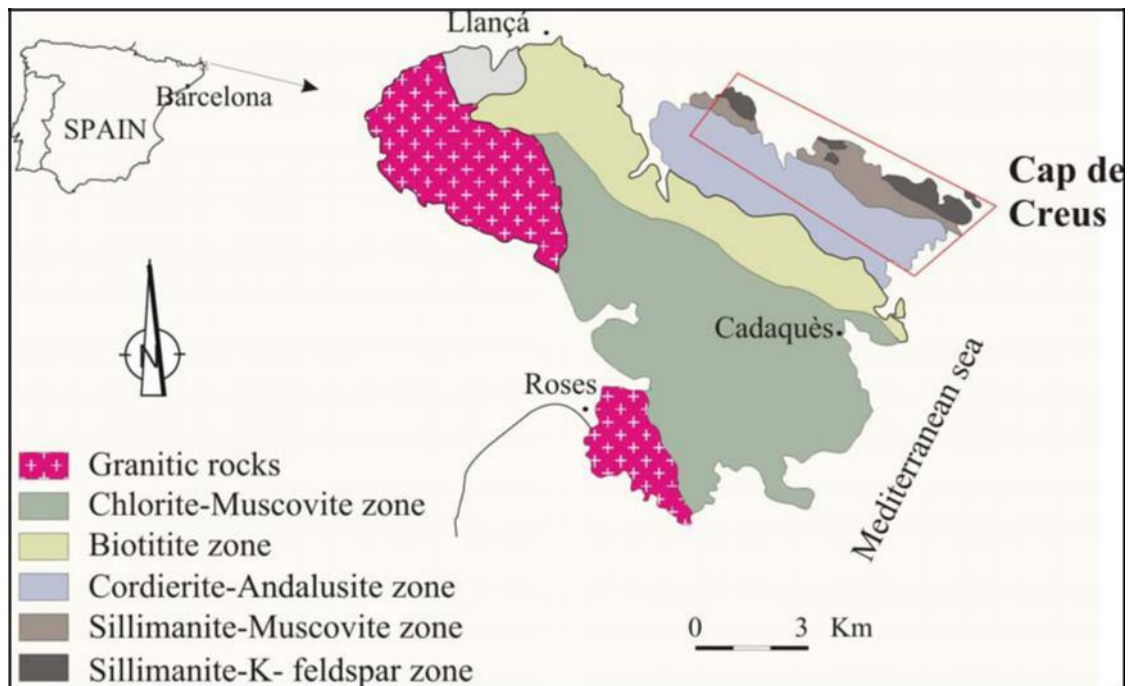


Figure 1.2 Geology of the Cap de Creus Peninsula (Carreras et al. 1975).

The Paleozoic series consists of a 2000 m-thick metapelitic sequence with minor limestones/marbles, felsic volcanic and coarser sedimentary rocks. Zircons from these felsic volcanics have been dated by SHRIMP as Vendian (554 ± 4 Ma at the basis and 560 ± 10 Ma at the top; Castiñeiras et al., 2008). These series can be correlated with the Canavelles sèries from the Eastern Pyrenees, dated also as Late Proterozoic (Vendian, 581 ± 10 Ma, Cocherie et al., 2005). This sequence has been affected by two main phases of Hercynian deformation. Phase one produced the main foliation, and the succeeding episode of deformation induced folding that ended with the development of NW-SE-trending shear bands (Carreras, 1975; Carreras & Casas 1987). A low pressure, high-temperature regional metamorphism, which increases from a chlorite-muscovite zone in the south to cordierite-andalusite, sillimanite-muscovite and K-feldspar-sillimanite zones in the north, with isograds trending NW, occurred between the two episodes of deformation (Druguet, 1997; Druguet & Hutton, 1998; Druguet, 2001).

The intrusive rocks in the Cap de Creus area consist of pre-Hercynian porphyritic granites (probably of Lower Ordovician age, as are those from other places in the Eastern Pyrenees dated as 473 ± 4 Ma; Cocherie et al., 2005) and two types of Hercynian granitic rocks: (1) small bodies of syntectonic leucogranites to quartz gabbros related to the northern migmatite zone (Carreras et al. 1975, Carreras & Druguet 1994), and (2) the late Hercynian Roses and Rodes granodiorites and quartz diorite stocks emplaced within lower-grade rocks in the south and southwest.

1.3 Pegmatite typology

Pegmatites are found generally as dikes tending to follow the main foliation, and are affected by late shearing. Four types of granitic pegmatites have been established according to internal structure and mineralogical criteria (Corbella, 1990; Corbella & Melgarejo 1990; fig. 4). Detailed descriptions of their internal structure and mineralogy are reported in Corbella & Melgarejo (1990) and Alfonso *et al.* (1995).

The different types are type I, type II, type III, type IV, and they represent different grades of evolution of the pegmatites. Type I pegmatites are the most primitive and barren, and the other are mineralized and more evolved. Following the classical pegmatite classifications (Černý, 1989; Černý, 1991a; Černý *et al.*, 1995; Černý & Ercit, 2005), type II pegmatites are classified into the beryl-columbite subtype or represent intermediate types with the barren pegmatites; type III are included in the beryl-columbite phosphate subtype, and type IV, the most evolved pegmatites, are included in the albite subtype. All these types are progressively distributed according to the metamorphic zones: type I occur in the sillimanite-K feldspar zone, and type IV in the cordierite-andalusite zone (Fig. 1.3).

As stated before, most of the pegmatites are found as dikes. Type I and II pegmatite dikes are several hundreds of meters long and more than 50 m wide. Types III and IV tend to be smaller and less abundant (see Fig. 1.3).

In addition to the pegmatite dikes, large quartz dikes are found in the most external part of the pegmatite field.

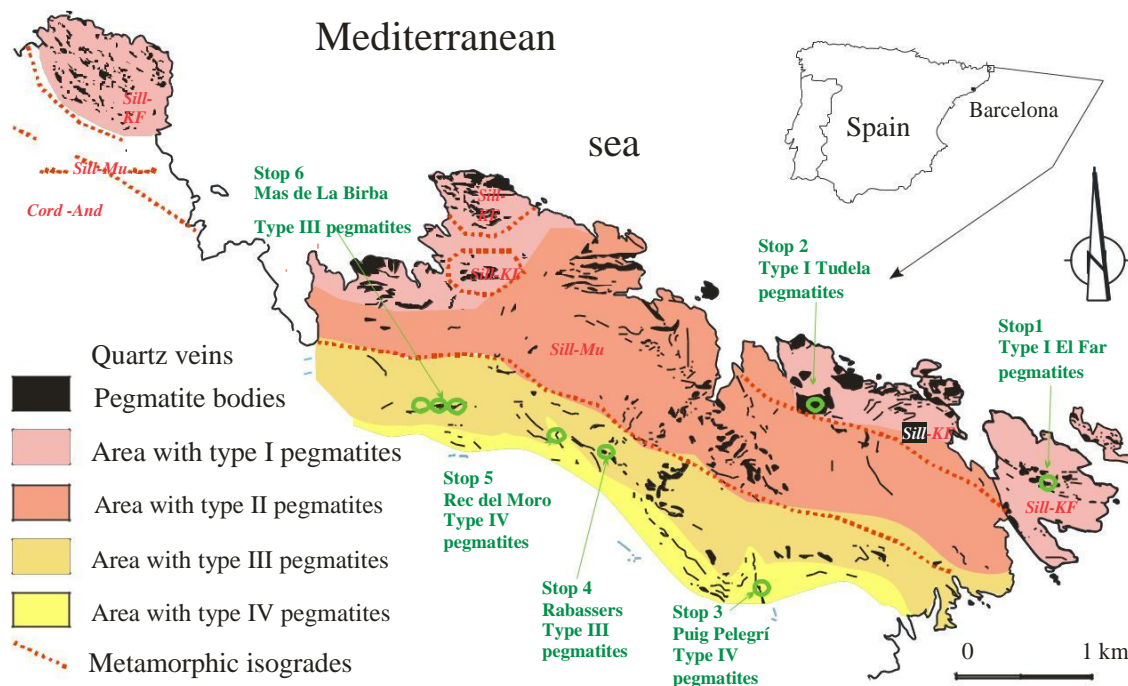


Figure 1.3 Distribution of the different pegmatite types at the Cap de Creus pegmatite field (modified from Carreras et al., 1975).

The pegmatites are syntectonic, and many of them are folded or display minor structures related to folding, as boudinage and pinch and swell. In some pegmatites of type-I a late pegmatitic crystal growth occur in the necking zones associated with the boudins.

Type I pegmatites: Internal structure and mineralogy

Type I or microclitic pegmatites are poorly zoned (Fig. 1.4). The typical outcrop is at the Lighthouse of the Cap de Creus. There is a centimeter-size border zone followed by the wall aplitic units and intermediate zones (first and second, according to the grain size). Synkinematic crystallization in necking zones, quartz and schorl veins also occur. Major minerals in all these zones are quartz, perthitic microcline and oligoclase. Common accessory minerals are peraluminous (cordierite, sillimanite, andalusite, almandine-rich garnet), biotite, muscovite and tourmaline. Many of these minerals have a skeletal habit and tend to have a grain size between some millimeters to several centimeters. Alignment of these accessory minerals can define internal banding in these units. Quartz cores are very small or absent in these pegmatites.

Rare-element minerals and phosphates are extremely scarce. Excluding few and small grains of apatite, xenotime and monazite, these pegmatites are phosphorus-poor. Ore minerals consist in fine-grained and very rare Sc- and W-rich ixiolite and ferrocolumbite.

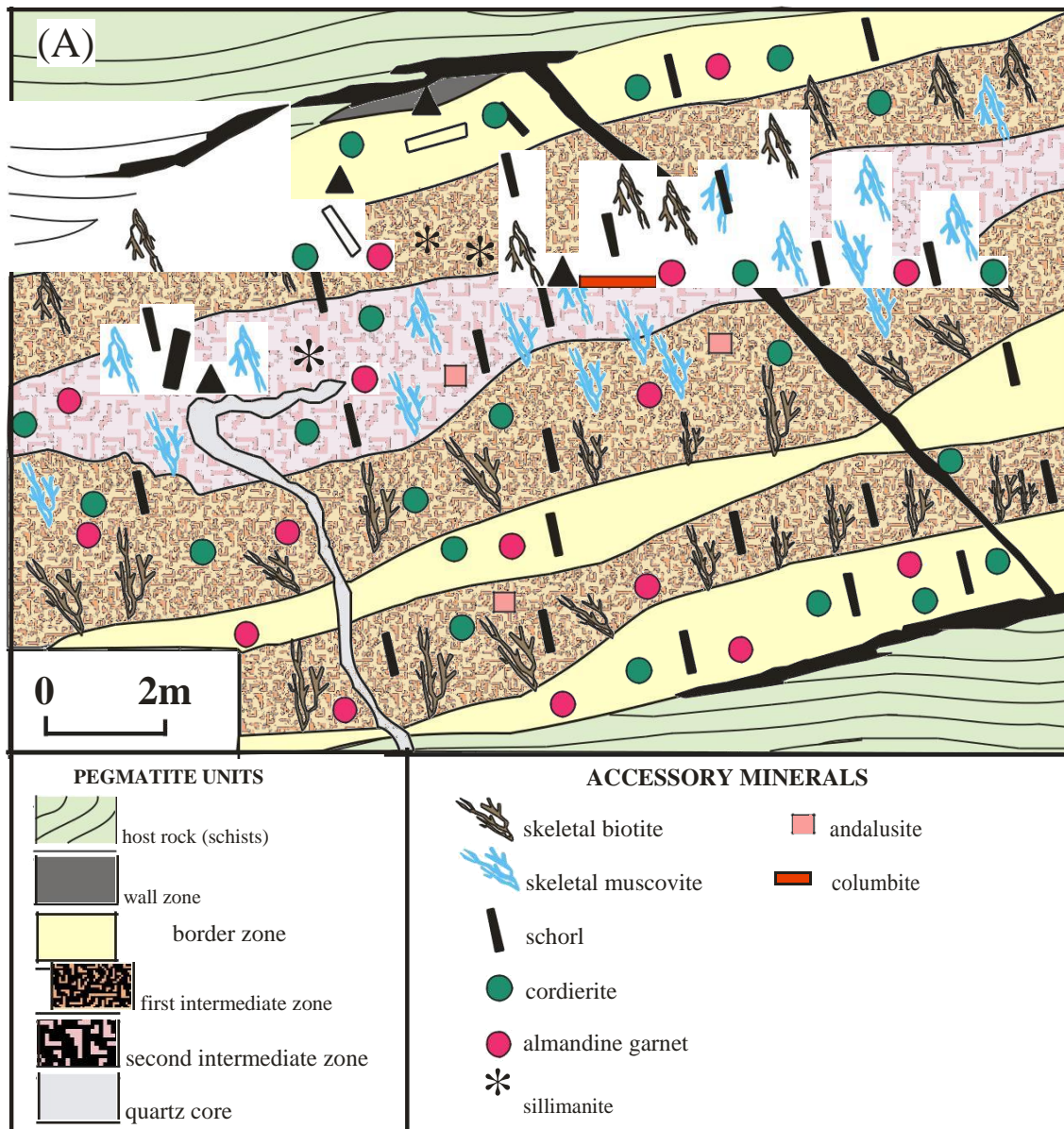


Figure 1.4 Internal structure of the type I pegmatites and distribution of minerals.

Type I pegmatites, similar as those of de Lighthouse, but of large size, are found at Tudela (stop 2). Some of them could be considered, in fact, as pegmatitic granites. Some of them have been affected by deformation as evidenced by boudinage structures, and some late pegmatite units are found in the necking zones (Fig 1.5). Minerals from these late units are slightly enriched on incompatible elements. Sequence in type I pegmatites is described in Table 1.1.

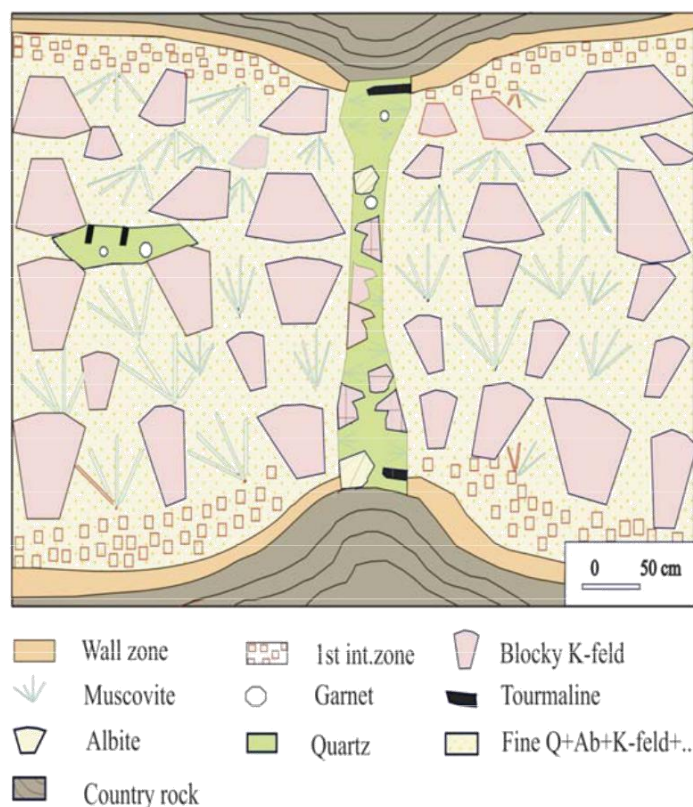


Figure 1.5 Internal structure of pegmatites type I at Tudela.

Table 1.1 Sequence of the type I pegmatites. Green, peraluminic minerals; red, rare-element minerals.

Zone		Formula	Stage				II	III	IV
			Intermediate zones				Core	F Boudins	F Veins
Border	Quartz	SiO_2							
	Muscovite	$\text{KAl}_2(\text{Si}_3\text{AlO}_{10})(\text{OH})_2$							
	Tourmaline	$\text{Na}(\text{Fe,Mg})_3\text{Al}_6(\text{BO}_3)_3\text{Si}_6\text{O}_{18}(\text{OH})_4$							
	Cordierite	$\text{Mg}_3\text{Al}_2\text{Si}_5\text{O}_{18}$							
	Almandine	$(\text{Fe,Mn})_3\text{Al}_2(\text{SiO}_4)_3$							
	Sillimanite	Al_2SiO_5							
Wall	Microcline	KAISi_3O_8							
	Oligoclase	$(\text{Na,Ca})\text{Al}(\text{Si,Al})_3\text{O}_8$							
	Quartz	SiO_2							
	Muscovite	$\text{KAl}_2(\text{Si}_3\text{AlO}_{10})(\text{OH})_2$							
	Tourmaline	$\text{Na}(\text{Fe,Mg})_3\text{Al}_6(\text{BO}_3)_3\text{Si}_6\text{O}_{18}(\text{OH})_4$							
	Biotite	$\text{K}(\text{Fe,Mg})_3(\text{Si}_3\text{AlO}_{10})(\text{OH})_2$							
	Cordierite	$\text{Mg}_3\text{Al}_2\text{Si}_5\text{O}_{18}$							
	Almandine	$(\text{Fe,Mn})_3\text{Al}_2(\text{SiO}_4)_3$							
	Sillimanite	Al_2SiO_5							
First intermediate zone	Microcline	KAISi_3O_8							
	Albite	$\text{NaAlSi}_3\text{O}_8$							
	Muscovite	$\text{KAl}_2(\text{Si}_3\text{AlO}_{10})(\text{OH})_2$							
	Quartz	SiO_2							
	Schorl	$\text{Na}(\text{Fe,Mg})_3\text{Al}_6(\text{BO}_3)_3\text{Si}_6\text{O}_{18}(\text{OH})_4$							
	Almandine	$(\text{Fe,Mn})_3\text{Al}_2(\text{SiO}_4)_3$							
	Cordierite	$\text{Mg}_3\text{Al}_2\text{Si}_5\text{O}_{18}$							
	Biotite	$\text{K}(\text{Fe,Mg})_3(\text{Si}_3\text{AlO}_{10})(\text{OH})_2$							
	Sillimanite	Al_2SiO_5							
Second intermediate zone	Quartz	SiO_2							
	Albite	$\text{NaAlSi}_3\text{O}_8$							
	Microcline	KAISi_3O_8							
	Garnet	$(\text{Fe,Mn})_3\text{Al}_2(\text{SiO}_4)_3$							
	Tourmaline	$\text{Na}(\text{Fe,Mg})_3\text{Al}_6(\text{BO}_3)_3\text{Si}_6\text{O}_{18}(\text{OH})_4$							
	Sillimanite	Al_2SiO_5							
	Biotite	$\text{K}(\text{Fe,Mg})_3(\text{Si}_3\text{AlO}_{10})(\text{OH})_2$							
	Muscovite	$\text{KAl}_2(\text{Si}_3\text{AlO}_{10})(\text{OH})_2$							
	Cordierite	$\text{Mg}_3\text{Al}_2\text{Si}_5\text{O}_{18}$							
	Ferrocolumbite	$(\text{Fe,Mn})(\text{Nb,Ta})_2\text{O}_6$							
	Ixiolite	$(\text{Ta,Nb,Sn,Fe,Mn})_4\text{O}_{84}$							
Core	Quartz	SiO_2							

Type II pegmatites: internal structure and mineralogy

Type II or beryl-columbite pegmatites exhibit, in addition to the above zones, a quartz core, albitic veins and albitic replacement bodies (Fig. 1.6). Accessory minerals are: biotite, muscovite, zircon, beryl, chrysoberyl, scarce Nb-Ta oxides and peraluminic minerals as gahnite, cordierite, garnet, andalusite and sillimanite. Beryl may be abundant in some pegmatites, generally in the vicinity of cores and in the albitic units. It is green in color and may achieve some cm in diameter.

Ore minerals are not so scarce, and some mm-sized ferrocolumbite grains are common in the intermediate zones and in the albitized units. In some cases, small amounts of mm-sized wolframite crystals may be also found. Uraninite is common as inclusions in zircon crystals.

Phosphates are not rare in some of these pegmatites. Ca-Fe-Mn-(Mg) phosphates, as triplite, sarcopside and graftonite occur as centimeter-sized rounded crystals in the intermediate zones, especially close to the quartz core. Moreover, some hydrothermal phosphates appear as a pseudomorph product of the above minerals. Fillowite is common as a replacement product of sarcopside and graftonite. Na-rich phosphates as alluaudite occur in the albitic units. Be phosphates as herderite may replace chrysoberyl in late stages. Late phosphates related to weathering are common. The sequence is in Table 1.2, and the detailed phosphate sequence in table 1.3.

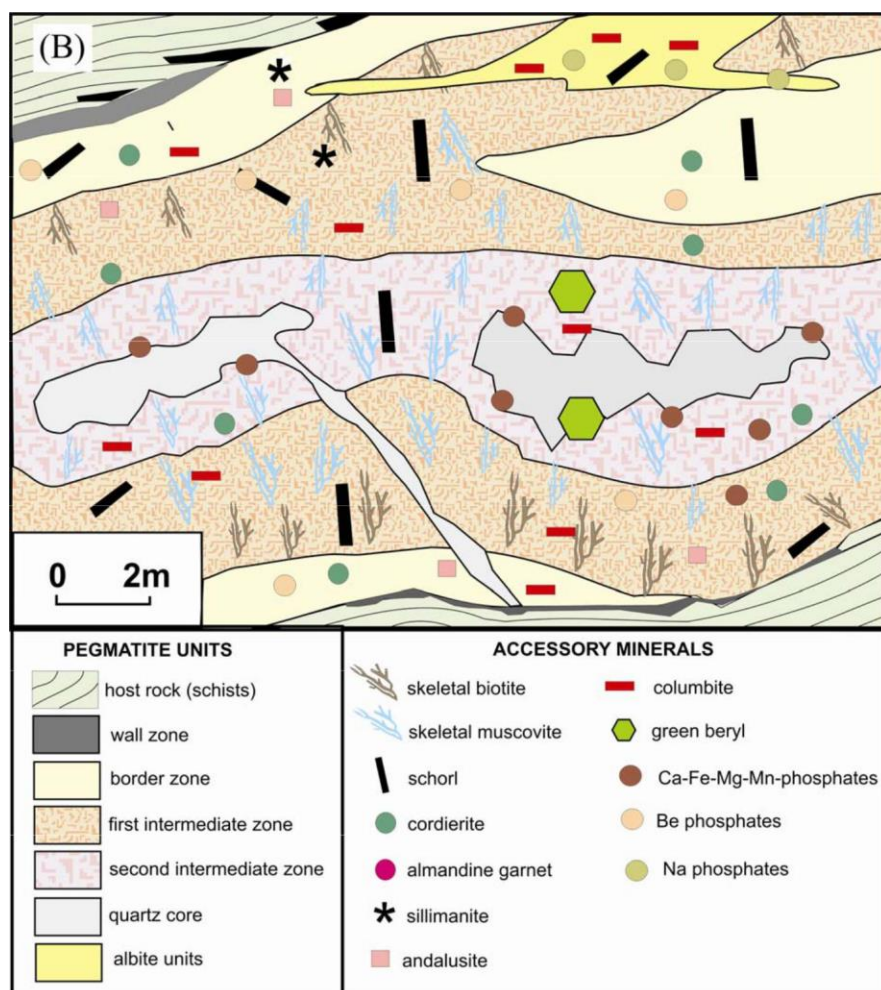


Figure 1.6 Internal structure of the type II pegmatites and distribution of minerals.

Table 1.2. Mineral sequence in type II pegmatites. Economic minerals, in red; peraluminic, in green; phosphates, in blue.

Zone		Stage Formula	I				II	III	IV
			Intermediate zones				Core	F Albitiz.	F Veins
Border	Quartz	SiO_2							
	Muscovite	$\text{KAl}_2(\text{Si}_3\text{AlO}_{10})(\text{OH})_2$							
	Tourmaline	$\text{Na}(\text{Fe,Mg})_3\text{Al}_6(\text{BO}_3)_3\text{Si}_6\text{O}_{18}(\text{OH})_4$							
	Cordierite	$\text{Mg}_3\text{Al}_2\text{Si}_5\text{O}_{18}$							
	Almandine	$(\text{Fe,Mn})_3\text{Al}_2(\text{SiO}_4)_3$							
	Sillimanite	Al_2SiO_5							
Wall	Microcline	KAlSi_3O_8							
	Oligoclase	$(\text{Na,Ca})\text{Al}(\text{Si,Al})_3\text{O}_8$							
	Quartz	SiO_2							
	Muscovite	$\text{KAl}_2(\text{Si}_3\text{AlO}_{10})(\text{OH})_2$							
	Tourmaline	$\text{Na}(\text{Fe,Mg})_3\text{Al}_6(\text{BO}_3)_3\text{Si}_6\text{O}_{18}(\text{OH})_4$							
	Biotite	$\text{K}(\text{Fe,Mg})_3(\text{Si}_3\text{AlO}_{10})(\text{OH})_2$							
	Cordierite	$\text{Mg}_3\text{Al}_2\text{Si}_5\text{O}_{18}$							
	Almandine	$(\text{Fe,Mn})_3\text{Al}_2(\text{SiO}_4)_3$							
First Intermediate zone	Sillimanite	Al_2SiO_5							
	Microcline	KAlSi_3O_8							
	Albite	$\text{NaAlSi}_3\text{O}_8$							
	Muscovite	$\text{KAl}_2(\text{Si}_3\text{AlO}_{10})(\text{OH})_2$							
	Quartz	SiO_2							
	Tourmaline	$\text{Na}(\text{Fe,Mg})_3\text{Al}_6(\text{BO}_3)_3\text{Si}_6\text{O}_{18}(\text{OH})_4$							
	Almandine	$(\text{Fe,Mn})_3\text{Al}_2(\text{SiO}_4)_3$							
	Cordierite	$\text{Mg}_3\text{Al}_2\text{Si}_5\text{O}_{18}$							
Second intermediate zone	Biotite	$\text{K}(\text{Fe,Mg})_3(\text{Si}_3\text{AlO}_{10})(\text{OH})_2$							
	Sillimanite	Al_2SiO_5							
	Quartz	SiO_2							
	Albite	$\text{NaAlSi}_3\text{O}_8$							
	Microcline	KAlSi_3O_8							
	Garnet	$(\text{Fe,Mn})_3\text{Al}_2(\text{SiO}_4)_3$							
	Tourmaline	$\text{Na}(\text{Fe,Mg})_3\text{Al}_6(\text{BO}_3)_3\text{Si}_6\text{O}_{18}(\text{OH})_4$							
	Sillimanite	Al_2SiO_5							
	Biotite	$\text{K}(\text{Fe,Mg})_3(\text{Si}_3\text{AlO}_{10})(\text{OH})_2$							
	Muscovite	$\text{KAl}_2(\text{Si}_3\text{AlO}_{10})(\text{OH})_2$							
	Cordierite	$\text{Mg}_3\text{Al}_2\text{Si}_5\text{O}_{18}$							
	Columbite	$(\text{Fe,Mn})(\text{Nb,Ta})_2\text{O}_6$							
	Beryl	$\text{Be}_3\text{Al}_2\text{Si}_6\text{O}_{18}$							
	CaFe-Phosph.	$\text{Na}_x(\text{FeMn})_x(\text{PO}_4)_x$							
Core	Be phosphates	$\text{Ca}_x(\text{FeMn})_x\text{Be}_x(\text{PO}_4)_x$							
	Na phosphates	$\text{Na}_x(\text{FeMn})_x(\text{PO}_4)_x$							
	Quartz	SiO_2							
Albitites	Albite	$\text{NaAlSi}_3\text{O}_8$							
	Na phosphates	$\text{Na}_x(\text{FeMn})_x(\text{PO}_4)_x$							
	Columbite	$(\text{Fe,Mn})(\text{Nb,Ta})_2\text{O}_6$							

Table 1.3 Mineral sequence of phosphates in type II pegmatites

Table 3. Sequence of phosphates in type II pegmatites

ZONE	MINERAL	FORMULA	STAGE I	LATE STAGES	WEATHERING
FIRST INTERMEDIATE	Lazulite	$(\text{Mg,Fe})\text{Al}_2(\text{PO}_4)(\text{OH})_2$	█		
	Scorzalite	$(\text{Fe,Mg})\text{Al}_2(\text{PO}_4)(\text{OH})_2$	█		
	Vivianite	$\text{Fe}^{2+}_3(\text{PO}_4)_2 \cdot 8\text{H}_2\text{O}$			█
	Rockbridgeite	$(\text{Fe}^{2+}, \text{Mn}^{2+})\text{Fe}^{2+}_4(\text{PO}_4)_4(\text{OH})_5$			█
	Cacoxenite	$(\text{Fe,Al})_{25}(\text{PO}_4)_{10}\text{O}_6(\text{OH})_{12} \cdot 75\text{H}_2\text{O}$			█
	Autunite	$\text{Ca}(\text{UO}_2)_3(\text{PO}_4)_2 \cdot 10\text{H}_2\text{O}$			█
SECOND INTERMEDIATE	Wyllieite	$(\text{Na,Ca,Mn}^{2+})(\text{Mn}^{2+}, \text{Fe}^{2+})(\text{Fe}^{2+}, \text{Fe}^{3+}, \text{Mg})\text{Al}(\text{PO}_4)_3$	█		
	Rosemaryite	$(\text{Na,Ca,Mn}^{2+})(\text{Mn}^{2+}, \text{Fe}^{2+})(\text{Fe}^{2+}, \text{Fe}^{3+}, \text{Mg})\text{Al}(\text{PO}_4)_3$		█	
	Sarcopside	$(\text{Fe}^{2+}, \text{Mn}^{2+}, \text{Mg})_3(\text{PO}_4)_2$	█		
	Graftonite	$(\text{Fe}^{2+}, \text{Mn}^{2+}, \text{Ca})_3(\text{PO}_4)_2$		█	
	Magniotriplite	$(\text{Mg,Fe}^{2+}, \text{Mn}^{2+})_3\text{PO}_4\text{F}$		█	
	Wolfeite	$(\text{Fe}^{2+}, \text{Mn}^{2+})_2(\text{PO}_4)(\text{OH})$		█	
	Fillowite	$\text{Na}_2\text{Ca}(\text{Mn,Fe}^{2+})_4(\text{PO}_4)_6$		█	
	Arrojadite	$\text{KNa}_4\text{CaMn}^{2+}_4\text{Fe}^{2+}_{10}\text{Al}(\text{PO}_4)_{12}(\text{OH,F})_2$		█	
	Alluaudite	$\text{NaCaFe}^{2+}_2(\text{Mn}^{2+}, \text{Fe}^{2+}, \text{Fe}^{3+}, \text{Mg})_2(\text{PO}_4)_3$		█	
	Stanekite	$\text{Fe}^{3+}(\text{Mn,Fe}^{2+}, \text{Mg})\text{PO}_4\text{O}$		█	
	Fluorapatite	$\text{Ca}_5(\text{PO}_4)_3\text{F}$		█	█
	Herderite	CaBePO_4F		█	
	Lazulite	$(\text{Mg,Fe})\text{Al}_2(\text{PO}_4)(\text{OH})_2$		█	
	Scorzalite	$(\text{Fe,Mg})\text{Al}_2(\text{PO}_4)(\text{OH})_2$		█	
	Souzalite	$(\text{Mg,Fe}^{2+})_3(\text{Al,Fe}^{2+})_4(\text{PO}_4)_4(\text{OH})_6 \cdot 2\text{H}_2\text{O}$		█	
	Lipscombite	$(\text{Fe}^{2+}, \text{Mn}^{2+})\text{Fe}^{2+}_3(\text{PO}_4)_4(\text{OH})_2$			█
	Rockbridgeite	$(\text{Fe}^{2+}, \text{Mn}^{2+})\text{Fe}^{2+}_4(\text{PO}_4)_4(\text{OH})_5$			█
	Jahnsite	$\text{CaMn}^{2+}\text{Fe}^{2+}_2\text{Fe}^{2+}_3(\text{PO}_4)_4(\text{OH})_2 \cdot 8\text{H}_2\text{O}$			█
	Cyrilovite	$\text{NaFe}^{2+}(\text{PO}_4)(\text{OH})_4 \cdot 2\text{H}_2\text{O}$			█
	Mitridatite	$\text{Fe}^{2+}_3(\text{PO}_4)_2 \cdot 8\text{H}_2\text{O}$			█
	Vivianite	$\text{Fe}^{2+}_3(\text{PO}_4)_2 \cdot 8\text{H}_2\text{O}$			█
	Dufrenite	$\text{Ca}_{10}\text{Fe}_6(\text{PO}_4)_4(\text{OH})_6 \cdot 2\text{H}_2\text{O}$			█
	Autunite	$\text{Ca}(\text{UO}_2)_3(\text{PO}_4)_2 \cdot 10\text{H}_2\text{O}$			█

Type III pegmatites, internal structure and mineralogy

Type III or beryl-columbite-phosphate pegmatites are more evolved. They have a similar concentric zoning (Fig 1.7), but the quartz core is well developed, and albitic veins and albitic replacement bodies are widespread; in addition, late quartz-muscovite veins appear. Accessory minerals in these pegmatites are beryl (green in the early units and white in the late ones), chrysoberyl, Nb-Ta-,U-oxides (specially concentrated in the albite veins, where they are enriched in Ta), gahnite, arsenopyrite (sometimes, enclosing small grains of gold, native bismuth and bismuthinite), and minor amounts of schorl and spessartine-rich garnet. Cordierite is absent, thus indicating decreasing of Mg content in the most evolved pegmatites in the field. Primary phosphates are abundant in all the pegmatitic units, both as skeletal crystals or as rounded anhedral crystals. They can be Li-phosphates (tryphylite, montebrasite) or Ca-Mn-Fe phosphates as sarcopside and graftonite. Triphylite is altered to the typical Quensel-Mason sequence: tryphylite-ferrisicklerite-heterosite). Alkaline phosphates as alluaudite are common in the albitic units, as are Be phosphates as hurlbutite. Strongly coloured secondary phosphates are well developed, and their presence can be interpreted as indicative of the presence of primary phosphates and, therefore, as an indicative of the evolution of the pegmatite. As a general rule, the content of rare elements is large in the pegmatites enriched in phosphates. Hence, the occurrence of high contents of secondary phosphates has proven to be a very successful tool for exploration of rare-elements in pegmatites. The sequence of mineralisation can be found in Table 1.4.

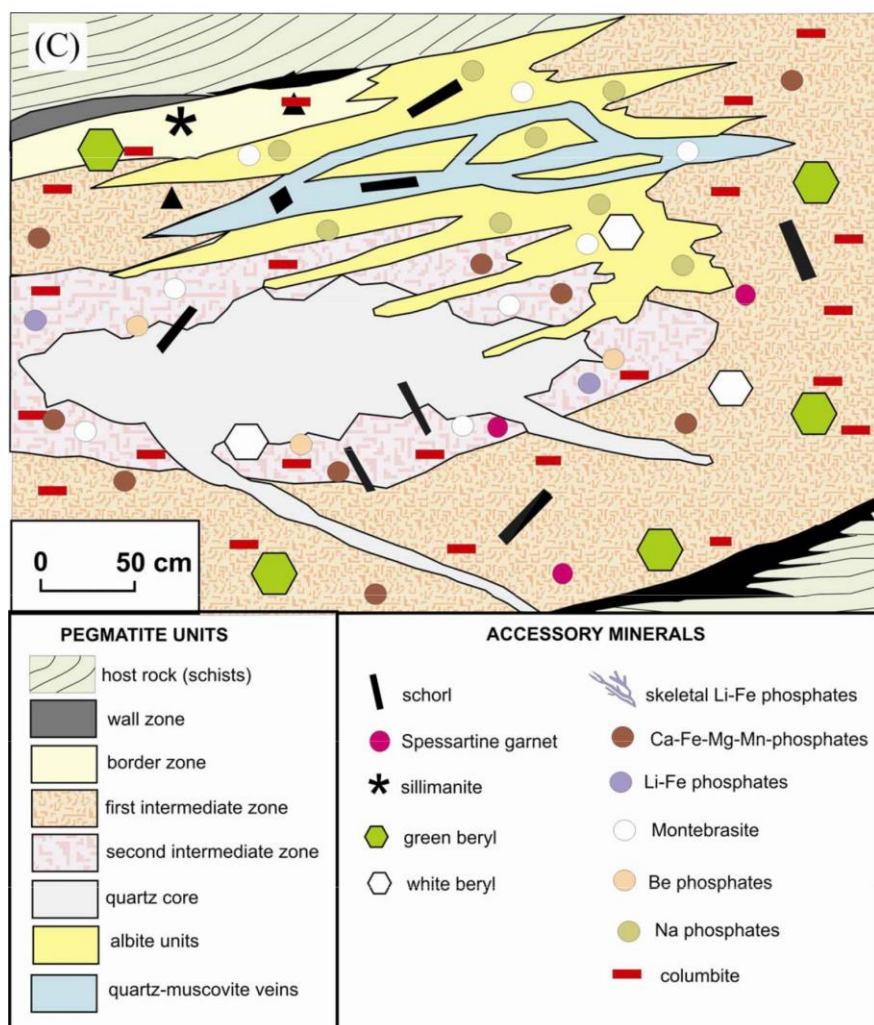


Figure 1.7 Internal structure of the type III pegmatites and distribution of minerals.

Table 1.4. Mineral sequence in type III pegmatites. Economic minerals, in red; peraluminic, in green; phosphates, in blue.

Zone		Formula	Stage I			II F	III F	IV	V	VI
			Intermediate zones			Core	Albitiz.	Greisen	Sul.	Fosf.
Border	Quartz	SiO ₂								
	Muscovite	KAl ₂ (Si ₃ AlO ₁₀)(OH) ₂								
	Tourmaline	Na(Fe,Mg) ₃ Al ₆ (BO ₃) ₃ Si ₆ O ₁₈ (OH) ₄								
	Beryl	Be ₃ Al ₂ Si ₆ O ₁₈								
	Montebrasite	LiAlPO ₄								
Wall	Columbite	(Fe,Mn)(Nb,Ta) ₂ O ₆								
	Microcline	KAlSi ₃ O ₈								
	Albite	NaAlSi ₃ O ₈								
	Quartz	SiO ₂								
	Muscovite	KAl ₂ (Si ₃ AlO ₁₀)(OH) ₂								
First intermediate zone	Tourmaline	Na(Fe,Mg) ₃ Al ₆ (BO ₃) ₃ Si ₆ O ₁₈ (OH) ₄								
	Beryl	Be ₃ Al ₂ Si ₆ O ₁₈								
	Montebrasite	LiAlPO ₄								
	Columbite	(Fe,Mn)(Nb,Ta) ₂ O ₆								
	Ixiolite	(Ta,Nb,Sn,Fe,Mn) ₄ O ₆								
	Uraninite	SrUO ₄								
	Zircon	ZrSiO ₄								
	Tapiolite	(Fe,Mn)(Ta,Nb) ₂ O ₆								
	Quartz	SiO ₂								
	Albite	NaAlSi ₃ O ₈								
Second intermediate zone	Microcline	KAlSi ₃ O ₈								
	Garnet	(Fe,Mn) ₃ Al ₂ (SiO ₄) ₃								
	Tourmaline	Na(Fe,Mg) ₃ Al ₆ (BO ₃) ₃ Si ₆ O ₁₈ (OH) ₄								
	Beryl	Be ₃ Al ₂ Si ₆ O ₁₈								
	Montebrasite	LiAlPO ₄								
	LiFe phosph.	Li(Fe,Mn)PO ₄								
	Metasom. Pho.	Li(Fe,Mn)PO ₄								
	Columbite	(Fe,Mn)(Nb,Ta) ₂ O ₆								
	Ixiolite	(Ta,Nb,Sn,Fe,Mn) ₄ O ₆								
	Tapiolite	(Fe,Mn)(Ta,Nb) ₂ O ₆								
	Casiterite	SnO ₂								
	Zircon	ZrSiO ₄								
	Uraninite	UO ₂								
	Fergusonite	(Y,HREE)NbO ₄								
	Quartz	SiO ₂								
Core	Albite	NaAlSi ₃ O ₈								
	Quartz	SiO ₂								
	Muscovite	KAl ₂ (Si ₃ AlO ₁₀)(OH) ₂								
	Columbite	(Fe,Mn)(Ta,Nb) ₂ O ₆								
	Ixiolite	(Ta,Nb,Sn,Fe,Mn) ₄ O ₆								
	Wodginite	(Ta,Nb,Sn,Fe,Mn) ₁₆ O ₃₂								
	Tapiolite	(Fe,Mn)(Ta,Nb) ₂ O ₆								
	Casiterite	SnO ₂								
	Fergusonite	(Y,HREE)NbO ₄								
	Gahnite	(Zn,Fe)(Al,Fe) ₂ O ₄								
Albite veins	Graphite	C								
	Quartz	SiO ₂								
	Muscovite	KAl ₂ (Si ₃ AlO ₁₀)(OH) ₂								
	Columbite	(Fe,Mn)(Ta,Nb) ₂ O ₆								
	Tapiolite	(Fe,Mn)(Ta,Nb) ₂ O ₆								
Quartz-muscovite veins	Chrysoberyl	BeAl ₂ O ₄								
	Gahnite	(Zn,Fe)(Al,Fe) ₂ O ₄								
	Graphite	C								
	Apatite	Ca ₅ (PO ₄) ₃ (F,OH)								
	Quartz	SiO ₂								
Sulphide veins	Arsenopyrite	FeAsS								
	Gold	Au								
	Bismuth	Bi								
	Bismutite	Bi ₂ S ₃								
Phosphate v.	Berlinite	AlPO ₄								

Type IV pegmatites, internal structure and mineralogy

Type IV or albite pegmatites represent the most evolved ones in the field. In addition to the border, wall, intermediate zones and the quartz core, quartz muscovite veins appear (Fig. 1.8). Thin late phosphate veins crosscut these veins. Accessory minerals are andalusite, sillimanite, muscovite, Ta>Nb-, Sn-, REE- minerals, beryl and chrysoberyl, gahnite, nigerite and phosphates. Phosphates are very abundant in these pegmatites. Apatite crystals appear in the exocontact of the pegmatite, associated to tourmaline, graphite and muscovite. Phosphates occur in all the concentric zones, forming nodules with variable size. Metasomatic phosphates are very common, as do the corresponding weathering products.

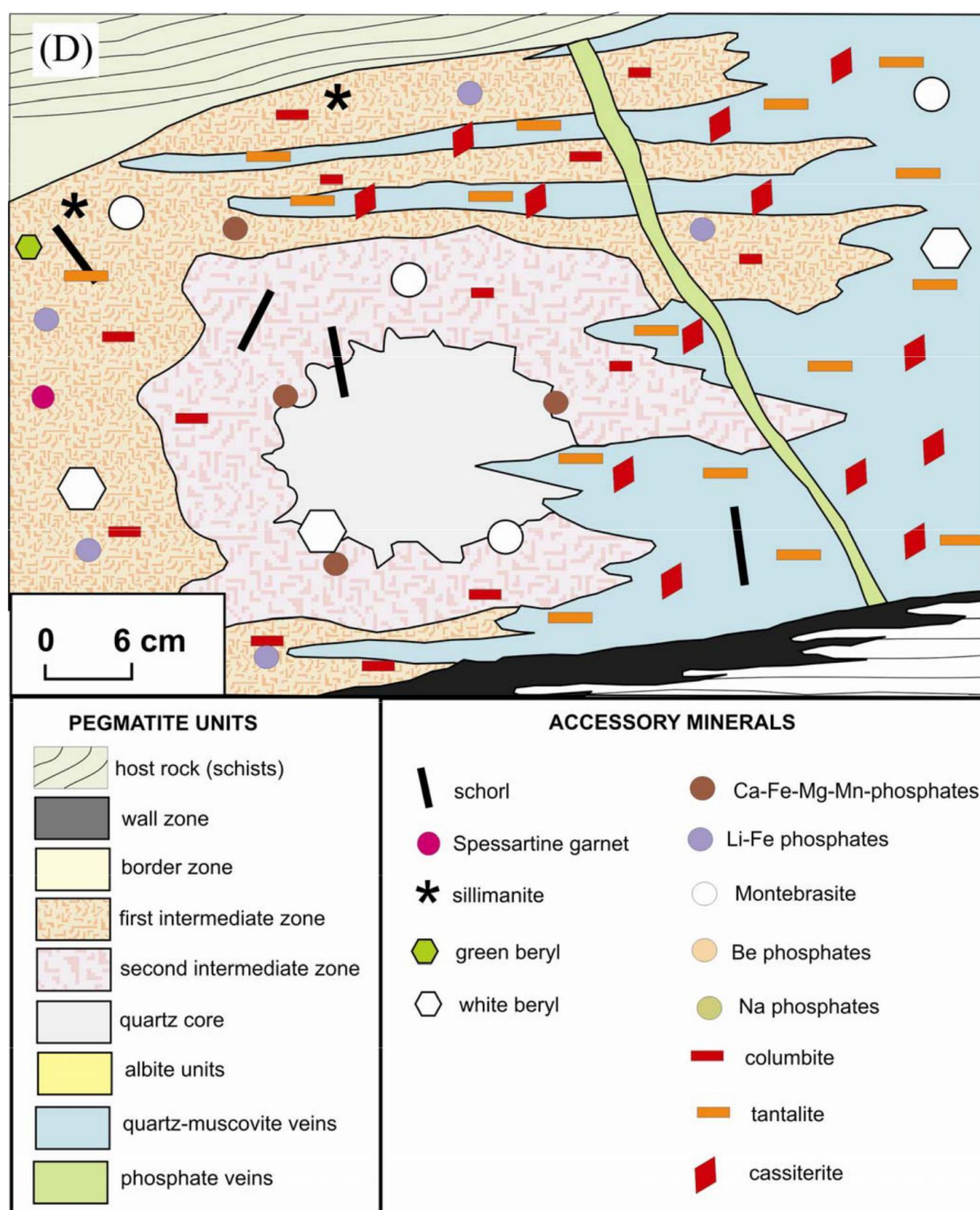


Figure 1.8 Internal structure of the type IV pegmatites and distribution of minerals.

1.4 Age of pegmatites

Pegmatite geochronology of the Cap de Creus pegmatites has been recently established as $297,1 \pm 1,9$ Ma by using U/Pb dating on zircon and columbite crystals (Grand'Homme, 2012). This age is similar to the age of a leucogranite of the Albera massif ($298,5 \pm 1,8$ Ma by the U/Pb method on monazite using microprobe data; BRGM, 2008). Hence, these pegmatites could be produced by fractionation of granitic magmas, in agreement with the tendencies found in rare element pegmatite fields worldwide (Černý, 1991b).

1.5 Conclusions

The most striking geochemical variations from type I to type IV pegmatites are: (1) increase of albitization and replacement phenomena, (2) increase of the P, Li mineralization, (3) increase in the ratios Ta/(Ta + Nb) and Mn/(Fe + Mn) in columbite-tantalite minerals (Alfonso *et al.* 1995).

The distribution of the different types of pegmatites and the mineralogical and geochemical data suggest that all these pegmatites were formed by fractionation operating from a single petrogenetic source (Corbella & Melgarejo 1993, Alfonso 1995). Moreover, in the Albera pegmatite field, 50 km at the northwest of Cap de Creus, similar pegmatite types are zonally arranged around a leucogranite intrusion (Malló *et al.*, 1995).

References

- Alfonso, P., Corbella, M., Melgarejo, J.C. (1995): Nb–Ta minerals from the Cap de Creus pegmatite field, eastern Pyrenees: distribution and geochemical trends. *Mineral. Petrol.* 55, 53-69.
- BRGM (2008): Notice explicative carte géologique 1:50.000 Feuille 1097 Argelès sur mer.
- Carreras, J. (1975): Las deformaciones tardi-hercínicas en el litoral septentrional de la península del Cap de Creus (prov. Gerona, España): la génesis de las bandas miloníticas. *Acta Geol. Hisp.* 10, 109-115.
- Carreras, J., Casas, J.M. (1987): On folding and Shear Zone development: a mesoscale structural study on the transition between two different tectonic styles. *Tectonophysics*, 135, 87-98.
- Carreras, J., Druguet, E. (1994): Structural Zonation as a result of inhomogeneous non-coaxial deformation and its control on syntectonic intrusions: an example from the Cap de Creus area (eastern-Pyrenees). *J. Struct. Geol.* 16, 1525-1534.
- Carreras, J., Orta, J.M., San Miguel, A. (1975): El área pegmatítica del litoral N. de la península del Cap de Creus y su contexto metamórfico y estructural. *Publ. Inst. Invest. Geol., Univ. Barcelona* 30, 11-34.
- Castiñeiras, P., Navidad, M., Montserrat, L., Carreras, J., Casas, J.M. (2008): U–Pb zircon ages (SHRIMP) for Cadomian and Early Ordovician magmatism in the Eastern Pyrenees: New insights into the pre-Variscan evolution of the northern Gondwana margin. *Tectonophysics* 461, 228-239.

- Černý, P. (1989): Characteristics of pegmatite deposits of tantalum. In Lanthanides, Tantalum and Niobium (P. Möller, P. Černý, P., F. Saupé, eds.), SGA Spec. Publ. 7, Springer Verlag, Berlin, Germany (192-236).
- Černý, P. (1991a): Rare-element granitic pegmatites. I. Anatomy and internal evolution of pegmatite deposits. *Geosci. Can.* 18, 49-67.
- Černý, P. (1991b): Rare-element granitic pegmatites. II. Regional to global environments and petrogenesis. *Geosci. Can.* 18, 49-67
- Černý, P., Alfonso, P.; Melgarejo, J.C. (1995): Pegmatitas graníticas. In Melgarejo, J.C. (ed.): Atlas de asociaciones minerales en lámina delgada. Edicions de la Universitat de Barcelona, Barcelona, 129-152.
- Černý, P., Ercit, T.S. (2005): The classification of granitic pegmatites revisited. *Can. Mineral.* 43, 2005-2026.
- Corbella, M. (1990): Estudi metal-logenètic del camp pegmatític del Cap de Creus. Unpubl. Grad. Thesis. Univ. Barcelona.
- Corbella, M., Melgarejo, J.C. (1993): Rare-element pegmatites of Cap de Creus Peninsula, northeast Spain: a new field of the beryl-phosphate subtype. Proc. 8th IAGOD Symp. E. Schweizerbart'sche Verlagsbuchhandlung (Nägele u. Obermiller), Stuttgart, Germany 295-302.
- Druguet, E. (1997): *The Structure of the NE Cap de Creus Peninsula*. Relationships with Metamorphism and Magmatism. Unpublished thesis. Universitat Autònoma de Barcelona.
- Druguet, E., Hutton, D.H.W. (1998): Syntectonic anatexis and magmatism in a mid-crustal transpressional shear zone: an example from the Hercynian rocks of the eastern Pyrenees. *J. Structural Geol.* 20, 905-916.
- Druguet, E. (2001): Development of high thermal gradients by coeval transpression and magmatism during the Variscan orogeny: insights from the Cap de Creus (Eastern Pyrenees). *Tectonophysics* 332, 275-293.
- Cocherie, A., Baudin, Th., Autran, A., Guerrot, C., Fanning, M., Laumonier, B. (2005): U-Pb zircon (ID-TIMS and SHRIMP) evidence for the early Ordovician intrusion of metagranites in the late Proterozoic Canaveilles Group of the Pyrenees and the Montagne Noire (France). *Bull. Soc. géol. Fr.* 176(3), 269-282.
- Grand'Homme, A. (2012): Pétrologie et géochronologie U-Pb sur zircons et colombo-tantalites des pegmatites du Cap de Creus. Unpublished Master 2 Recherche. Sciences de la Terre et des Planètes. GET-Univ. Paul Sabatier, Toulouse. 42 pp.
- Malló, A., Fontan, F., Melgarejo, J.C. & Mata, J.M. (1995): The Albera zoned pegmatite field, Eastern Pyrenees, France. *Mineral. Petrol.* 55, 103-116.

2. Introduction to the geology of SW Catalonia

J.C. Melgarejo¹

1. Departament de Cristal·lografia, Mineralogia i Dipòsits Minerals. Facultat de Geologia, Universitat de Barcelona

2.1 Geographical situation

The studied area is located in southwestern Catalonia, and includes the counties of Alt Camp, Conca de Barberà, Baix Camp and Priorat.

2.2 Geological setting

The outcrops are located in the Catalan Prelitoral Mountain Range (Serralada Prelitoral Catalana), in the Catalan Coastal Ranges (Serralades Costaneres Catalanes). The area was affected by three geologic cycles: a pre-hercynian cycle, a hercynian cycle, and an alpine cycle.

2.3 Pre-hercynian cycle

The outcrops that show the oldest materials are found in the south-western ends of the El Priorat and Baix Camp. Highly metamorphosed series outcrop in the core of a big hercynian anticlinal fold. These series are affected by different phases of folding that are not present in the rest of Paleozoic materials on the area. The basal part of the series consists in over 200 m of shales and brown greywacke known as the Marçà Unit (Melgarejo, 1987). The top of the series consists in 50 m of black slates. These are followed by the Molar Unit, a unit of calcosilicate rocks well characterized by the occurrence of dolomite associated with scapolite (Fig 2.1a), which has been related with the metamorphism of precursor evaporates (Melgarejo and Ayora, 1990). The discordantly overlying Pinyeres Unit is formed by brown quartzite with intercalations of shales (Fig 2.1b).

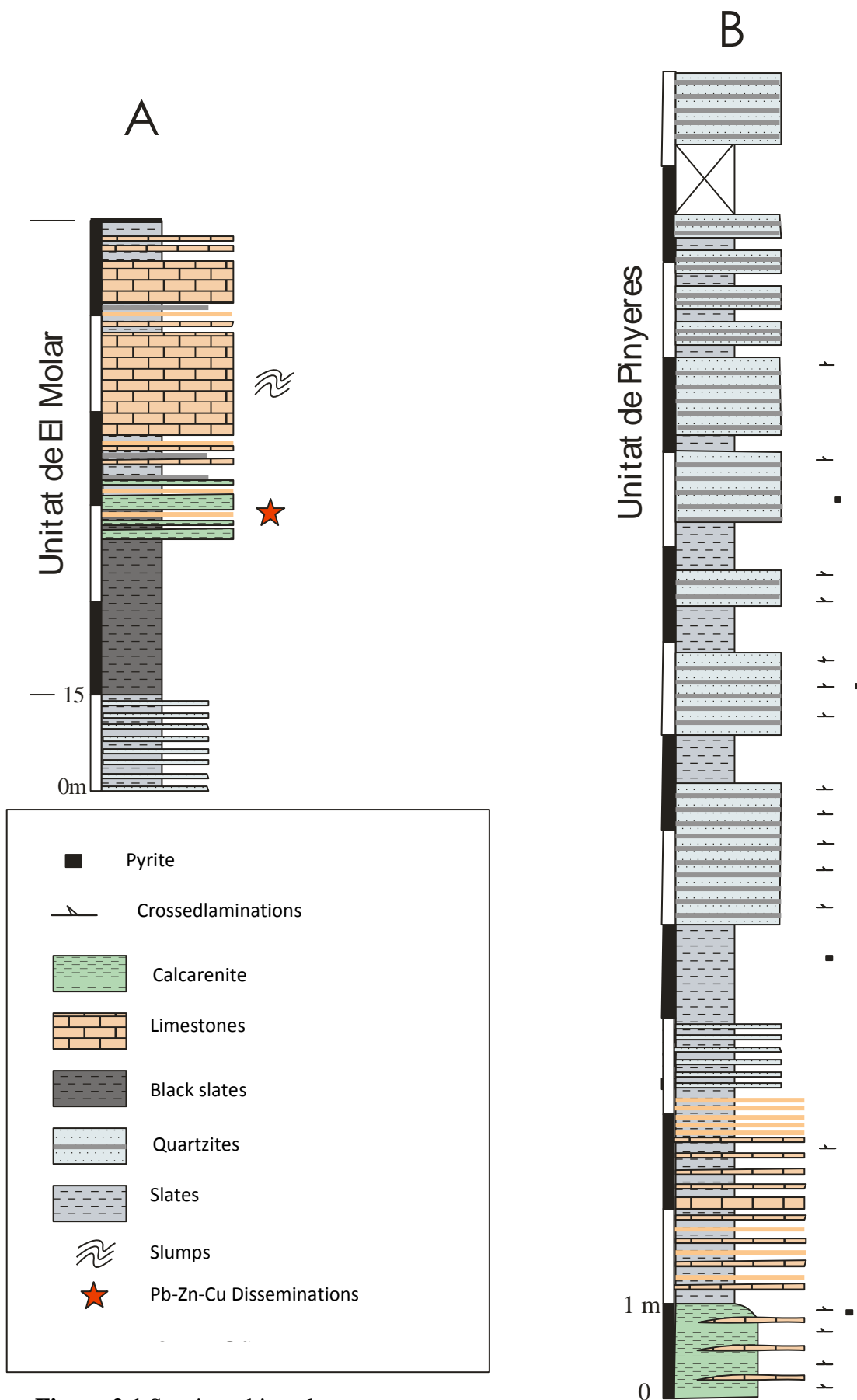


Figure 2.1 Stratigraphic columns

These materials were attributed to the Ordovician by Crespo and Michel (1980) based on lithofacies studies. Moreover, the Upper Ordovician materials of the rest of the Catalan Coastal Ranges are not affected by the complex folding observed in the materials of this area. For this reason, Melgarejo (1987) proposed that this

series could be Precambrian. However, later explorations of the area allowed finding possible segments of trilobites, which would date the materials Paleozoic and not Precambrian.

2.4 Hercynian cycle

Most of the mineralization of the Priorat area is hosted in Hercynian rocks. Therefore, these materials will be described in more detail. The Hercynian series are important for the mineralization and for the soils that have allowed the development of vineyards that produce famous wine of the highest quality. The shales that are found in this area are commonly known as “licorella”, and the best wines of Priorat are found in the vineyards on top of these slates. The landscapes of the areas occupied by materials from the Paleozoic, and in particular by “licorelles”, are very characteristic. They consist of hills rounded by erosion and generally brown in colour. This type of landscape is the one that dominates the Central Priorat.

Within the Hercynian cycle, two main series can be differentiated separated by an unconformity: the pre-carboniferous series and the carboniferous series.

2.4.1 The pre-carboniferous hercynian series

They are formed by materials deposited from the Upper Ordovician to the Upper Devonian (Fig 2.2). The Silurian series form the detachment levels of thrust faults, and therefore they are very segmented. The older materials are black shales, with intercalations of massive sulphide with mineralization of Cu-Au-PGE-As-Ni-Co-Ag-Bi-Te. These series have been dated by the graptolites found in them (Melgarejo, 1987). The Ludlovian series also consist of black shales with pyrite disseminations.

The Devonian series start with 200 m of marls and marly-limestones with tentaculites. They evolve into calcarenites with intercalations of slates towards the top of the series, finally giving place to thick series of black shales with intercalations of quartzites and lidites at the top (Melgarejo, 1987).

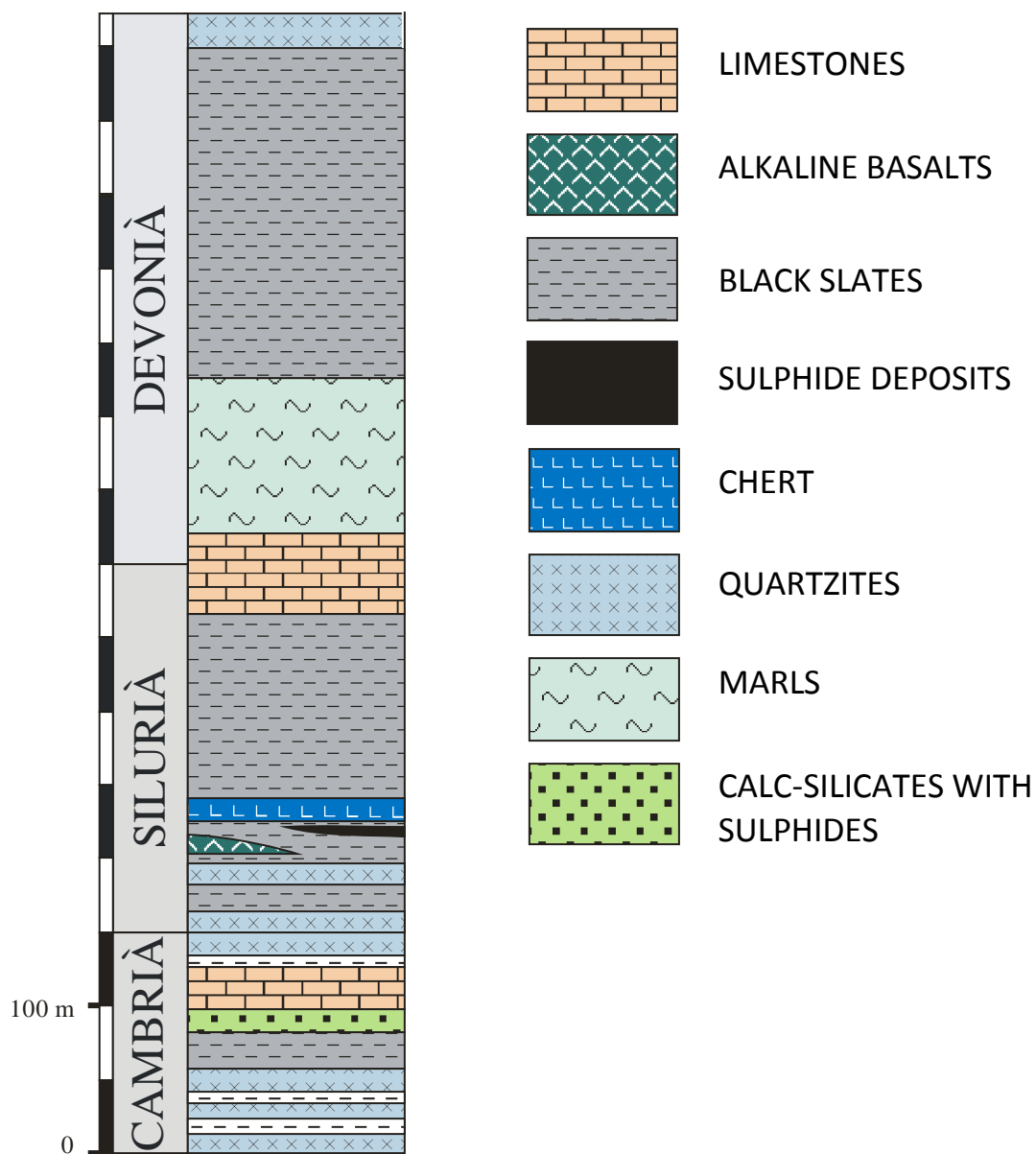


Figure 2.2 Stratigraphic column of the Lower Paleozoic in Priorat-Muntanyes de Prades

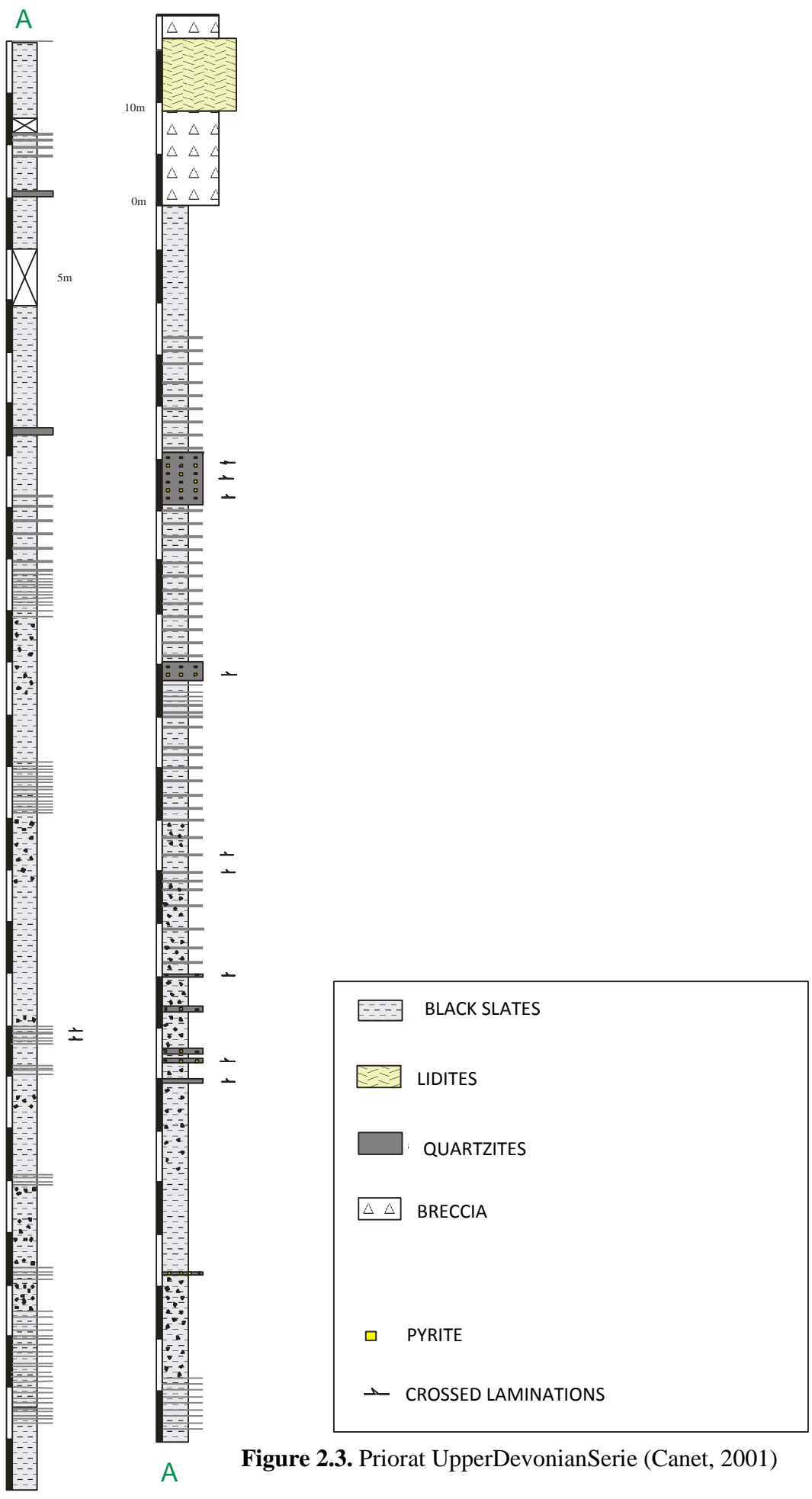


Figure 2.3. Priorat Upper Devonian Serie (Canet, 2001)

2.4.2 The Carboniferous series

The Carboniferous series are the most common from the SW Catalan Paleozoic materials. In the Priorat region, these materials appear low to non-metamorphized with flattened folds. Their great exposure allowed comprehensive studies of the Carboniferous (Sáez, 1982; Anadón et al., 1985 a,b; Sáez&Anadón, 1989). This series was initially established by Sáez (1982), who associated it with a submarine turbiditic depositional environment; although afterwards new sedimentologic interpretations have been suggested.

The Carboniferous through the Catalan Coastal Ridge is discordantly deposited onto the prior series (Ashauer&Teichmüller, 1935), even though in certain locations such as Central Priorat and Miramar the Carboniferous appears in a transition between the Upper Devonian. Therefore, it is suggested that the Upper Paleozoic basins in the Catalan Coastal Ridge are controlled by synsedimentary faults.

The Carboniferous in the Prades-Priorat Ridge is essentially turbiditic in most of its outcrops (Fig. 2.4) and it has kilometre-sized thickness, except for the southern side of Miramar Ridge where there is a compacted carbonatic series (80 m thick micrite) that ranges from the Upper Tournasian-Lower Visean to the Namurian shown by conodont dating (Sanz López et al., 2000). This carbonatic unit may contain cephalopods, crinoids and algae fossil remains. It is made up of meter-sized layers of white to purple micrite, locally nodular, with interbedded millimetre-sized layers of shale. This Carboniferous series is settled discordantly onto the Lower Cambrian quartzites basement.

On the northern side of Miramar Ridge the Carboniferous is placed discordantly onto the Silurian or Devonian. In Figuerola del Camp, the Carboniferous contains olistostromic bodies with carbonatic fragments of the Upper Silurian (5-15m). Above it appears a layer of green shales with nodular phosphates (5-10 m). The upper layer consists in hyaloclastitic splitic lavas sealed by lidites (Tournesian). Overlain discordantly by a 400m thick, coarse-grained alternation essentially made of grauwackes and shales with packets of Ludlovianolistostromic limestones and interspersed layers of spilites that belong to the Visean. The volcanic basement is absent along the Carboniferous logging performed in Masmolets or the northern side of Miramar Ridge, towards Selmella. In these cases, the Viseandetritic material is deposited on the previous materials of Carboniferous. Thus, there is an erosive discordance between Tournasian and Visean.

In the Priorat region, the lowermost Carboniferous member is likely to be a 5-10 m thick layer of lidites (which occasionally may have a thickness up to 40 m, as in Central Priorat and Torroja del Priorat area). These lidites have been attributed to the Tournasian (Scherer, 1969). The contact between lidites and the underlying prehercynian material is featured by an angular discordance, unless the upper layer is the Upper Devonian; then the contact is gradual. This suggests an unstable Carboniferous basin (Melgarejo&Ayora, 1988,1992).

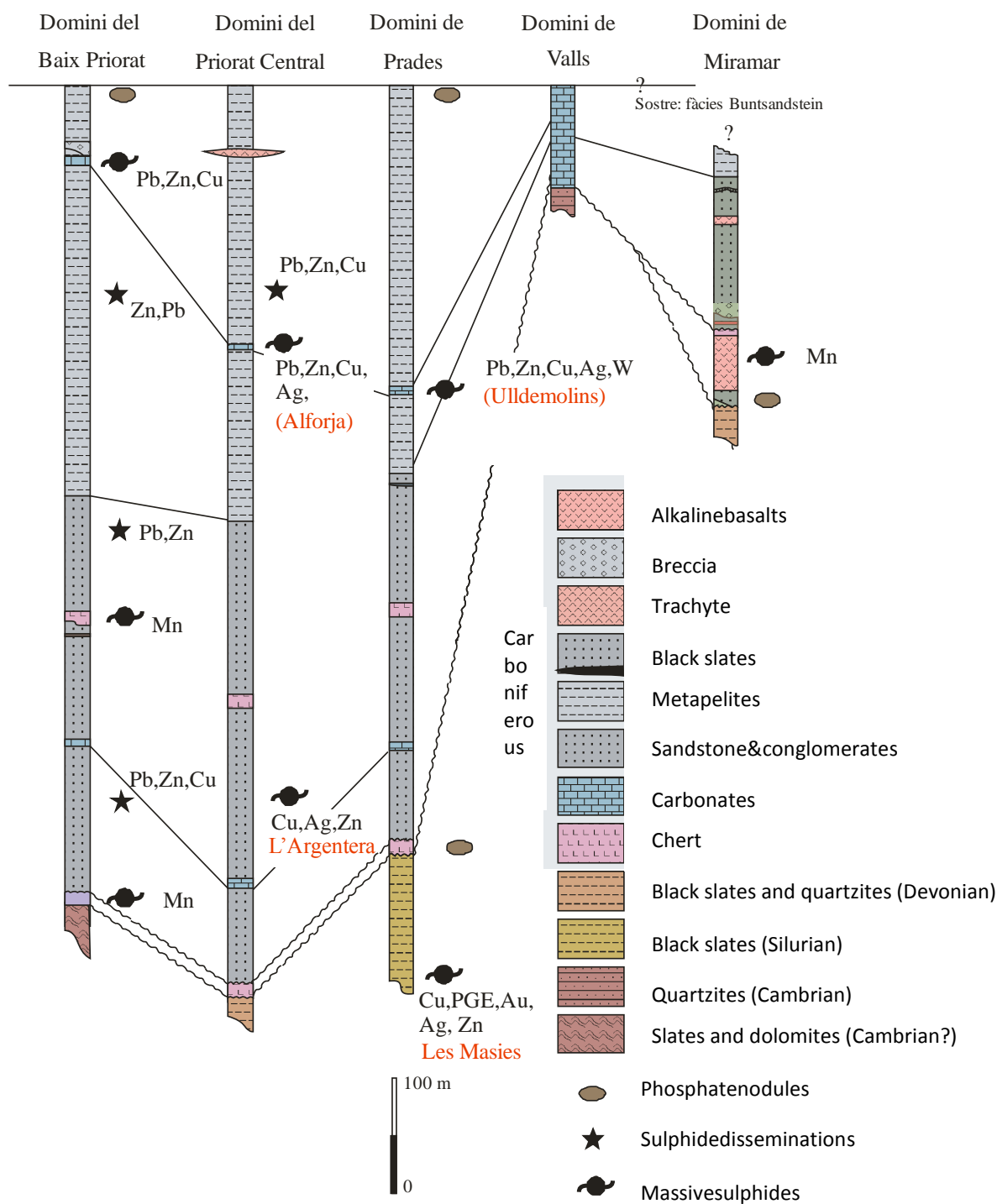


Figure 2.4. Stratigraphic columns of the Lower and Mid Carboniferous in the SW Catalonia (Melgarejo, 1987)

The Visean is deposited discordantly either with limestones or Pre-Carboniferous material. The contact between this unit and the previous is vastly irregular and often erosive. Visean series consist in detritic and coarse-grained material (200-400 m thick) accompanied of vegetation remains dragged from the continent (Villalba-Breva & Martín-Closas, 2009) and scarce interbedded carbonatic layers with conodonts (allowing its dating), tuff and intraplate alkaline spilites (Melgarejo & Martí, 1989), and restricted massive sulphides. Melgarejo (1987) distinguished the Bellmunt, Bassetes and l'Espluga units.

The Namurian series, around 400 m thick, consist in pelitic material all over the Priorat region. In the Central Priorat, Sáez (1982) named it as Escaladei Unit. Besides the presence of shales, the unit also contains interbedded pockets of conglomerate and certain limestone packets up to 5 m thick, which supposedly correspond to olistostromes.

This series is overlain by thick turbidite packets arranged in megasequences (Maestro et al., 1998), their whole thickness is about 200 m. It was named Poboleda Unit by Sáez (1982). These series consist in rhythmic alternation of sandstones, conglomerates and shales.

2.4.3 Hercynian deformation and metamorphism

Paleozoic materials were deformed and metamorphised in epizonal and shallow conditions. Therefore, the regional metamorphism is low-graded to absent (Melgarejo, 1987; Valenzuela, 2005). The Hercynian deformation caused flattened folds with low axial plane schistosity. The deformation was polyphasic. The first deformation phase was the main one; it produced NW-SE trending folds, slightly tilted towards NW (figure 2.5). The fold vergence is SW and their flanks are often thrust faulted. The Devonian black shales act as decollement due to the ductility that resulted from the graphite presence. Although the more evident folds are encompassed in the Devonian ductile material, folding affected to the whole Paleozoic series, though in Carboniferous, folds are often not observed in the outcrops. This phase affected prior thrust faults which ended up inverted. The second deformation phase produced chevron shaped folds with the same direction (NW-SE) but opposite vergence. It also triggered thrust faulting in minor scale. The Hercynian cycle finished forming regionally kink-band microstructures and Tardi-Hercynian pregrantic faults with NE-SW strike (Melgarejo, 1987).

2.4.4 The Tardi-Hercynian granite intrusions and associated porphyry

The Paleozoic series are intruded by Tardi-Hercynian plutonic bodies and their filonian cortex (Fig 2.5), like it occurs along the Catalan Coastal Ranges.

The outcropping plutons of Prades-Priorat Ridge consist in calcoalcaline rocks (Enrique, 1981; Melgarejo, 1987; Enrique, 1990). The more important pluton in Priorat is the one located in Falset and extends until Marçà. In this pluton, rocks range from granitic to granodioritic composition with biotite and hornblende as accessories. Biotitic leucogranites differentiates are found in the cupola of the pluton. In the Baix Camp, the more important plutons are in Alforja and Argentera with quartzioritic to leucogranitic composition, and in the Conca de Barberà the more relevant are in Prades, mostly granodioritic in composition (Melgarejo, 1987), and certain intrusions near Poblet with dioritic to leucogranitic in composition (Melgarejo, 1987).

The plutons give certain geomorphological features at the landscape. They can be found in depressed and limited areas surrounded by small hills made up of Paleozoic host rock. This happens since the erosionability of granitoids is greater than the surrounding rocks.

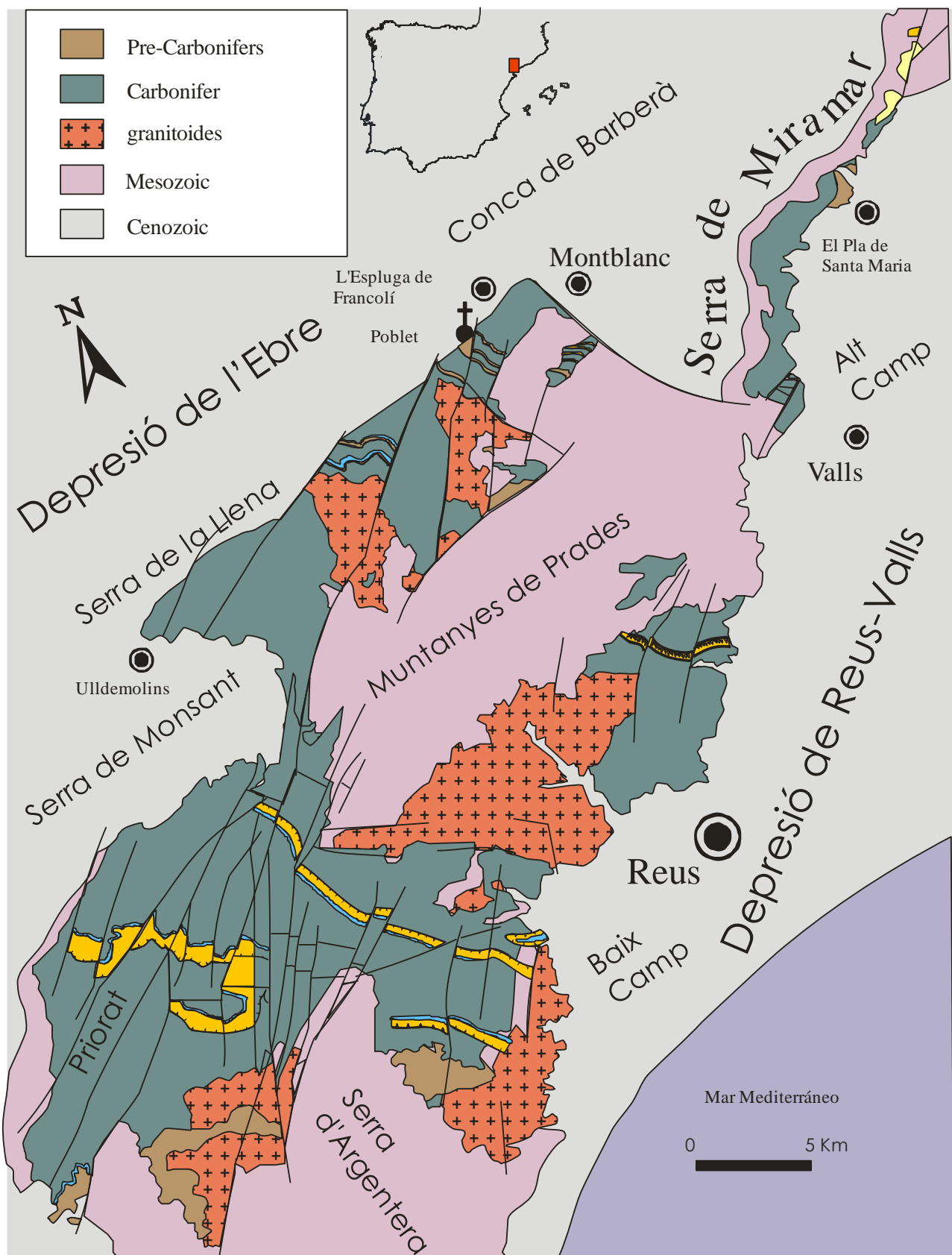


Figure 2.5. Muntanyes de Prades- Priorat-Serra de Miramar geologicalmap

Its contact with the host rock is sharp, and the granites may incorporate host rock xenoliths. The texture is phenocrystalline with millimetric grainsize, holocrystalline to allotriomorph. The main accessory mineral is biotite and hornblende. Sometimes, muscovite can also be found. Orto and clinopyroxenes are common accessories in the Prades Ridge granitoids and especially in Baix Camp. Granites are accompanied with an important filonian cortex

Andesitic porphyries are typically subvertical dikes with NE-SW direction, but also WNW-ESE and NNW-SSE. They are probably associated with the Tardi-Hercynian faults and are intruded in the granitic plutons or in its thermal metamorphic area. They show grey to dark colouration, present phenocrystals of plagioclase, quartz, biotite, calcic amphibole and occasionally pyroxenes.

Riodacitic porphyries are much different than the mentioned above. They outcrop in sills, intruding subconcordantly to the layering or Paleozoic material schistosity, either far from the pluton or within it. They cross-cut the porphyries and therefore are the most recent igneous rocks of the area. Their colouration is yellowish to orange. Quartz and biotite are the main phenocrysts, but often are rich in devitrified glass. Fluidal textures typically seen in rhyolites are recognized together with phenocrysts of quartz englobed by a microcrystalline to glassy matrix. The sills of Bellmunt-El Molar are considerably thick, reaching hundreds of meters. Towards the E, these porphyries shorten gradually and branch to smaller dykes, which height tens of meters in the Règia mine of Bellmunt del Priorat, and vanish completely in Gratallops. This might be indicative that the El Molar area is the deepest part of the intrusion and towards the E gradually outcrops the shallower parts. If this is true, and thus the andesitic sills correspond to the same complex, an interesting aspect comes out; Hercynian materials are eroded prior to the formation of the Pretriassic erosional surface. This surface, next to el Molar, is located at great depth, whereas in Bellmunt is shallower. This could be explained by Tardi-Hercynian faulting before the Pre-Triassic erosion and after the dyke emplacement.

Finally, it is remarkable that the pegmatitic and aplitic dykes are low-developed and their size is centimetric. The composition is similar to the granitoids that they come from and they do not present relevant accessory minerals. Typically, their extension is restricted into the granites.

2.4.5 Contact metamorphism.

The diffusion of heat produced by the granitoids intrusion determined the development of the contact metamorphism aureole to the metasedimentary Paleozoic rocks located near the intrusions. The wide of the aureole varies and has hundreds of meters. The contact metamorphism very rarely reaches high-grade and generally middle-grade metamorphic mineral assemblages are identified. The metasedimentary rocks of Carboniferous are grauwackes and lutites rich in quartz clasts, rock fragments and chlorite. As they are Fe-, Mg- and Si-bearing, and relatively depleted in Al, the poikiloblastic recognition is difficult. When they appear are likely cordierite. Whereas the Devonian and Silurian black shales, richer in Al, contain cordierite and andalusite.

2.5 Preorogenic alpine cycle stage: the Mesozoic megasequence

The alpine cycle begins with a strong erosive stage. On its top, Mesozoic series were deposited. Mesozoic series can be divided in a group of sedimentary sequences, separated by smaller discontinuities (Virgili, 1958). Mesozoic series are formed by Triassic facies, thick series of Jurassic and Cretaceous (Fig 2.6). All these series

are formed in an extensional context of rifting. The first depositional sequence is formed by Upper Permian, Buntsandstein and part of lower Muschelkalk (Calvet, 1986).

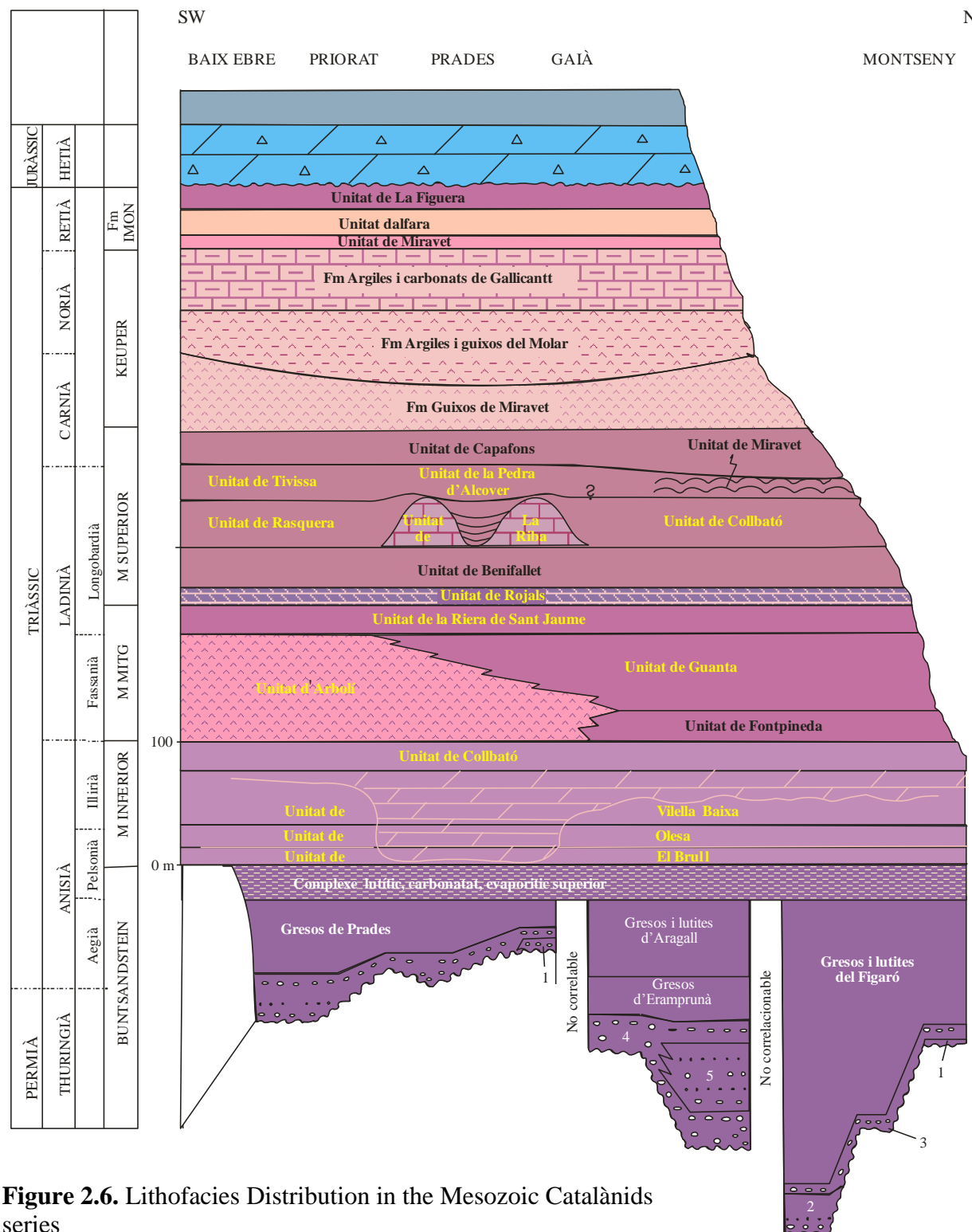


Figure 2.6. Lithofacies Distribution in the Mesozoic Catalànids series

2.5.1 Buntsandstein

The base of the sequence is discordant to hercynic basement. Buntsandstein is formed by red sediments (20-150m), arranged in a coarsening upward sequence (March, 1980). Locally, breccia and conglomerates occur at the base, which have been regionally attributed to Permian, near the Eugènia Mine. However, thicker packages of clusters, with quartz pebbles and metamorphic and igneous rocks, occur more often

from the erosion of Paleozoic materials. The cement is ferruginous, silicic or carbonatic, but locally it presents barite.

The intermediate section of the sequence is generally sandy, often displaying cross bedding textures. The upper part of the series consists in clays.

2.5.2 Muschelkalk

Muschelkalk is subdivided into a lower section of limestone, locally dolomitized, (50-100 m of thickness), an intermediate section (50-100 m of thickness) with evaporites, red lutites, sandstones and dolomites, and a higher section with limestones and marls (50-150 m of thickness). The first section of carbonates (lower Muschelkalk) is quite resistant to erosion and constitutes the most important associated structural cliffs and surfaces in the Prades mountains. The middle Muschelkalk consists of red clays and gypsum, materials that indicate a regressive episode. The upper Muschelkalk, indicates a transgressive episode, in which thick carbonates were deposited.

2.5.3 Keuper

The third depositional sequence is regressive. It is formed by the top materials of the Muschelkalk Superior facies and the versicolor clay rich in gypsum sections of the Keuper (Salvany and Ortí, 1985). In the Priorat these materials are only recognized in the south, because towards the northwest they are eroded.

2.5.4 Jurassic

This sequence (Robles, 1975; Salas, 1987) is under an important surface of discontinuity, which corresponds to an erosive stage, and consists of carbonated breccia (150 m of thickness) that grade to dolomites. These levels are associated with a sequence Hettangian - Carixian (Salas, 1987).

Domerian sequence is located between two small discontinuities. This sequence is formed by marls and limestones (shallowing sequence towards the top) (Salas, 1987).

2.6 The synorogenic state from the Alpine cycle (Paleogene)

The paleogenic materials outcropping at the borders of the Ebro Depression record the tectonic evolution of the Catalan Coastal Ranges that took place during the Paleogene due to a compressive period. The studies of Anadón et al (1979) and Colombo (1986 a,b), among others, summarize this evolution. At the Priorat, the paleogenic series are mainly continental detrital series.

2.6.1 The Palocene series

Mediona Formation represents the Paleocene materials of the region. It lies discordantly over Mesozoic material. The formation is constituted by a thin section of red lutites containing *Vidaliella Gerundensis*, from the Upper Paleocene. Edaphic features are conspicuous and silex nodules of metric order are locally found. The thickness of the formation is always lower than 30 m. The materials from these series already present lateral and vertical facies changes, which is indicative of an instable basin.

2.6.2 The Eocene series

The Cornudella Group overlies concordantly the Paleocene materials (Colombo et al., 1995). This unit is subdivided into two subunits: Ulldemolins Complex and La Morera de Montsant Limestones Formation.

Ulldemolins Complex is constituted by and alternation of red lutites and gypsum levels, and sandstones and carbonates, with a total thickness of 200-300 m. The age of the complex is Lower-Middle Eocene (Colombo and Escarré, 1994).

La Morera de Montsant Limestones Formation presents thickness of 70-80 m. It is constituted by yellowish limestones with intercalation of lutites. The age of the formation is Upper Eocene (Colombo and Barbé, 1994).

2.6.3 The Oligocene series

The Eocene materials are overlaid by the Escaladei Group (Allen et al., 1983; Pérez Lacunza and Colombo, 2001). This unit is also subdivided into two subunits (Colombo, 1986): Conglomerates of Montsant Formation and Margalef Formation.

The Conglomerates of Montsant Formation presents up until >1000 m and was formed at the Lower and Middle Oligocene. It is constituted by two members: Sant Joan del Codolar Member, and Creu Corbatera Member. The Sant Joan del Codolar Member consists of lutites with thin intercalations of conglomerates, which present channel forms and are laterally discontinuous. The Creu Corbatera Member consists essentially of massive conglomerates, laterally continuous, with thicknesses up to tens of meters.

The Margalef Formation is constituted by sandstones and conglomerates, with some intercalations of gypsum. Its thickness is around 400 m and the age is Middle Oligocene.

2.6.4 The Alpine compressive structures

During the Eocene – Oligocene, the late-hercynian faults were activated as strike slip faults due to a compressive period (Teixell, 1986, 1988). These faults generally present high dip angles at the Paleozoic basement and at the lower part of the Mesozoic cover, but they become flexures or folds at the upper part of the Mesozoic cover. The main faults display NE-SW direction, although other faults present NW-SE and WNW-ESE directions. These faults caused the progressive uprising of the Catalan Coastal Ranges relative to the Ebro Depression. The new formed relief was being synchronously eroded. As a result, the materials deformed by the faults were rapidly covered by subhorizontal layers of detrital material originated by the erosion. These layers were also deformed and straightened by the faults and once again covered by subhorizontal detrital layers. The repetition of this cycle resulted in the formation of progressive discordances (Anadón et al., 1979, 1985c; Colombo and Vergés, 1992). These materials are syntectonic and hence their age is the same as the age of the deformation. Therefore, we can conclude that the main activity of these faults occurred during the Oligocene.

2.6.5 Late-orogenic stage of the Alpine Cycle (Neogene)

This stage is characterized by the occurrence of a regional extension which was accompanied by volcanism at the northern part of the Catalan Coastal Ranges. As a result of the extension, the pre-existent faults were inversed as normal faults. These normal faults led to the formation of big tectonic basins all along the Catalan Coastal Ranges (Guimerà, 1988). The basins were filled with detrital material coming from the erosion of the adjacent horsts. The Móra Depression is interpreted as a Miocene basin filled with conglomerates. These materials do not outcrop significantly in the Priorat.

2.6.6 Quaternary

The Quaternary sedimentary deposits are conditioned by the present relieves: slope sediments, alluvial fans, and river terraces. At the Priorat, big river terraces are only formed by the lower course of the Siurana River. The terraces, arranged in several levels, can be observed at the lower part of the Siurana River course, between Bellmunt and the Ebro. As an overall, the majority of these materials are poorly consolidated.

References

- Allen, P., Cabrera, L., Colombo, F., Matter, A. (1983): Variations in fluvial style on the Eocene Oligocene alluvial fan of the Scala Dei Group, SE Ebro Basin, Spain. *Journal of the Geological Society of London*, 140: 133-146.
- Anadón, P., Julivert, M., Sáez, A. (1983): El Carbonífero de las Cadenas Costero-Catalanas. In: *Carbonífero i Pérmico de España. X Cong. Int. Estr. i Geol. del Carbonífero. I.G.M.E.* pp. 332-336.
- Anadón, P., Julivert, M., Sáez, A. (1985a): El Carbonífero de las Cadenas Costeras-Catalanas. In C. Martínez. (ed.), *X Congr., Int. Estrat. Geol. Carbonífero y Pérmico en España, Inst. Geol. Min. España*, 1: 99-106.
- Anadón, P., Julivert, M., Sáez, A. (1985b): Aportación al conocimiento del Carbonífero de las Cadenas Costeras-Catalanas. *C.R. Xème. Congr. Int. Strat. Géol. Carbon. (Madrid, 1983)*, I: 99-106.
- Anadón, P., Cabrera, L., Guimerà, J., Santanach, P. (1985c): Paleogene strike-slip deformation and sedimentation along the South eastern margin of the Ebro basin. In K.T. Biddle, N. Christie-Blick. (eds.): *Spec. Publ. 37 on strike-slip deformation, basin formation and sedimentation*: 303-318.
- Anadón, P., Colombo, F., Esteban, M., Marzo, M., Robles, M.S., Santanach, P., Solé Sugrañes, L. (1979): Evolución tectono-estratigráfica de los Catalánides. *Acta Geol. Hisp.* 14: 242-270.
- Ashauer, H., Teichmüller, R. (1935): Die variscische und alpidische Gebirgsbildung Kataloniens. Versión castellana de J.M. Ríos en *Publicaciones extranjeras sobre Geología de España. CSIC (1946)*, 3: 7-102.
- Barnolas-Cortinas, A., López, F., Anadón, P., Ardévol, L., Cabra, P., Cabrera, L., Calvet, F., Enrique, P., Fernández, P., Giner, J., Guimerà, J., González, J., Julivert, J., Marzo, M., Orti, F., Salas, R. (1987): *Mapa geológico de España, Tarragona. IGME, Madrid.*

- Calvet, F. (1986): El cicle Triàsic al marge oriental d'Ibèria. In: Història Natural dels Països Catalans. Vol. 1. (Geologia-I). Fundació Enciclopèdia Catalana, 253-280.
- Castellort, F.X. (1986): Estratigrafia del Muschelkalk mitjà dels Catalànids i sedimentologia de les seves unitats detrítiques. Tesi de llicenciatura inèdita. Departament d'Estratigrafia. Universitat de Barcelona. 102 pp.
- Canet, C. (2001): Dipòsits sedimentari-exhalatius del Paleozoic del SW dels Catalànids: model de dipòsit. Tesi doctoral inèdita. Departament de Cristal·lografia, Mineralogia i Dipòsits Minerals. Universitat de Barcelona. 442 pp.
- Colombo, F. (1980a): Estratigrafía y sedimentología del paleógeno continental del borde meridional occidental de los Catalánides. Cuadernos de Geología Ibérica, 10, 44-115.
- Colombo, F. (1980b): Estratigrafía y sedimentología del terciario inferior continental de los Catalánides, Tesi Doctoral, Universitat de Barcelona, 606 p.
- Colombo, F., Vergés, J. (1992): Geometría del margen SE de la Cuenca del Ebro: discordancias progresivas en el Grupo Scala Dei, Serra de la Llena (Tarragona). Acta Geologica Hispanica 27: 33-54. Libro Homenaje a Oriol Riba Arderiu.
- Colombo, F., Barbé, D. (1994): Ciclicidad en carbonatos lacustres paleógenos: Formación Morera del Montsant, Tarragona. Geogaceta, 15: 41-44.
- Colombo, F., Barbé, D., Escarré, V. (1995): Controles alocíclicos en el relleno sedimentario de una cuenca paleógena: arquitectura deposicional del Grupo Cornudella, Cuenca del Ebro (Tarragona). Geogaceta, 17: 27-30.
- Colombo, F., Escarré, V. (1994): Arquitectura deposicional y sedimentología del Complejo de Ulldemolins (Paleógeno), Tarragona. Geogaceta, 15: 37-40.
- Colodron, I., Cabañas, I., Martínez, C. (1979): Mapa geológico de España. Escala 1:50000. Hoja núm. 444, Flix. IGME, 24 p.
- Colodrón, I., Núñez, A., Ruiz, V. (1976): Memoria y hoja geológica número 472 (Reus). Mapa geológico de España 1:50.000 (segunda serie). IGME, Madrid.
- Colodrón, I., Núñez, A., Ruiz, V. (1978): Memoria y hoja geológica número 445 (Cornudella). Mapa geológico de España 1:50.000 (segunda serie). IGME, Madrid.
- Crespo, J.L., Michel, B. (1980): Estudio Geológico de los yacimientos minerales del Macizo Catalán entre Bellmunt de Ciurana y Mola, Priorato (Tarragona). Studia Geologica Salmanticensia 16: 123-149.
- Enrique, P. (1981): Late tectonic granitoids of the Catalanian Coastal Ranges. Guide to the field trips in the Eastern Pyrenees and Catalanian Coastal Ranges. IGCP proj. 5: 44-52.
- Enrique, P. (1990): The Hercynian intrusive rocks of the Catalanian Coastal Ranges (NE Spain). Acta Geologica Hispanica, 25, nº 1-2: 39-64.
- Giner, J. (1980): Estudio sedimentológico y diagenético de las facies carbonatadas del Jurásico de las Catalánides, Maestrazgo y Rama Aragonesa de la Cordillera Ibérica. Tesi Doctoral inèdita. Dpt. Estratigrafia Universidad de Barcelona, 315 pp.

- Guimerà, J. (1988): Estudi estructural de l'enllaç entre la Serralada Ibèrica i la Serralada Costanera Catalana. Tesi doctoral. Universitat de Barcelona.
- De Haller, A. (1997): Le complexefilonien à Pb (\pm Zn \pm Ag \pm Ba \pm Cu \pm Ni \pm Co \pm Fe) de Bellmunt del Priorat (Tarragona, Espagne). Cartographie, minéralogie, pétrographie magmatique, lithogéochimie, altérations, typologie filonienne, séquences paragénetiques et textures intrafiloniennes. Diplôme Sciences de la Terre. Univ. Genève, 135 pp.
- Hernández-Sampelayo, P. (1935). El Sistema Cambriano. Explicación del Nuevo Mapa Geológico de España en Escala 1:1.000.000, I. El Sistema Cambriano. Memorias del Instituto Geológico y Minero de España 41, 291-528.
- Maestro-Maideu, E.; Estrada, R., Remacha, E. (1998): La Sección del Carbonífero en el Priorat central (prov. de Tarragona). Geogaceta 23: 91-94.
- Melgarejo, J.C. (1987): Estudi geològic i metal·logenètic del Paleozoic del Sud de les Serralades Costaneres Catalanes. Tesi doctoral inèdita. Departament de Cristal·lografia, Mineralogia i Dipòsits Minerals. Universitat de Barcelona. 615 p.
- Melgarejo, J.C. (1993): Estudio geológico y metalogenético del Paleozoico del sector sur de las Cordilleras Costeras Catalanas. Col. Monografías ITGE 103: 1-605.
- Melgarejo, J.C., Ayora, C. (1989): Mineralizaciones sedex de manganeso en tramos basales de la serie carbonífera del Priorato-Sierra de Miramar (Cataluña). Bol. Geol. y Min. 103: 544-550.
- Melgarejo, J.C., Ayora, C. (1990): Escapolita en metasedimentos precarboníferos del Priorato (Cataluña). Bol. Soc. Española Mineral. 13: 43-49.
- Marzo, M. (1980): El Buntsandstein de los Catalánides: estratigrafía y procesos de sedimentación. Tesi doctoral inèdita. Dept. Estratigrafía, Universitat de Barcelona.
- Melgarejo, J.C., Martí, J. (1989): El vulcanisme bàsic del Carbonífer inferior de la serra de Miramar. Acta Geol. Hisp. 24,2: 131-138.
- Melgarejo, J.C., Salas, R., Corbella, M., Querol, X. (1989): Geologia del sector comprès entre el Massís de Garraf i els Ports de Beseit. Aspectes d'Història Natural de les Comarques de Tarragona, 69-125.
- Melgarejo, J.C., Ayora, C. (1988): Mineralizaciones SEDEX de Mn en tramos basales de la serie carbonífera del Priorat-Serra de Miramar (Cataluña). Bol. Soc. Española Mineral., 11(2):157-158.
- Melgarejo, J.C., Ayora, C. (1992): Mineralizacionessedex de manganeso en tramosbasales de la serie carbonífera del Priorato-Sierra de Miramar (Cataluña). Boletín Geológico y Minero, 103(3): 544-550.
- Orche, E., Colodrón, I. (1976): Memoria y hoja geológica número 444 (Flix). Mapa geológico de España 1:50.000 (segunda serie). IGME, Madrid.
- Orche, E., Robles, S., Rosell, J. (1977): Memoria y hoja geológica número 471 (Mora de Ebro). Mapa geológico de España 1:50.000 (segundaserie). IGME, Madrid.
- Pérez Lacunza, E., Colombo, F. (2001): Variaciones del estilo deposicional en el Grupo aluvial Scala Dei, Cuenca del Ebro (Provincias de Tarragona y Lleida): Características y significado sedimentológico. Geogaceta 30: 211-214.

- Raymond, D., Caridroit, M. (1990): Le Dévonien-Carbonifère inférieur du Priorat (Catalogne, Espagne): nouvelles données micropaléontologiques et interprétation paléogéographique. *Acta Geologica Hispanica* 28(1): 27-31.
- Robles Orozco, S. (1975): Síntesis de la evolución estratigráfica y tectónica de los materiales secundarios del bloque del Cardó y sectores adyacentes (Provincia de Tarragona). *Acta Geol. Hisp.* 10(2): 59-66.
- Sáez, A. (1982): Estudio estratigráfico y sedimentológico de los materiales paleozoicos de la parte central del Priorat (Tarragona). Tesis de Licenciatura inédita. Dept. Estratigrafia, Univ. Barcelona, 86 pp.
- Sáez, A., Anadón, P. (1989): El complejo turbidítico del paleozoico del Priorato (Tarragona). *Acta Geologica Hispanica* 24: 33-47.
- Salas, R. (1987): El Malm i el Cretaci inferior entre el Massís de Garraf i la Serra d'Espadà. Anàlisi de conca. Tesis Doctoral inédita. Universitat de Barcelona. Dpt. de Geoquímica, Petrologia i Prospecció geològica, 3 tomos, 345 pp., 133 figs.
- Salas, R. (1989): Evolución estratigráfica secuencial y tipos de plataformas de carbonatos del intervalo Oxfordiense-Berriasiense en las Cordilleras Ibérica Oriental y Costero Catalana Meridional. *Cuadernos de Geología. Ibérica*, 13: 121-157.
- Salas, R. (1991): Historia de la subsidencia durante el Mesozoico y evolución tectono-sedimentaria Cretácica de las cuencas del margen oriental de Iberia. III Coloq. Cretácico España, Resumen comunicaciones, 61.
- Salvany, J., Ortí, F. (1985): El Keuper de los Catalánides. In F. Mateu Ibarz i M. Marzo (eds.): "Resúmenes II Coloquio de estratigrafía y paleogeografía del Pérmico y Triásico de España ", 105-106.
- San Miguel de la Cámara, M., San Miguel Arribas, A. (1948): Las rocas eruptivas y metamórficas de las comarcas del Priorato y Campo de Tarragona. *Estudios Geológicos*, 9: 107-132.
- Sanz López, J., Melgarejo, J.C., Crimes, Th. J. (2000): Stratigraphy of Lower Cambrian and unconformable Lower Carboniferous beds from the Valls unit (Catalonian Coastal Ranges). *Comptes Rendus Academies des Sciences de Paris, série IIa, Sciences de la Terre*, 330,2: 147-153.
- Scherer, N. (1969). Faltung von Lyditen am Beispiel des Unterkarbons in Südostkatalonien (Spanien). *Geologie* 18:1190-1198.
- Teixell, A. (1986) : Estudi geològic de les Serres de Pàndols, de Cavalls i del Montsant i de les seves relacions amb les depressions de l'Ebre i de Móra (Tarragona). Tesis de Licenciatura, Univ. de Barcelona, 149 p.
- Teixell, A. (1988): Desarrollo de un anticlinorio por transpresión, aislando una cuenca sedimentaria marginal (borde oriental de la cuenca del Ebro, Tarragona). *Rev. Soc. Geol. España*, 1, 229-238.
- Valenzuela, S. (2005): Cristalinidad de la illita y de la clorita: aplicación en la caracterización del metamorfismo de gradomuybajo, límite diagénesis-metamorfismo, del Priorat (Tarragona). Tesis de màster inédita. Dept. Petrologia, Geoquímica i Prospecció Geològica, Universitat de Barcelona. 248 pp.

- Villalba-Breva, Sh., Martín-Closas, C. (2009): Plant Taphonomy from the Mississippian Flysch Facies of the El Priorat Massif (Catalonia, Spain). *J. Taphonomy* 7(3-4), 249-262.
- Virgili, C. (1958): El Triásico de los Catalánides. *Bol. Inst. Geol. Min. España*, 69: 858 p.

3. Mineral deposit types of the SW of Catalonia

J.C. Melgarejo¹, C. Canet², P. Alfoso³, J. Proenza¹, C. Cirera¹, A. Escusa¹

1. *Departament de Cristal·lografia, Mineralogia i Dipòsits Minerals. Facultat de Geologia, Universitat de Barcelona*

2. *Instituto de Geofísica, Universidad Nacional Autónoma de México, México*

3. *Departament d'Enginyeria Minera i Recursos Naturals, Universitat Politècnica de Catalunya, Manresa.*

3.1 Introduction

In Priorat – Prades Mountains there are some lead mines. Lead mines contain other resources, like Ag, Petroleum and Al. These mines were explored to mine other minerals and rocks, like fluorite (composed by Cu, Mn), Barite, Gypsum, Clay, Flint, Limestone and Marble.

Priorat mineral resources are distributed around all Priorat regions, the most economic area is the region comprised between Falset and el Molar. Traditionally, this region was named as Priorat Mineral Basin, Falset Mineral Basin or Bellmunt-Molar Mineral Basin. There is more complementary information in Melgarejo (1987, 1993) and in the metallogenic map (ITGE, 1994)

There are 3 classifications of these mineral resources:

1. Depending on the moment when it was formed.
2. Depending on its morphology.
3. Depending on what's the most important resource.

3.2 Stratabound mineralizations (Pb- Zn- Cu- W) in pre-Hercynian series

At 500m NE from the bridge on Siurana River, on the road that connect El Molar with Masroig there is a black shale outcrop (El Molar Unit). Some decimetres of metacalcarenites are intercalated with black shales; on metacalcarenites there are crossed laminations. The metacalcarenites present sulphur dissemination. There is a predominance of sphalerite, galena and chalcopyrite, and fewer amounts of pyrrhotite, pyrite and scheelite. There are some outcrops on the shore of Siurana tributaries, near the silver Falset mine (Melgarejo and Ayora, 1990). These mineralizations were not explored. Based in lead isotopic analysis, galena and its texture, it is unlikely that they were metaevaporites ore deposits. Canet (2001) proposed that the mineralizations were formed by calcium silicate with hydrothermal contamination during Post-Hercynian age.

Lower Silurian series appear at N of Prades Mountains and it contains stratabound polymetallic mineralizations, which are rich in Cu, V and Cr and it contain PGE, REE, U, Th and Au too. Its thickness is 25m. Llandovery series was affected by contact metamorphism and they are interpreted as Sedex (Melgarejo, 1987; Canet 2001).

3.3 Mineralizations associated with the dynamics of Hercynian basins

Devonian series contains pyrite disseminations, but their mining is not economic. The economic mineralizations are hosted by the Carboniferous series (Ayora et al, 1990).

3.3.1 Petroleum in Upper Devonian shales

Priorat Upper Devonian black shales contain petroleum that was extracted in the 16th Century. For petroleum formation organic matter is needed in sediment, maturation and a trap to fix the components and preserve petroleum. For the petroleum preservation a low grade metamorphism that never exceeds the critical threshold is needed.

During the Upper Devonian there was a closed basin in the Priorat Region, which constituted a poor oxygen environment. This event allowed the formation of thick levels of black shales with organic matter that appear in Central Priorat.

In Priorat, regional Hercynian metamorphism was weak but some Devonian materials were affected by contact metamorphism. The carbonaceous materials turned into graphite so graphite inclusions often occur in andalusite (chiastolite) poikiloblast near the Falset intrusion. However, near Vilelles there was weak metamorphism or the rocks are not metamorphosed, and it is preserved some organic components. Some of these black shales can burn in a fire.

Some fluid components of petroleum strain in rocks cracks and imprint these rocks. In open pits, petroleum drops, slide on the wall.

3.3.2 Alum and Phosphate mineralizations in Devonian Materials

Devonian black shales contain pyrite disseminations. The pyrite is oxidized and transformed in H_2SO_4 . This H_2SO_4 reacts with the shale hosting the pyrite and attacks the silicate minerals, releasing SiO_2 and cations (Al, K, Fe, and Mg). The resulting acid waters enriched in these components circulate through the materials by capillarity towards the surface. Close to the surface, the waters can evaporate, giving place to sulfate precipitation. These minerals were used for alum production.

The upper Devonian and Tournaisian series are formed by phosphates (cryptocrystalline apatite). The same acids, formed by pyrite dissolution, can dissolve apatite and precipitate as Al phosphates (evasite, variscite or calcioferrite).

3.3.3 Phosphate mineralization in Tournaisian Lydites

Tournaisian lydites levels contain phosphate nodes (cryptocrystalline apatite). The phosphate concentration was not enough for their exploitation. However, this stratiform phosphate of sedimentary origin was a pre-concentration for later events, like meteoric waters. These waters are able to mobilize phosphate, especially if sulfurs are being altered at the same time. In this context, variscite or turquoise mineralisations can form during weathering. If there are Cu lydites, turquoise will form associated with other amorphous and cryptocrystalline phosphates (crandalite).

3.3.4 Manganese levels in Tournaisian lydites

Carboniferous lydites levels in south Priorat have stratiform manganese intercalations (Melgarejo and Ayora, 1988, 1989, 1992) with long lateral continuity. Locally, the lydites and hosted manganese levels were affected by synsedimentary landslides within the carboniferous basin and they were resedimented as olistostromes in Visean materials. Similar mineralizations are always associated with lydites and Tournaisian volcanism (Melgarejo and Marti, 1989).

The mineralization presents banded textures with different colorations for the bands. Manganese mineralizations consist in associations of Mn silicates of very small grain. Three different bands, mm to cm wide, can be distinguished: a) spessartine with amphibole, b) tephroite, and c) piroxangite (Sanz Balagué, 1980).

The whole is cross-cut by irregular rhodonite veins. This mineral association was formed during prograde contact metamorphism of rocks initially formed by alternances of rhodocrosite levels, chert and clay. During retrograde metamorphism tephroite was replaced by friedelite or natronambulite. The result of these processes is a very hard rock with conchoidal fracture and ornamental value.

As accessory minerals, arsenides, nickel and cobalt sulfoarsenides (nickeline, skutterudite, gersdorffite), galena, sphalerite, chalcopryite, pyrite, chalcostibite, molibdenite, melonite, hesite, breithauptite, scheelite, apatite, monazite, geikelite and manganochromite grains (20-100 μm) occur disseminated. The primary mineralization indicates low S fugacity of the ore deposit forming fluids, but the nickeline being replaced by gersdorffite indicates a later sulfuration (Escusa and Melgarejo, 1998).

The geological context of the deposits and their mineralogy suggest that this volcanic stratiform deposit was formed under sea level, where there was very low oxygen content, and it was formed by a hydrothermal fluid (sedimentary-exhalative deposit or Sedex) (Melgarejo, 1987).

On the surface, under the effect of weathering agents, manganese silicates were oxidized into black manganese oxides with low hardness that were exploited. The change of altered rock to non-altered rock is gradual. The most important Mn mine is Serrana Mine, also known as Manganese Molar mine.

3.3.5 Olistostromic level in lydites with Mn mineralizations

Lydite and manganese levels from the Tournaisian base were reworked by submarine streams during the Visean age and later stages of the collapse of the turbiditic basin of the Priorat. Big lydite blocks slid down into deeper basin zones and resedimented with detrital sediments, forming olistostromic blocs. Therefore the mineralization is less continuous due to the fracturation resulting from this process. The mineralization does not present economic interest nowadays.

3.3.6 Massive Sulphide levels in Visean Series

In Priorat Region, massive sulphides have not been found in this series. However, fragments of massive sulphide mineralization have been found in the dumps of some very old mines that end up buried. The samples from the dumps are composed by pyrrhotite with low quantities of chalcopryite and sphalerite (Canet, 2001).

3.3.7 Dissemination in Visean series

Visean series contain some sulphide disseminations, generally consisting in galena, sphalerite and chalcopyrite in a matrix of sandstones and conglomerates. They occur together with fine grained calc-silicates (diopside, tremolite, prehnite, epidote, clinozoisite) that gives a greenish coloration to the rock. In the outcrop, these rocks are altered and present brownish to white decolorations depending on sulphides concentration. The mineralization appears forming metric lenses. The mineralization was initially proposed to be the result of the erosion of previous stratiform mineralizations (Melgarejo, 1987). However, it seems more likely that they were formed from the circulation of hydrothermal fluids through poorly consolidated sediments. The mineralization is not economically valuable to be exploited but it gives information of fluid circulation in a sedimentary basin.

3.3.8 Massive sulphides levels in Namurian Series

One gallery of lower mine in el Mas del Licort, Porrera, intersects one decimetric stratiform deposit of massive sulphides embedded in slates. Sulphides are fine grained and consist in pyrite, sphalerite, galena and chalcopyrite, with small quantities of hessite and tetradrite. It is thought that this body could extend to Cortiella Valley deposits (Jorge et al., 1994).

3.3.9 Disseminations in Namurian Series (Cu, Pb, Zn)

Namurian series contain sulphide disseminations located in Ulldemolins, Cornudella del Montsant, Torroja, Gratallops, Porrera and Bellmunt del Priorat. They are similar to Visean disseminations but located in slates where these mineralizations are fine grained (Melgarejo 1987).

3.3.10 Sulphide disseminations (Pb, Zn, Cu) in Westfalian series

There is only one example in Cornudella de Montsant, in an open pit located in Argentera. The outcrop is found within turbidites from Poboleda unit where the fine-grained sulphides occur in sandstones levels (Melgarejo 1987). They are rounded grains, which could indicate a detritic origin, but they could also be epigenetic as the result of fluid circulation through the sandstones.

3.4 Mineralization related to late-hercynian tectonic and magmatic activity.

In Priorat zone, metalogenic events related to folding are of little importance. This effect is only observed very locally. On the other hand, thermal metamorphism is more important: it is almost always present in those areas where stratiform deposits have been located, favouring the development of polygonal textures and increase of grain size. The grain size increasement eases the metallurgical treatment, making the deposit easier profit.

However the fluids associated to granitic intrusions are of much more importance, and can generate several types of deposits, some of them will be described next.

3.4.1 Skarns (Pb, Zn, Cu, W)

This mineralization is recognised in Bessó to Ulldemolins mines (Melgarejo and Ayora, 1994) and in several trial pits in Ulldemolins near to Molí del Pont and in Segalassos east zone (Canet and Melgarejo, 1997, 1998; Canet, 2001; Alfonso et al., 2012).

Bessó Mines

Bessó Mines represent the best example of this mineralization. It consists on a layer of 400m length with 2 m thick. This layer is embedded by carbonates, sandstones, conglomerates and slates. Mineralization is located in the inverted flank of a folded fold, so the ore is within a complex structure. Sulphide alteration presents secondary minerals like malachite, atzurite, serpentinite and greenockite. Outcrops are cut by riodacitic porphyric sills with magmatic breccia. This mineralization is interpreted as SEDEX tipology by some authors (Canet and Melgarejo, 1998; Canet, 1998; Alfonso et al., 1998, 1999; Canet, 2002). However, recent isotopic studies reinterpreted this mineralization as a skarn (Alfonso, 2012).

3.4.2 Cu seams within the batholites

Intrabatholytic seams are located at the top part of granitic bodies. They are small, with centimetric thickness and up to metric lateral continuity. It is frequent that the seams form net textures, which makes the exploitation of the mineralization not viable economically. In Flaset pluton, fine grained scheelite, chalcopryrite and bismut thelurides are found.

Peribatholytic seams are disposed near intrusions in host rocks and present higher dimensions than intrabatholytic seams. They appear in fractures with hercynian orogenic directions, which coincide with the same fractures that favoured the emplacement of granitic intrusive bodies.

There are two examples of this ore type in Priorat zone, one is Candida Mine, in Falset, and Barranc Fondo Mine, in Cornudella del Montsant (Melgarejo 1987). These mineralizations are related to hydrothermal fluids from granitic intrusions.

Candida Mine

Near Falset, Candida Mine is found. From this mine, chalcopryrite, galena, pyrite, tennantite, and Ni-Co arsenides were exploited in the past. Chalcopryrite is enriched by supergenic events becoming calcocite and bornite, and altered sometimes to malachite and atzurite. Tennantite is altered to conicalcite, and arsenide to eritrite and annabergite.

This mine has a vertical 40 m hole flooded. Several seams with decametric thickness are found in the road to Falset. These seams present chalcopryrite, pyrite and tennantite altered to conicalcite.

Barranc Fondo Mine (also called Núria Mine) in Cornudella de Montsant

The seam in the Barranc Fondo Mine has a NE-SW strike and a 70° SW dip. It is hosted in sericitic and chloritic altered Carboniferous metapelites.

The seam can be as wide as 1 or 2m, and basically consists in quartz with disseminated chalcopyrite. Pyrite can also be found in large quantities. Those minerals are common; their sizes vary from 500 µm to several centimeters. Other minerals, like sphalerite, galena, scheelite, cassiterite, stannite or molybdenite, are also present in this mineralization, but those are less common with smaller grain size.

3.5 Mineralizations related to the Alpine cycle

3.5.1 Pb-Zn-Ag Seams in the basement

This mineral typology is one of the most important typologies in Catalonia due to its historical exploitation and strong incidence in the economy of Catalonia. Most of the deposits of this typology are found between the villages of El Molar and Bellmunt del Priorat. The mineralization has an E–W strike within an area of 4km width and 6km long. The seams are hosted in a large variety of rocks: Cambrian rocks, Carboniferous turbidites (like in Eugenia Mine), and Hercynian porphyry dikes. Finally all the seams are cut by the Permian – Triassic discordance, as it can be seen in Linda Mariquita Mine, or near Eugenia Mine.

The seams have a vertical dip, with a lateral continuity that ranges from meters to hectometers. The width of the seams goes from a few millimeters to some decimeters. The seams generally present <75 m depth, but they can be found at depths of 600m. The classification of the seams has been based on the host rock, although some seams can cut different types of rock at the same time (Crespo and Michel, 1982; de Haller, 1997). The seams are classified as: a) net of Pb seams restricted to rhyodacitic porphyrys, b) Pb seams located in the fault planes within slates, c) Ag-rich seams, and d) seams found in mylonites. It has to be considered that two or more of these types of seams can be found in the same mine.

In this mine field, two big areas can be distinguished, one in the west of the Siurana Fault, and the other one in the east. In the western zone, the mineralization is mainly hosted in thick porphyrys. In the eastern zone, the seams are hosted either by slates or porphyrys. So according to that, the western part represents a deeper sector of the porphyric intrusions than the eastern zone. The first three types of seams (a, b and c) are synchronic, while the fourth type (d) is more recent.

The mineralogy of these seams is simple. Basically they are formed by galena and other accessory sulphides within a carbonate matrix (Coy-III and Font-Altaba, 1966a, 1966b; Coy-III and Font-Altaba, 1969; Mata and Montoriol, 1974; Mata, 1981, 1990).

(a) Pb-(Zn) seam network hosted in joints within rhyodacitic sills

This typology is especially developed in Bellmunt area. This typology is present in the next mines: Linda Mariquita, Raimunda and Jalapa mines from El Molar, and Blancardera, Espinòs, Règia Antiga and Règia mines from Bellmunt del Priorat. The thickness of the seams is usually of several centimeters, and its strike is NW–SE, perpendicular to the Hercynian rhyodacitic sills. Seams present adular-sericitic alteration, sometimes with silicification too.

Mineralized bodies present different kind of shapes. They can be inside subparallel joints, or in fault breccia. The contact between the host rock and the mineralized bodies is usually sharp. In the areas where

the mineralization is within joints, the mineralized bodies can reach widths up to 400m and they were exploited in the past (de Haller, 1997).

Sulphide mineralization of the seams mainly consists in galena, but also sphalerite, pyrite, marcasite and chalcopyrite. Seams porosity is filled by crystallization sequence of carbonates. The sequence of crystallizations is: ankerite-dolomite-calcite-siderite. Both, carbonates and sulphides tend to have idiomorphic morphologies. They also present druse porosity within the host rock. Idiomorphic crystals of quartz, dickite and barite have also been found in small quantities. These minerals were formed later than the main mineralogy.

These deposits were exploited with wells and tunnels at different levels. Many of these tunnels reached depth of hundreds of meters, but nowadays are inaccessible.

(b) Pb-(Zn)-(Ni) seams hosted in slates

The clearest example is present in Eugènia Mine, but they are also in other mines like Renània Mine, Grinyons Mine and La Ramona Mine. Unlike other mineralized seams, these ones are well-defined and concentrated in very long seamy zones, whose strike is NNW–SSE. The seams appear to be subparallel. In Eugènia Mine, seams are separated 5 to 20 m from each other and they are located above a fracture area of 400 m width, 2 km long and 600 m depth. They were exploited in the past.

Texturally, two types of mineralization have been defined. The first type is present within hydraulic breccia in fault zones. The second one fills the joints associated to these faults. Seams have adular-sericitic alteration. The dimensions and strike of the seams are variable.

In Eugènia Mine it is very particular the crystallization sequence of Ni sulphides associated with the galena crystallization. This sequence can only be observed in the most superficial parts of certain local areas. The sequence of crystallization starts with the formation of millerite, which is replaced by gerdorffite, tiospinel and chalcopyrite. Millerite has a capillary development, which was originally confused with pyrite (Tomás, 1920). Those millerite crystals are between the largest ever found in the world, and can be considered as first class museum pieces.

(c) Ag-Ni seams

This mineralization was very exploited during the Middle Ages as silver mines (Abella, 2001). The seams have small dimensions, generally about several tens of meters long and a few meters depth. Thickness is usually less than 10 cm. However, several parallel seam networks can be found in some locations, like in Balcoll Mine in the village of Falset. Texturally, seams present abundance of druse textures and collapse breccia.

The contact between the seams and metapelites – calc-silicated host rocks is generally altered to sericite and fine grain adularia. This could suggest that the alteration was produced by an alkaline fluid (Alfonso et al., 2002).

Seams filling sequence can be compared to the other sequences in Priorat. The sequence starts with the crystallization of idiomorphic and small (less than 1 mm) adularia and quartz crystals. It follows with the development of pink ankerite and zoned, white dolomite. These crystals measure between 3 mm and 1 cm. Their crystal faces are rounded, like the ones present in hydrothermal dolomites. Later, another generation of white dolomite is developed together with native silver. Native silver presents skeletal and dendritic shapes. In this stage, radial berthierite and nickelite can also crystallize.

A second seam filling stage produces the precipitation of calcite. In this stage, the Sulphur fugacity was much higher, causing the crystallization of many sulphides. Thus, native silver is replaced by acantite, and other sulphides, like pyrite, galena and sphalerite, between others, precipitate. Finally, in geodic cavities can crystallize other minerals, like silver sulfosalts (stannite, pyrargirite, xanthoconite) and a second generation of native silver (with filamentous textures), that can also be replaced again by acantite.

(d) Breccia veins

They are found in fractures which can be regional scale faults, with well developed fault-breccias. The faults present a prevailing direction N030, which could be both associated with the hercynian and alpine faults direction.

The veins present an intense alteration of their host rock, especially an important silicification with seritization and sometimes chloritization. The filling is constituted by irregular fragments of the host rock (Palaeozoic porphyries or metasediments), generally strongly milonitized and altered, cemented by carbonated gangue or, more rarely, silicic (belonging to a later stage than the previous) with galena, sphalerite and pyrite disseminations. Due to this feature, these veins can be differentiated from others by the absence of drussic growth and for presenting even more altered vein boxes. Another distinctive feature of these mineralizations is the appearance of galena mineralization: the galena has undergone milonization phenomena, and often is very fine-grained with matt lustre (matt veins). Finally, another distinctive aspect is the presence of a vertical zonation: the deepest levels tend to be enriched in sphalerite. Sphalerite crystals grew up to some mm in size within geodic cavities together with quartz.

In the case of the Mineralogia Mine, the hydrothermal alteration superimposes to an intense supergene alteration that produces the development of important quantities of carbonates and lead sulphates (cerussite and anglesite) which once were considered as possible Pb ores during the previous mine exploitation period.

The Montse Mine is located in a fracture zone, and presents veins similar to those for the Mineralogia Mine but with larger amounts of sphalerite, which would indicate a deeper origin. Other mineralizations comparable to those from the Mineralogia Mine are found in numerous locations in the Priorat, outside the Mining Basin. It would take long to detail the characteristics of dozens of mines located at the Priorat. We will only mention the most remarkable characteristics.

The Cornudella Mines, the most important outside the Bellmunt-El Molar zone, are found to the East of the town. They consist of subvertical veins, with mostly silicic gangue, and bearing scarce amount of

galena and sphalerite. Above them, several mines were opened, probably during the Middle Ages. However, their development is referred to the twenties, giving place to the Mercedes, San Fernando, Santa Bàrbara Anita and Teresina concessions (Havre, 1920; Fonrodona, 1926). Through systems involving shafts and galleries, at the Mercedes Mine a vein up to 1 m wide was exploited. The Ag content in the veins was very variable, between 170 ppm up to 280 ppm. At the Anita Mine there was a shaft and gallery system too. This one followed a vein up to 80 cm wide and with an extension of 700 m following a NW–SE direction. The Ag grade was of 190 ppm approximately. No vein data is known from the Santa Bàrbara and San Fernando mines, though in Santa Bàrbara a known iron vein should be pointed out as it could consist of the superficial expression. Finally, the Teresina Mine is the only one which was located to the west of the town. Galena was found in the shape of big isolated crystals in it.

The Porrera exploitations were located in two different areas; at the Mas de Licort zone and at the south of the town. At the Licort Mines, a series of labours in shafts and galleries were carried out on veins with NW–SE direction. The veins are found in strongly silicified fracture zones and the mineralization is poor. It comprises galena and sphalerite disseminations. Sometimes, this silicification replaces a previous mineralization consisting of calcite with sulphur disseminations. Galleries were made over diverse veins. Some galleries belonging to the area are over various hundreds of meters long and diverse counterweights, getting to run through the ridge (Muñoz and García-Lomas, 1913). However, most of them are up to only few dozen metres long. Some galleries cut decimetric stratiform Pb-Zn mineralizations interspersed with shales.

The mine located at the south of the Porrera town is associated with a large fracture: the Marçà-Porrera fault. This fault has produced diverse mineralizations throughout its trail, all of them of little importance; such as the one located at the South of the Porrera town. In this case, a shaft was carried out, from where galena associated to calcite was extracted. However, on other spots intense silicification of the host-rock was produced, like at the quartz vein belonging to the chapel zone near the town. It should be stressed that this fracture system is mineralized with fluorite, though these veins seem to be posterior. This would bear witness to hydrothermal processes linked to the alpine movement of these faults.

The lead mines of the Pradell consist too of an example of small veins associated to silification processes of the host-rock. Entrenchment was practiced.

In Torroja, exploitations by means shaft system over silicified zones bearing galena were located too. The mines are very ancient, and probably argent was searched within them. The same can be applied to the shafts belonging to the Escaladei and the Pobleda zone.

The age of the Pb veins

The age of the Regia and Eugènia type veins could be approximated using textural information. They cut Permian porphyries and they never have been registered in the upper Permian discordance. Therefore, their age should be delimited between the beginnings of the Permian and the late stages of the Permian, confirming that

they are Permian in age. However, recent completed dating with Ar/Ar from the Adularias of the Ballcoll Mine result in Jurassic age, allowing them to be associated with the rest of vein type deposits in the area.

The age of the Mineralogia type veins reveals to be more doubtful because the fractures found could correspond to those that have their movement during the compressive stages of the alpine cycle.

Formation Model of the lead veins

The spatial relationship of the majority of these evidences with pre-concentrations in the carboniferous or precarboniferous series suggests a genetic mechanism based on the remobilization of the pre-concentrations at the basement by means of the circulation of hydrothermal fluids throughout late hercynian fractures. However, some Pb analyses of galenas (Canals and Cardellach, 1994, 1995, 1997; Llinares, 1997) indicated a lixiviation of Pb from the late hercynian granitoids, and possibly from the metasediments, though in less proportion.

In the case of the Eugènia Mine, modelization of the ore-forming fluids of the deposit was performed (Canals and Cardellach, 1990; Cardellach et al., 1990). According to the stable isotopic data of both fluid inclusions and mineral associations, the authors conclude that the fluids were saline (15% NaCl eq), moderately acids (pH 5-6.2), with an oxygen fugacity between 10-50.5 and 10-48.5, $\delta^{13}\text{CO}_2 = -8.1\text{‰}$, $\delta^{18}\text{O}_{\text{H}_2\text{O}} = 3\text{‰}$, $\delta^{34}\text{S} = 1\text{‰}$, and of low temperature (around 150°C). According to Cardellach et al. (1990) these type of solutions suggest that the fluids were not magmatic, but with a meteoric origin. The mineral precipitation is explained by the changes in pH in the solutions and by slight fallings regarding the fluid temperature.

3.5.2 Barite veins

The deposits of this typology were exploited at small or large scale. They consist of veins, which cut through both the basement (the granites or the Palaeozoic metasedimentary rocks) and the Triassic covering (Font et al., 1985). This category includes a great number of veins with kilometric order lateral continuity, hectometric order depth and with a thickness up to two meters. In close proximity to these veins, poor developed hydrothermal alterations can be observed, such as chloritization or seritization. The veins are located in fractures, clearly of alpine origin (though with an initial late hercynian activity) with to N030 and N110 directions.

The main mineral is barite, typically white to pink in colour, which usually presents itself in the shape of tabular crystals and often in geodic cavities. Locally, the minerals present in the vein can be milonitized as the result of the reactivation of the fracture they filled. Variable amounts of galena, pyrite, chalcopyrite, tennantite and Ni-Co arsenides are common, though mostly as accessory minerals.

In the Priorat, the barite veins are less important than in the neighbouring regions. Nevertheless, many of them were exploited in several mines. These veins never produced great tonnages, plus the active period of these mines was always very short. The most important mine was Atrevida Mine, located at Vimbodí (Barberà Basin).

When coming down to establishing a genetic model for these concentrations it has to be taken into account, on a first place, an irrefutable fact: the veins cut through the Mesozoic series and therefore cannot be linked

either to the granites or to the late hercynian tectonic. The model that has been proposed to explain the formation of these veins suggests that the precipitation of barite could be the result of the mixture of two solutions. One of them; superficial, would provide sulphate anions whilst the other, coming from deep conductive cells, would be a possible metal and Ba supplier. Canals (1989) provides data regarding the isotopic relationships (for S) which work with this mechanism. As regards to the metal source, it has to be taken into account that Ba substitutes potassium in the structure of many minerals, particularly in potassic feldspars and micas. These minerals are the components which make up the basement rocks. Canals and Cardellach (1991, 1993), basing on the isotopic analysis of Sr found barite, concluded that the Ba source of the ensemble of mineralizations of the Catalan Coastal Ranges partly comes from the lixiviation of the basement rocks and partly from the Triassic to Jurassic evaporites of marine origin. Regarding the metal source, it should be remembered that both barium and lead substitute potassium in the structure of many minerals, such as micas (constituents of Palaeozoic rocks) and feldspars (in granitoids). Thus, it is easy to imagine that a fluid circulating in depth through the basement rocks, when equilibrating itself with these can be loaded with these metals. Canals and Cardellach (1994, 1995, 1997) have provided isotopic data of Pb that is in agreement with this mechanism.

3.5.3 Baritic cement in Buntsandstein sandstones and conglomerates

When finding themselves near the Ba mineralized veins, the Buntsandstein facies presents a scarce proportion of oxidized iron cement, which translates in the absence of the typical reddish colour of the sediment. On the other hand, they present abundant barite cement. This cement is usually microcrystalline, though in some cases the barite crystals grow up to have millimetric dimensions, like in the conglomeratic outcrop found in the roadway from Reus to Móra (specifically in the intersection with Guiaments) or in the Trias cement near Linda Mariquita mine. This cement has been also observed around the Catalànides, in the proximities to other barite veins. Due to this cause, it can be interpreted as the result of the circulation of the same ore-forming fluids belonging to the vein structures through the permeable host-rock. Either of these mineralizations have economic interest. On the other hand, it is important that their existence in an outcrop can be used as exploration criteria for other new barite veins in the surroundings.

3.5.4 Pb-Zn disseminations in the lower Muschelkalk

The laminated dolomitic levels belonging to the Brull unit, located at the base of the lower Muschelkalk, can contain galena and sphalerite disseminations. These minerals occur as millimetric size grains, scattered throughout the rock porosity. Andreu (1986) and Andreu et al. (1987) describe and example in Siurana. These signs have never been exploited, but are important as they reflex that the diagenetic fluids could have developed a metalogenetic role during the Mesozoic.

3.5.5 Fluorite veins

In the Priorat, there are several mineralizations of fluorite veins. Although much less important than the fluorite veins of the Montseny-Guilleries area, we can mention the existence of two vetiform fields rich in fluorite: one in Ulldemolins and one in Porrera. Numerous mines have been exploited in both fields.

The Porrera vetiform field

The Vetiform field of Porrera is constituted by a set of veins direction NE–SW. The main signs are located directly on a fault zone corresponding to a regional accident, the Marçà-Porrera-Cornudella fault, while other small mineralizations are located in several satellite faults of the main one, located in a strip that covers approximately 500 m away from the main fault. In the Porrera fault, a zone of hydrothermal alteration of the host rock product of intense silicification and sericitization is identified. In some places, like the hermitage of San Antonio, in addition to the silicification you can see quartz veins that constitute an element of landscape.

Mineralization in the host rock area is different: black shales of the Upper Devonian and Carboniferous, lidites (banded siliceous rocks, cherts), greywacke and shales. Veins are more potent when fractures cut rocks of more fragile behavior, such as lidites and greywacke. The most important veins are located on the fault of Porrera. The length of the mineralized zone is quite extensive, with a minimum length of 500 m and up to 50 m in the vertical. The continuity of this vein can reach 50 m if one takes into account the difference between the main gallery next to the river and several holes located on the ridge. The width of the veins is very variable, but they can become metric.

The filling of the veins is very complex; much silicified hydraulic breccias are seen. The growth of the mineralization in the generated porosity is of geode type. The sequence begins with the crystallization of quartz with comb growths, which cover the fracture surfaces and the breeched fragments. There follows a crystallization of calcite which in many cases becomes fluorite. This is evidenced by the presence of cubic crystals of fluorite overgrown in the remains of crystals of dissolved calcite. Fluorite is generally yellow honey, but also white, pink and violet. In association with fluorite, there are small amounts of sulphides (galena, sphalerite and pyrite) that form grains of millimetric to centimetric size dispersed in fluorite. Finally, where there is geode-like porosity, one can see the precipitation of a very late generation of barite crystals. This barite forms book growths on fluorite.

The Ulldemolins vetiform field

It is the most important of the fields of fluorite of the Priorat. In it stands the Magdalena Mine, which was more intensely exploited. The field of veins is located to the north of Ulldemolins, in the right bank of the Montsant. They are veins of main direction ENE–WSW, embedded in turbidites and in late hercynian granitic porphyries that cross them. Similar to what happens in the Porrera field, there is an intensive silicification and sericitization of the host rocks. In addition, the broader mineralizations occur where faults cut the most fragile materials, such as porphyries, conglomerates and greywacke, while they tend to

disappear on the shales. The most important vein exploited in the Magdalena mine is on a direction fault. In the family of fractures and diaclasses of the main structure, there are many other veinlets, often millimeter to centimeter wide. The outcrops of these veins are numerous, and many of them were recognized from small trenches, usually of depth less than one meter. Altogether, these mineralizations help to see the trace of the mineralized zone and to be able to identify the zone of hydrothermal fluids circulation. For Porrera, this area extended to more than 500 m away from the main vein, so there may be other veins in the area.

On the main vein, there are several mining works in galleries, trenches and pits. This vein is located in porphyries, in which it produces an intense silicification and kaolinite and sericite alteration. The veins lose power and become sterilized when they fail through shales and turbidites sandstones of the Carboniferous. This is because during the deformation the porphyries have a more rigid behavior than the most plastic slates. Because of this, porphyry tends to exhibit more fracturing and breccias in fault zones, while shales form folds. Porphyry dykes are wide in this area (more than 30 m) and the vein cuts almost longitudinally, so good traps are formed that allow the mine to have significant reserves. The main vein was of great width, between 20 and 50 cm in the present outcroppings. The crystallization sequence is very similar to that described in Porrera. In this case, the fluorite becomes solid, with yellowish or violet colors. Sulfides (galena, sphalerite, chalcopyrite, pyrite, marcasite) are also common, and they are disseminated in fluorite. There is a gallery located to the NE, upstream of the Montsant, in which also explorations were made. At this point, the host rock corresponds to conglomerates intercalated with turbidites. Similar to what happens in the case of porphyries, this package acted as a more fragile medium than the finer sections, which formed many fractures and diaclasses, all mineralized. This is why it is possible to speak of a system of veins that come to have until 30 cm of thickness of solid fluorite and of crystalline aspect. As a whole, the veins have a width of 50 cm. In addition to the main vein located on faults in direction that have a little horizontal displacement, there are several mineralized stepped diaclasses. In these faults, it is common to observe an important porosity that is partially filled by large crystals, some of which have up to 4 cm.

3.5.6 Celestine Mineralization

Celestine mineralizations appear at transit levels between the roof of Muschelkalk Superior facies and Keuper facies, typically in gypsum sections or in levels yellowish dolomites with a stromatolitic appearance and finely laminated. The Celestine replaces dolomite or gypsum crystals. It is usually cryptocrystalline, but in some geodes, the crystals of Celestine come to have centimetric dimensions. These mineralizations that are found between Falset and Pradell de Teixeta were evidenced when extending the road from Reus to Falset, and especially the mount of Gallicant.

3.5.7 Muschelkalk Karstic Mineralizations

Muschelkalk facies have suffered several episodes of karstification, and in some cases, Manganese oxide mineralization has occurred in association with this process. In the area of La Bisbal de Falset and La Figuera

de Falset, there are small signs of manganese oxides (Mata, 1982). The deposits have very irregular shapes since they inherit the karstic morphology. They are chimneys and small veins of variable directions, formed on karstic ducts that follow the structures. They are very irregular bodies formed from the replacement of the limestone from the layers joints. For this reason, the continuity of the mineralized zones is very difficult to predict, and that makes it difficult to evaluate the reserves. If this negative circumstance adds these bodies are always of very small dimensions (often of metrical order), it is understood that these circumstances hinder their exploitation, although in some cases small mining works were developed (Nolla et al., 1902). Several wells and trenches were made, almost all in reconnaissance work, and never entered the exploitation phase. Similar, much more important mines were in the vicinity of Aleixar (Andújar and Melgarejo, 2001). Minerals fillers are manganese oxides (pyrolusite and todorokite) that present in masses of botryoidal aspect.

References

- ABELLA, J. (2001): Bellmunt del Priorato. Historia, Geología y Mineralogía. *Bocamina***7**, 28-63.
- ABELLA, J. (2005): L'argent a la mina Ballcoll de Falset. *Mineralogistes de Catalunya***8(7)**, 6-22.
- ABELLA, J. (2008): Minerals i mines de la conca de Bellmunt del Priorat. Grup Mineralògic Català, Fons Mineralògic de Catalunya, 128 pp.
- ALFONSO, P., CANET, C., MELGAREJO, J.C., FALLICK, A. (1998): Composición isotópica del S de depósitos de edad Silúrica tipo sedex de las Montañas de Prades. 18 Reunión de la SEM, 150. Bilbo.
- ALFONSO, P., CANET, C., J.C. MELGAREJO, J.C., FALLICK, A., ELLAM, R. (1999): Isotope study of the Carboniferous sediment-hosted sulphide deposits from the Southern Catalan Coastal Ranges (Spain). In Stanley et al. (Eds.): *Mineral Deposits: Processes to processing*. Balkema, Rotterdam. vol. 2, 805-808. Rotterdam, Holanda.
- ALFONSO, P., GIMÉNEZ, F.X., CANET, C., J.C. MELGAREJO, J.C., ABELLA, J., FALLICK, A., ELLAM, R. (2002): Filones de plata de la mina Ballcoll, Priorato, Tarragona: mineralogía e isótopos estables. *Bol. Soc. Española Mineralogía***25a**: 1-2.
- ALFONSO, P., CANET, C., MELGAREJO, J.C., MATA-PERELLÓ, J.M., FALLICK, A. (2012): Stable isotope geochemistry of the Ulldemolins Pb-Zn-Cu deposit (SW Catalan Coastal Ranges, Spain). *Geologica Acta*, 10(2), 145-157.
- AMIGÓ, R., ESPASA, J.B. (1990): Noms actuals i pretèrits del terme antic de Cornudella de Montsant. Edicions Rosa de Reus, Reus. Col·lecció Biblioteca d'Autors Reusencs i d'obres d'interés local. Associació d'Estudis Reusencs . Publicació N° 77, 468 pp.
- ANDREU, A. (1986): *Las mineralizaciones de Pb-Zn-Ba en el Muschelkalk Inferior de los Catalánides*. Tesis de Llicenciatura inèdita. Universitat de Barcelona. 101 pp.
- ANDREU, A., CALVET, F., FONT CISTERÓ, X., VILADEVALL, M. (1987): Las mineralizaciones de Pb-Zn-Ba en el Muschelkalk inferior de los Catalánides. *Cuadernos de Geología Ibérica* **11**: 779-795.
- ANDÚJAR, J., MELGAREJO, J.C. (2001). Las mineralizaciones de manganeso de L'Aleixar comarca del Baix Camp (Tarragona). *Bol. Soc. Esp. Mineral.* **24-A**: 145-146.

- AYORA, C., SOLER, A., MELGAREJO, J.C. (1990): The hercynian ore deposits from the Catalanian Coastal Ranges. *Acta Geol. Hisp.* **25**, 1/2: 65-74.
- BIETE, V. (1991): Cabacés, un poble al peu del Montsant. Cabacés, 482 pp.
- BUATIER, D., TRAVÉ, A., LABAUME, P., POTDEVIN, J.L. (1997): Dickite related to fluid-sediment interaction and deformation in Pyrenean thrust fault zones. *European Journal of Mineralogy* **9**: 875-888.
- CANALS, A. (1989): *Contribució a la gènesi dels filons de baixa temperatura dels Catalànids*. Tesi doctoral. Inèdit. Universitat de Barcelona. 268 pp.
- CANALS, A., CARDELLACH, E. (1990): The Eugenia mine (Pb-Zn-Ag), Bellmunt del Priorat, (Tarragona, Spain): Fluid geochemistry and mechanisms of formation. *Bol. Soc. Esp. Mineral.* **13**: 195-208.
- CANALS, A., CARDELLACH, E. (1991): Geoquímica isotòpica del S y del Sr en las mineralizaciones filonianas de Ba-F de los Catalánides. *Bol. Soc. Esp. Min.* **14**/1: 76-77.
- CANALS, A., CARDELLACH, E. (1993): Strontium and sulphur isotope geochemistry of the low temperature barite-fluorite veins of the Catalanian Coastal Ranges (NE Spain): a fluid mixing model and age constraints. *Chem. Geol. (Isotop. Geosc.)* **104**: 269-280.
- CANALS, A., CARDELLACH, E. (1994): Composición isotópica del plomo y del azufre en galenas de los filones de baja temperatura de las Cadenas Costeras Catalanas. *Bol. Soc. Esp. Min.* **17**/1: 200-201.
- CANALS, A., CARDELLACH, E. (1995): Lead and sulphur isotopes in galenas from the low-temperature veins of the Catalanian Coastal Ranges, Spain): metalogenetical implications. A: Pašava, J., Kíibek, B., ěak, K. (eds.): Mineral deposits: from their origin to their environmental impacts. Balkema, Rotterdam: 35-38.
- CANALS, A., CARDELLACH, E. (1997): Ore lead and sulphur isotope pattern from the low-temperature veins of the Catalanian Coastal Ranges (NE Spain). *Mineral. Deposita* **32**: 243-249
- CANET, C. (2001): *Dipòsits sedimentàrio-exhalatius del Paleozoic del SW dels Catalànides: model de dipòsit*. Tesi doctoral inèdita. Departament de Cristal·lografia, Mineralogia i Dipòsits Minerals. Universitat de Barcelona. 442 pp.
- CANET, C., MELGAREJO, J.C. (1997): Los depósitos de tipo sedex de Ulldemolins. XVII Reunión Sociedad Española de Mineralogía. Almagro.
- CANET, C., MELGAREJO, J.C. (1998): Contrasting mineralogy of Silurian and Carboniferous sedex deposits, SW Catalonia. *Abstracts 17th General Meeting IMA, Toronto, Canada*, A121.
- CANET, C.; ALFONSO, P.; MELGAREJO, J.C.; FALICK, A.E. (1998): Composición isotópica del azufre de los sulfuros de depósitos carboníferos tipo sedex del Priorato (SO de Cataluña). *Boletín de la Sociedad Española de Mineralogía*. **21**(A): 56-57.
- CARDELLACH, E., CANALS, A., TRITLLA, J. (1990): Late and post-hercynian low temperature veins in the Catalanian Coastal Ranges. *Acta Geol. Hisp.* **25**, 1/2: 75-82.
- COY YLL, R. (1964): Mineralogía y génesis del yacimiento de galena de Bellmunt de Ciurana (Tarragona). Tesi doctoral. Departament de Cristal·lografia, Mineralogia i Dipòsits Minerals. Universitat de Barcelona. Vol.I: 179 pp.; Vol.II: 139 pp.

- CRESPO, J.L., MICHEL, B. (1980): Estudio Geológico de los yacimientos minerales del Macizo Catalán entre Bellmunt de Ciurana y Mola, Priorato (Tarragona). *Studia Geologica Salmanticensia***16**: 123-149.
- ESCUSA, A., MELGAREJO, J.C. (1998): Mineralogy of the El Molar Metamorphized deposit of Mn, Catalonia. *Abstracts 17th IMA International Meeting, Toronto*.A-124.
- FONRODONA, F. (1926): *Traduction de la mémoire sur les mines «Mercedes», «San Fernando», «Santa Bárbara», «Anita» et «Teresina» situées à Cornudella & Ciurana (Priorato-Province de Tarragona)*. Informe inèdit. 7 pp.
- FONT, X., ANDREU, A., VILADEVALL, M., MELGAREJO, J.C. (1985): Metalogenia del Triásico de los Catalánides. II Coloquio de Estratigrafía y Paleogeografía del Pérmico-Trías.
- GIL, P. (1600): *Libre primer de la historia Cathalana en lo qual se tracta de Historia o descripció natural, ço es de casos naturals de Cathaluña*. Manuscrit al Seminari Conciliar de Barcelona. Transcrit per J. Iglésies (1949). Quaderns de Geografia. Barcelona, 194-225. També a J. Iglésies i Fort (2002): Pere Gil i la seva geografia de Catalunya. Institut d'Estudis Catalans, 329 pp.
- DE HALLER, A. (1997): *Le complexe filonien à Pb (\pm Zn \pm Ag \pm Ba \pm Cu \pm Ni \pm Co \pm Fe) de Bellmunt del Priorat (Tarragona, Espagne). Cartographie, minéralogie, pétrographie magmatique, lithogéochimie, altérations, typologie filonienne, séquences paragénetiques et textures intrafiloniennes*. Diplôme Sciences de la Terre. Univ. Genève, 135 pp.
- HÀVRE, H. (1920): *Rapport sur les mines de plomb d'Alforja et Cornudella*. Informe inèdit. 10 pp.
- ITGE (1994): Mapa metalogenético de España 1:200.000. Hoja 42 (Tarragona). Colección mapas metalogenéticos Instituto Tecnológico y Geominero de España (ITGE) 42(9/5). Madrid.
- JORGE, S., MELGAREJO, J.C., AYORA, C. (1994): Las mineralizaciones sedimentario-exhalativas carboníferas del Mas del Mestre, Alforja, Cataluña: zonación, estructura y mineralogía. *Boletín de la Sociedad Española de Mineralogía*. **17**, **1**: 172-173.
- LLINARES, L. (1997): *Le complexe filonien à Pb (\pm Zn \pm Ag \pm Ba \pm Cu \pm Ni \pm Co \pm Fe) de Bellmunt del Priorat (Tarragona, Espagne). Cartographie, approche structurale, inclusions fluides, caractérisation isotopique (C, O, S, Pb) et géochronologie*. Diplôme Ingénieur Geologue. Univ. Genève, 135 pp.
- MATA, J.M. (1982): Breus apunts sobre les mineralitzacions de reompliment de bossades càrstiques - situades a Catalunya. *Acta Grup Autònom de Manresa, Inst. Cat. Hist. Nat.* **2**: 31-37.
- MELGAREJO, J.C. (1987): *Estudi geològic i metal·logenètic del Paleozoic del Sud de les Serralades Costaneres Catalanes*. Tesis doctoral inèdita. Departament de Cristal·lografia, Mineralogia i Dipòsits Minerals. Universitat de Barcelona. 615 p.
- MELGAREJO, J.C. (1993): Estudio geológico y metalogenético del Paleozoico del sector sur de las Cordilleras Costeras Catalanas. *Col. Monografías ITGE* **103**: 1-605.
- MELGAREJO, J.C., AYORA, C. (1988): Mineralizaciones SEDEX de Mn en tramos basales de la serie carbonífera del Priorat-Serra de Miramar (Cataluña). *Boletín de la Sociedad Española de Mineralogía*, **11**(2):157-158.

- MELGAREJO, J.C., AYORA, C. (1989): Mineralizaciones sedex de manganeso en tramos basales de la serie carbonífera del Priorato-Sierra de Miramar (Cataluña). *Bol. Geol. y Min.* **103**: 544-550.
- MELGAREJO, J.C., MARTÍ, J. (1989): El vulcanisme bàsic del Carbonífer inferior de la serra de Miramar. *Acta Geol. Hisp.* **24,2**: 131-138.
- MELGAREJO, J.C., AYORA, C. (1990): Escapolita en metasedimentos precarboníferos del Priorato (Cataluña). *Boletín de la Sociedad Española de Mineralogía***13**: 43-49.
- MELGAREJO, J.C., AYORA, C. (1992): Mineralizaciones sedex de manganeso en tramos basales de la serie carbonífera del Priorato-Sierra de Miramar (Cataluña). *Boletín Geológico y Minero*,**103(3)**: 544-550.
- MUÑOZ Y GARCÍA-LOMAS, E. (1913): *Mines du Coto Mestres*. Informe inèdit. 15 pp.
- NOLLA, J., BARTOLOMÉ, M., MIR, J. (1902): *Algunos apuntes sobre las minas de bióxido de manganeso - de la Figuera*. Separata. Propiedad de la Razón Social. La Figuera de Falset, 1-23.
- SANZ BALAGUER, J. (1980): Breu estudi òptic de la piroxmanguita del Molar (Tarragona). *Acta de la Institució Catalana d'Història Natural*. Grup Autònom de Manresa. p.60.
- TOMAS, LL. (1919-1920): Els minerals de Catalunya. *Treballs de la Institució Catalana d'Història Natural*. Institut d'Estudis Catalans.129-357

4. Gavà mineralizations: Phosphate mineralization types

Aleu Andreazini

Centro de Instrumentación Científica, Universidad de Granada

In the Gavà Neolithic Mining Complex (GNMC) have been determined two phosphate mineralization types: stratabound layers and late veinlets.

- The phosphate stratabound layers are interbedded with grey shales of the lower Llandovery (Lower Silurian). The following series (Fig. 4.1) were determined in the *L* mine of the GNMC:
 - (1) Alternating dm-thick layers of grey shales and cherts (generally slumped), up to 1.5 m thick in section.
 - (2) grey shales with occasional thinner chert layers, and minor mm-thick phosphate layers, up to 1 m thick.
 - (3) grey shales with large chert nodules (diameter up to 50 cm) and mm-thick phosphate layers, up to 1.5 m thick.
 - (4) shales with very scarce chert and phosphate layers, up to 2 m thick.
 - (5) alternations of cherts and shales with local thin apatite layers, up to 1.5 m thick.

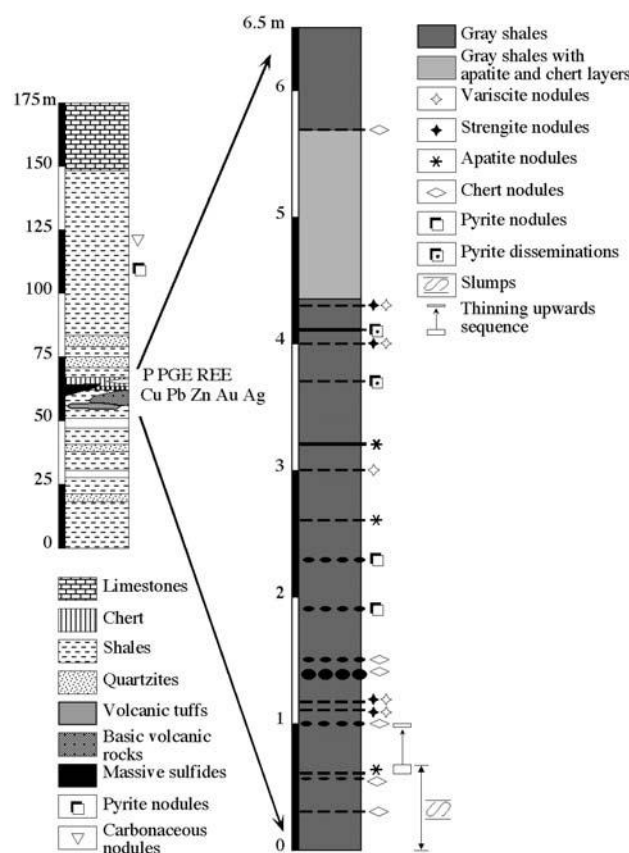


Figure 4.1. Detailed stratigraphic section of Silurian shales in the Gavà Neolithic Mining Complex (right), limited to the general stratigraphical section of the central part of the Catalan Coastal Ranges, or CCR (left). In the latter is indicated the position of the main elements that form significant deposits in the Catalan Coast Ranges. (Camprubí et al., 2003).

The phosphate layers observed in the *L* mine are stratabound, essentially monomineralic, very fine grained and between 1 mm and some cm-thick. They consist generally of apatite or variscite, although some layers are constituted by strengite or phosphosiderite.

In the *Can Tintorer* mine, the stratigraphic section has significant differences from the section described above, as the unit of grey shales with large chert nodules is overlain by a massive hematite layer (Fig.4.1), up to 1m thick, which is interlayered with brown shales. The latter becomes dominant upward. Thus, it is possible that the phosphate-rich section corresponds laterally to the iron oxide rich section. In addition, there are also thin nontronite layers interbedded within the shales. In the *Can Tintorer* mine, the phosphate-rich section is 50 cm thick and consists of strengite or phosphosiderite layers. It is overlain by a massive primary jarosite bed, up to 40 cm thick. The late veinlet mineralization is abundant in the study area. Although some veinlets in neighbouring areas show evidence of ductile deformation (some are clearly contemporaneous to schistosity and have the same mineralogy of post-schistosity mineralization). The dominant veinlet mineralization in the GNMC is undeformed and was produced long after the Hercynian deformation. The veinlets are generally monomineralic, and may contain Fe–Al–phosphates or Ca-phosphates as two different veinlet types and filled diaclasses with dominant N–S or NE–SW orientations. Some veinlets show features resembling hydraulic brecciation. These veinlets are usually 1 to 5 mm thick, up to 3 cm. The Fe–Al–phosphate veinlets are formed by variscite, strengite or phosphosiderite or, less commonly, turquoise. The electron probe microanalyses on the minerals of these veinlets (Camprubí et al., 1994) do not show significant chemical variations with respect to the same species found in the stratabound mineralization. The slight content of some trace elements (Cr, V) of phosphate minerals of this association may be due to leaching of host shales, which are relatively rich in these elements. The phosphate minerals of this association are frequently associated with jarosite and alunite. All these minerals are texturally microcrystalline and, locally, spherulitic due to a slight increase in crystal size, indicating some degree of recrystallization in the veinlets. Frequently, it was observed that this recrystallization progressed from tiny cracks in the mineralization or from the contact with host rocks.

In the *Can Badosa* mine, away from the area of GNMC, variscite was seldom found associated with quartz in veinlets. The Ca-phosphate veinlets are also found there and they were formed later. Montgomeryite ($\text{Ca}_4\text{MgAl}_4(\text{PO}_4)_6(\text{OH})_4 \cdot 12\text{H}_2\text{O}$) partially filled some fractures in the shales. These veinlets show irregular morphologies and orientations. Montgomeryite is displayed as micron-sized individual platy crystals, or as radial aggregates thereof, commonly directly implanted on the fracture gauge or on goethite film-like coatings. Crandallite ($\text{CaAl}_3(\text{PO}_4)_2(\text{OH})_5 \cdot \text{H}_2\text{O}$) is microcrystalline and is found in veinlets or replacing phosphates of the Fe–Al association. The latter occurred from tiny cracks in the Fe–Al phosphate veinlets or from the contact with host rocks.

4.1 Origin of phosphate mineralizations

The phosphate stratabound mineralizations are good guide beds for the bottom of the Silurian in the region. Appropriate conditions for the biochemical precipitation of phosphates appear to have been absent. Therefore, Camprubí et al., 2003 suggests a primary exhalative genesis of the primary phosphate deposits (apatite-rich layers), based on the following evidence:

1. The phosphate mineralizations are stratabound, hosted in submarine sediments, and prior to the Hercynian deformation.
2. The phosphate minerals are stratigraphically associated with levels with a mineralogy that can be interpreted as exhalative, with the formation of chert, hematite, nontronite and jarosite.
3. These deposits are associated with positive anomalies of V, Ba, Cu and rare earth elements.
4. These deposits are contemporaneous with basic alkaline volcanism (not present in the area, but located in other spots of the Catalanian Coastal Ranges), and with massive sulfide deposits hosting Zn–Cu–PGE mineralizations with interbedded apatite layers (Melgarejo et al., 1994, Alfonso et al., 2002). The close association of phosphate minerals with jarosite and hematite suggests that their deposition occurred from very acid and oxidizing fluids.

Subsequently, the apatite-rich layers would have been partially replaced by Al and Fe-phosphates after fluids of undetermined source, either hydrothermal or meteoric, that leached Fe and Al from host shales. Also, in the Silurian strata there are abundant levels with disseminated pyrite that could provide the necessary sulfate anionic groups to carry metals in solution. The close association of phosphate stratabound layers with barite-rich shales may be congruent with this explanation, as barite is not primary and may result from the fixing of sulfate derived from disseminated sulfides, and Ba released after weathering or hydrothermal alteration of Ba-rich muscovite, a widespread mineral in the series. The direct exhalative formation of Fe- and Al-phosphates may be a geochemical cause (Nriagu, 1972; Stumm & Morgan, 1981), but in this case, the possibility of a formation of the stratabound Fe- and Al-phosphate mineralization after replacement of apatite-rich layers is more plausible. The stratabound phosphate mineralizations can be, in turn, easily remobilized by any type of oxidizing solution, either hydrothermal or meteoric. As an analogous argument to explain the formation of phosphate-rich stratabound layers, the leaching of pyrite from the series would provide the acid and oxidizing solutions necessary to mobilize phosphorus from the series. The P-rich solutions would circulate through fractures or other pores, and deposit secondary phosphates, the composition of which depends on the composition of host rocks in the GNMC, triggered by faulting. Thus, Fe-Al phosphates form from Fe- and Al-rich rocks and the, eventually, turquoise may form from leaching of disseminated chalcopyrite. The association of phosphates with alunite or jarosite, and the composition of phosphates itself, provide evidence for the precipitation of phosphates in acidic and oxidizing environments. As in the *Can Badosa* mine some veinlets show variscite associated with quartz, it may be argued that at least part of this type of mineralization may have been originally hydrothermal. An alunite sample from late phosphate veinlets of the GNMC yielded a K–Ar age of 1.20 ± 0.05 Ma. Another alunite sample from phosphate veinlets with similar mineralogy and in the same

geological context from Montcada i Reixac (5 km N of Barcelona) yielded a K–Ar age of 1.33 ± 0.05 Ma. However, Al-phosphate and sulfate veinlets may also have been formed by recent or ancient meteoric phenomena. Dill et al. (1991) describe a similar deposit in Sudan, demonstrating that the veinlet mineralizations there are Quaternary in age and that have a meteoric origin.

References

- Camprubí, A., Costa, F. and Melgarejo, J.C., 1994, Mineralizaciones de fosfatos fèrrico-alumínicos de Gavà (Catalunya): tipología: Bol. Geol. Min., 105/5, 444-453 (in Spanish).
- Camprubí, A., Melgarejo, J. C., Proenza, J. A., Costa, F., Bosch, J., Estrada, A., ... & Andreiche, V. L. (2003). Mining and geological knowledge during the Neolithic: a geological study on the variscite mines at Gavà, Catalonia. *Episodes*, 26(4), 295-301.
- Dill, H.G., Busch, K. and Blum, N., 1991, Chemistry and origin of vein-like phosphate mineralization, Nuba Mountains (Sudan): Ore Geol. Rev., 6, 924.
- Melgarejo, J.C., Jorge, S., Taylor, R.P. and Jones, P., 1994, The occurrence of platinum group and Au-Ag-V-Cr-REE minerals in Lower Silurian sedimentary-exhalative (SEDEX) sulphide mineralization, Poblet, Catalonia, Spain: Abstracts of the 16th General Meeting, International Mineralogical Association, Pisa (Italy), 274.
- Nriagu, J.O., 1972, Stability of vivianite and ion-pair formation in the system $\text{Fe}_2(\text{PO}_4)_2\text{-H}_3\text{PO}_4\text{-H}_2\text{O}$: Geochim. Cosmochim. Acta, 36, 459-470.
- Stumm, W. and Morgan, J.J., 1981, Aquatic chemistry. 2nd edition: Wiley Interscience, 780 p.

5. Cardona salt diapir

Aleu Andreazini

Centro de Instrumentación Científica, Universidad de Granada

5.1 Geological setting

The Cardona salt diapir is located in the eastern sector of the Ebro Tertiary Basin, in the southern foreland basin of the Pyrenees (Fig. 5.1). The sediments that crop out in the area correspond to the marine Cardona Saline Formation, Upper Eocene in age and a series of Upper Eocene–Lower Oligocene detrital continental formations deposited after the Priabonian regression (Saéz and Riba, 1986). These formations are affected by fold structures with prevailing NE–SW and NW–SE trends (Fig. 5.1). The tectonic style shows the typical characteristics of folded strata overlying evaporites, with wide and flat-bottomed synclines and narrow anticlines related to the migration of salt from the adjacent synclines and controlled by thrust structures (Sans and Verges, 1995; Sans et al., 1996).

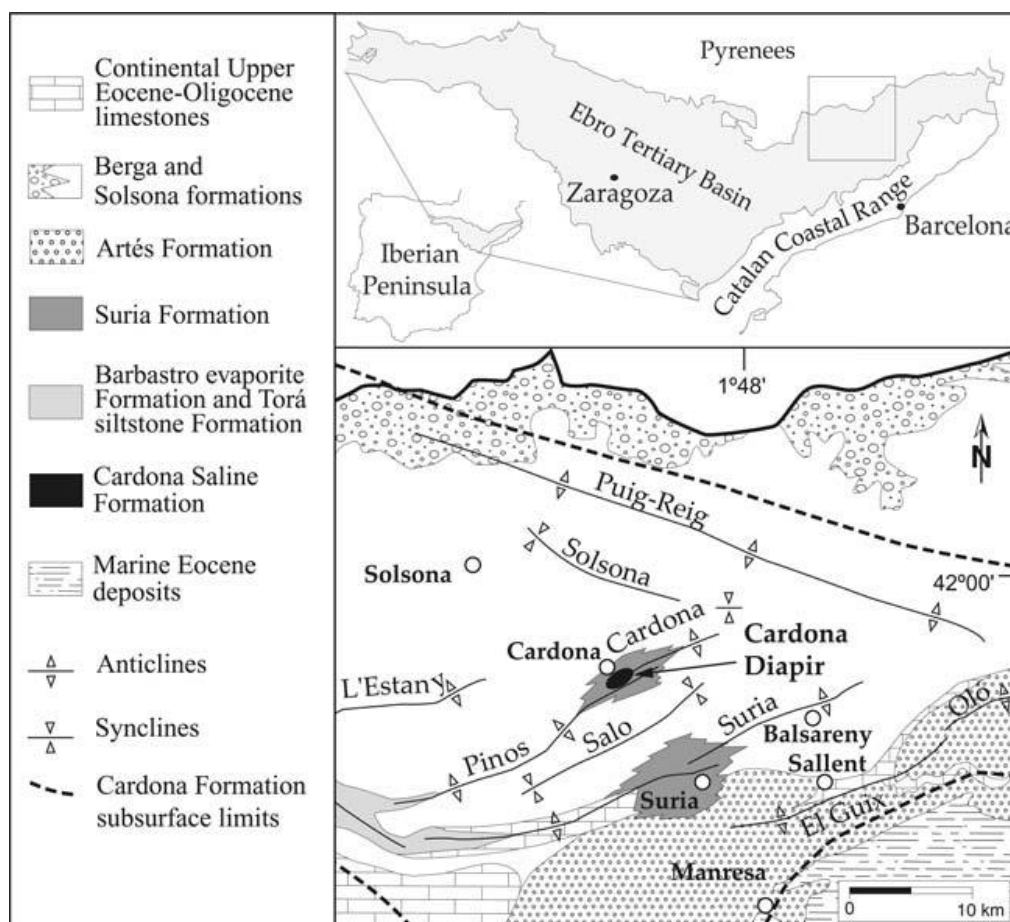


Figure 5.1. Geological setting of the Cardona salt diapir in the eastern sector of the Ebro Tertiary Basin.

From Lucha et al. 2007.

Seismic data indicate that the planar base of the Cardona Saline Formation dips gently to the north and lies at a depth of 1,500 m (1,000 m below sea level) under the Cardona Diapir (Riba et al., 1975; Esbarrany, 1997).

In the diapir, the Cardona Saline Formation is overlain by the Suria Sandstone Formation and the Solsona Formation, upper Priabonian-Lower Oligocene and Lower Oligocene in age, respectively (Fig. 5.2). The Suria Sandstone Formation, around 325 m thick in the Cardona Diapir area, is composed of two members (Saéz and Riba, 1986; Esborrany, 1997): (a) a lower member, 95–110 m thick, made up of alternating grey-bluish tabular sandstone layer and grey-green siltstone layers. The absence of outcrops of this member in the Cardona Diapir is attributed to the diapiric piercing of the Suria Formation by the Cardona Saline Formation (Fig. 5.2), and (b) the upper member is made up of a 250-m-thick alternation of reddish tabular sandstone layers and siltstone layers. The Solsona Formation, locally more than 1,000 m thick, is formed by an alternation of arkosic sandstones and yellow-reddish shales.

The Cardona salt diapir is located next to Cardona village in the hinge zone of a composite NE–SW trending detachment antiform formed by the Cardona and Pinos anticlines and the Intermediate Syncline (Fig. 5.1 and 5.2). The Cardona Anticline has its south-western termination around the Bofia Gran (Big Sinkhole) in the Cardona Diapir, and the Pinos Anticline has its northern termination to the east of the Cardona Diapir (Fig. 5.1). This asymmetric and south verging anticlinal structure has a gentle northern limb, a steep southern forelimb, and a maximum amplitude of 1 km (Sans and Koyi, 2001; Sans, 2003; Fig. 5.2). According to Sans (2003), the Cardona–Pinos Anticline developed where the Cardona Saline Formation reaches its greatest thickness and its basal slope is nearly horizontal. The syncline located between the Cardona–Pinos Anticline and the L’Estany Anticline to the north is welded with the subsalt strata, leaving each anticline as a closed salt system (Sans, 2003; Fig. 5.1). The strongly folded exposed salt body in Cardona can be described as a diapir (O’Brien 1968; Jackson and Talbot 1986) as it has pierced more than 300 m of overburden, showing a 2–6-m-thick melange of country rock and sheared salt at the contact with the sedimentary cover. According to Jackson and Talbot’s (1986) classification, the Cardona diapiric structure can be classified as a salt stock (salt plug, *salzstock*, *noyau de sel*). It has a 250–500-m-wide and 250-m-high stem, and a 60–80-m-high and 400–700-m-wide bulb (Sans, 2003; Fig. 5.2). The overburden in the crest of the Cardona–Pinos Anticline is about 400 m thick, whereas in the adjacent Solsona and Salo synclines it reaches 2,000 and 1,200 m in thickness, respectively (Sans and Koyi 2001; Sans 2003; Fig. 5.1).

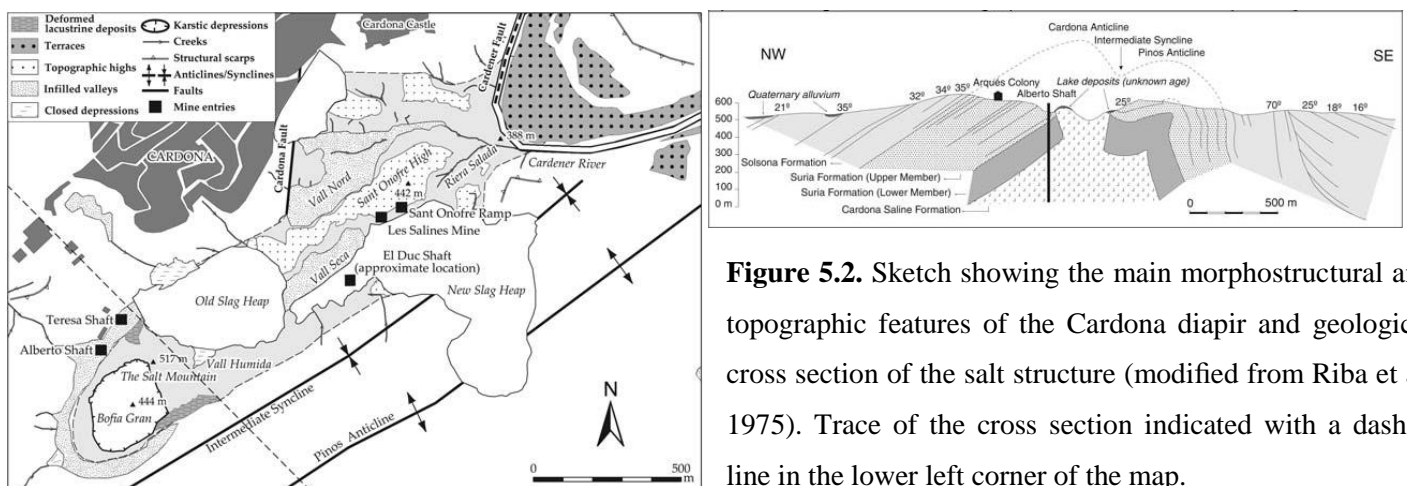


Figure 5.2. Sketch showing the main morphostructural and topographic features of the Cardona diapir and geological cross section of the salt structure (modified from Riba et al. 1975). Trace of the cross section indicated with a dashed line in the lower left corner of the map.

Folding during the Lower Oligocene caused the Cardona salt to flow and to accumulate in the Cardona–Pinos Anticlinecore from the adjacent synclines. Erosion in the crest of the growing anticline thinned the overburden above the salt, increasing the differential loading between the anticline and the synclines and aiding the salt to flow towards the Cardona–Pinos Anticline (Sans and Koyi 2001). In a subsequentstage, evaporites of the salt anticline started to pierce the overburden in the Cardona area. Physical analog models indicate that piercement of the Cardona Diapir occurred after 2.2 km of overburden was eroded from the crest of the Cardona–Pinos Anticline (Sans and Koyi, 2001). On and around the outcropping salts there is a 20–25-m-thick deformed, unconsolidated deposit made up of marls,sands and gravels that contain plant remnants, charophytes,gastropods and ostracods (Fig. 5.2). A poorly constrained Pliocene-Pleistocene age has been ascribed to these lacustrine sediments by Wagner et al. (1971). They show conspicuous drag folds with subvertical limbs at the diaper rim created by upward movement of the salt. The recent and present-day upward movement of the salt is evidenced by the existence of the salt outcrop (Riba et al. 1975) and geodetic measurements carried out between 1979 and 1986 that indicate an average rate of uplift of 1 mm/year (CardonaInternal Report in Sans 2003). The Roman writer Aulo Gelio reported in the second century about theCardona Diapir: *Quantum demas tantum acresc*, whichmeans, “the more it (salt) is mined the more it rises” (Cardona and Viver, 2002). The observation is probably the first written account of an active diapiric deformation everreported.

5.2 Mineralization

According to Pueyo (1975), the Cardona Saline Formation, which constitutes the Cardona salt diapir, from the bottom to the top is made up of: 5 m of anhydrite at the base, 200 m of massive halite (Lower Salt Member) and 50 m of halite and interbedded potassium chlorides (Upper Evaporitic Member). The tightly folded sediments exposed in the Cardona salt outcrop (Fig 5.3) correspond to the Upper Evaporitic Member, composed of three units: A lower unit bearing sylvite (KCl), whose top is at a depth of 600 m in the Cardona Diapir, an intermediate unit bearing carnalite ($\text{KClMgCl}_2 \cdot 6\text{H}_2\text{O}$) and an upper halite unit known as the “top salt”. The halite of the Upper Evaporitic Member forms layers with microcrystalline texture several centimetres thick separated by clay partings less than 1 cm thick. The sylvite, with micro-mesocrystalline texture, occurs in 10–30-cm-thick beds showing a red to brown colour due to hematite inclusions. The carnalite shows a microcrystalline texture with euhedral crystals (Esberrany, 1997).

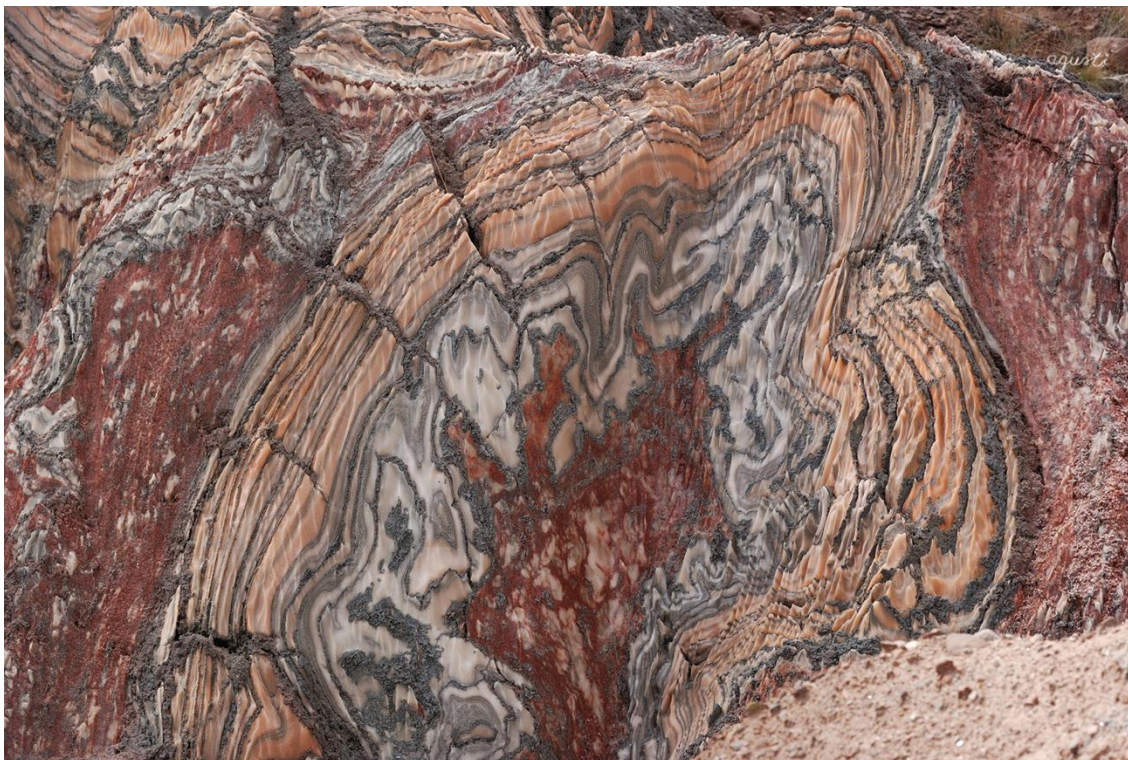


Figure 5.3. Interbedded and folded chlorides outcrop. Halite (white), sylvite (reddish and yellowish layers) and marls (greyish). From: *Fotografies de la naturalesa*.

References

- Cardona F., Viver J. (2002) Sota la sal de Cardona, p 128
- Esborrany (1997) Estudi de viabilitat d'un dipòsit subterrànic controlat de residus especials a l'antiga mina de sal de Cardona
- Jackson MPA., Talbot CJ. (1986) External shapes, strain rates, and dynamics of salt structures. *Geol Soc Am Bull* 97:305–323
- Lucha, P., Cardona, F., Gutiérrez, F., and Guerrero, J. (2008). Natural and human-induced dissolution and subsidence processes in the salt outcrop of the Cardona Diapir (NE Spain). *Environmental Geology*, 53(5), 1023-1035.
- O'Brien GD. (1968) Survey of diapirs and diapirism. In: Braunstein J, O'Brien GD (eds.) *Diapirism and diapirs*. AAPG, Tulsa, pp. 1–9
- Pueyo JJ. (1975) Estudio petrológico y geoquímico de los yacimientos potásicos de Cardona, Suria, Sallent (Barcelona, España), Doctoral thesis, Universitat de Barcelona, p. 351
- Riba O., Maldonado A., Ramírez J. (1975) Mapa Geológico de España, Scale 1:50.000, 2nd series, no. 330, Cardona, Madrid, Instituto Geológico y Minero de España, Servicio de Publicaciones del Ministerio de Industria, p. 58

- Saéz A., Riba O. (1986) Depósitos aluviales y lacustres paleógenos del margen catalán de la Cuenca del Ebro. In: Anadón P., Cabrera L. (eds.) Guía de las excursiones del XI Congreso Español de Sedimentología, Barcelona, pp. 1–29
- Sans M. (2003) From thrust tectonics to diapirism. The role of evaporites in the kinematic evolution of the eastern South Pyrenean front. *Geol Acta* 1(3):239–259
- Sans M., Koyi HA. (2001) Modelling the role of erosion in diapir development in contractional settings. In: Koyi HA, Mancktelow NS (eds.) *Tectonic modelling: a volume in honour of Hans Ramberg*: Boulder, Colorado, Geological Society of America memoir, vol. 193, pp. 111–122
- Sans M, Verges J (1995) Fold development related to contractional salt tectonics: Southeastern Pyrenean Thrust Front, Spain. In: Jackson MPA, Roberts DG, Snelson S. (eds.) *Salt tectonics: a global perspective*: AAPG Memoir 65, pp 369–378
- Sans M., Muñoz JA., Vergés J. (1996) Triangle zone and thrust wedge geometries related to evaporitic horizons (southern Pyrenees). *Bull. Can. Pet. Geol.* 44(2):375–384
- Wagner G., Mauthe F., Mensik H. (1971) Der Salzstock von Cardona in Nordostspanien. *Geol Rundschau* 60:970–996
- Fotografies de naturalesa, Geologia-formes a la natura. Consulta juliol 2017
URL: <http://agusti2.com/inici>

6. Field trip to the Western Pyrenees

J.C. Melgarejo¹, C. Villanova de Benavent¹, D. Domínguez¹

1. Departament de Cristal·lografia, Mineralogia i Dipòsits Minerals. Facultat de Geologia, Universitat de Barcelona

6.1 Catalonia Geological Units

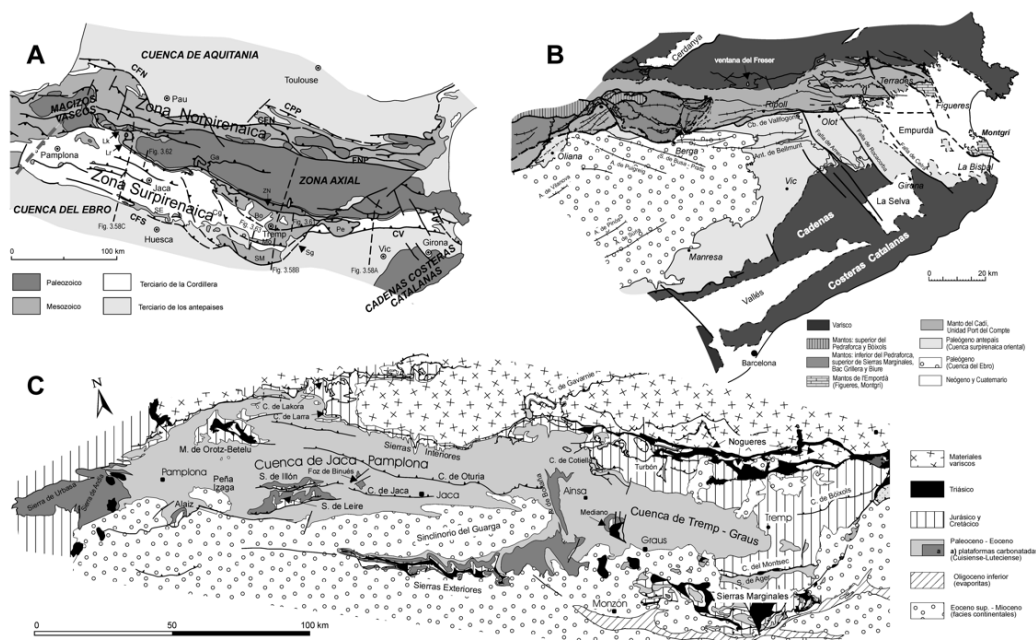


Figure 6.1. Geological maps of NW Iberian Peninsula (map adapted from Barnolas and Pujalte, 2004).

6.2 Eureka uranium mine

The Eureka mine is located near the Castell-Estaú town in the Pallars Jussà region (NW Catalonia). The mineralisation of the Eureka mine is located in Permian-Triassic, red, continental, detritic rocks. The mine was active in the 1950s (Arribas, 1966). Some galleries, open pits and mine dumps can be observed as a result of this activity from the mineral activity in the decade of 1950 (Figs 6.2, 6.3 and 6.4). The main minerals described in the Eureka mine can be found in Table 6.1.

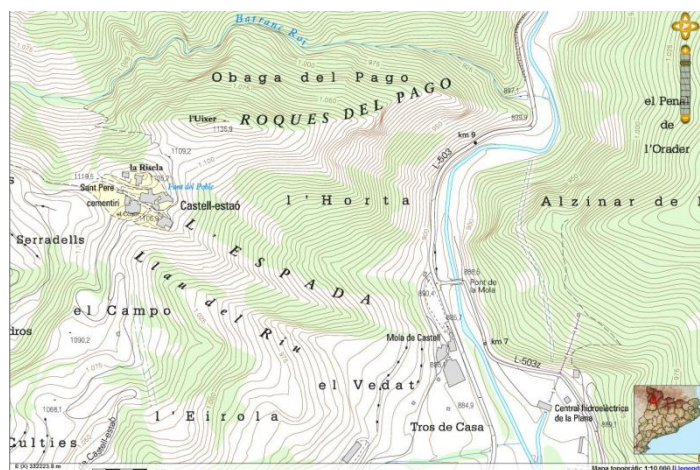


Figure 6.2. Topographic map of the Eureka mine (<http://www.icgc.cat>)



Figure 6.3. Google Earth image of Eureka mine (Google Earth ©)

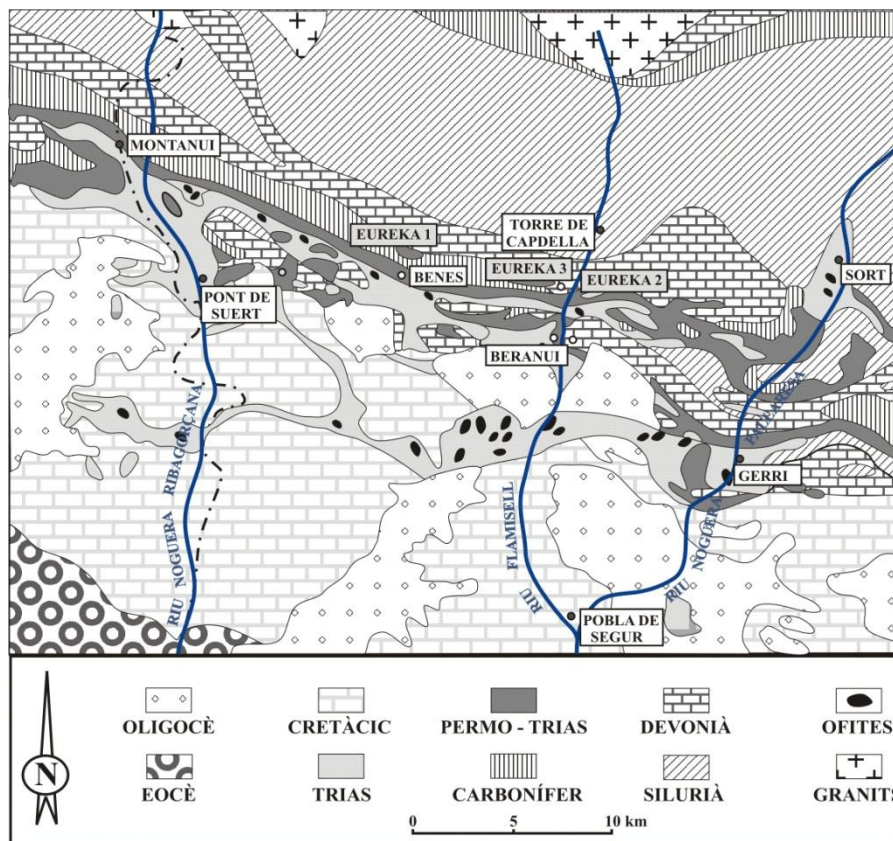


Figure 6.4. Geological map of the area surrounding the Eureka mine, showing three mining sites (Eureka 1, Eureka 2 and Eureka 3) (adapted from Almela i Ríos, 1947).

Table 6.1. Main mineral species in the Eureka mine (Castell-Estaó, Pallars Jussà).

Legend: AA: very abundant, A: abundant, C: common, R: rare, RR: very rare.

TEXTURE	MINERAL	FORMULA	%	Grain size
Disseminated	Bismuth	Bi	R	fine
	Chalcopyrite	FeCuS ₂	A	fine
	Chalcocite	Cu ₂ S	C	fine
	Covellite	CuS	C	fine
	Gersdorffite	(Ni,Co)AsS	R	fine
	Cobaltite	CoAsS	R	fine
	Aguilarite	Ag ₄ SeS	R	fine
	Tetrahedrite	(Cu,Fe) ₁₂ Sb ₄ S ₁₃	R	fine
	Galena	PbS	R	fine
	Bornite	Cu ₅ FeS ₄	C	fine
	Pyrite	FeS ₂	A	fine
	Coffinite	(USiO ₄) _{1-x} (OH) _{4x}	R	fine
	Roscoelite	K(V,Al,Mg) ₂ (AlSi ₃)O ₁₀ (OH) ₂	AA	medium
	Uraninite	(UO ₂)	C	fine
In veins	Carnotite	K(UO ₂) ₂ (V ₂ O ₈)·3H ₂ O	A	fine
	Zeunerite	Cu(UO ₂) ₂ (AsO ₄) ₂ ·10-16H ₂ O	R	fine
	Metatorbernite	Cu(UO ₂) ₂ (PO ₄) ₂ ·8H ₂ O	R	fine
	Johannite	Cu(UO ₂) ₂ (SO ₄) ₂ (OH) ₂ ·6H ₂ O	R	fine
	Volborthite	Cu ₃ (V ₂ O ₇)(OH) ₂ ·2H ₂ O	R	fine
	Antlerite	Cu ₃ (SO ₄)(OH) ₄	AA	fine
	Brochantite	Cu ₄ SO ₄ (OH) ₆	AA	fine
	Demesmaeckerite	Pb ₂ Cu ₅ (UO ₂) ₂ (SeO ₃) ₆ ·2H ₂ O	R	fine
	Calcite	CaCO ₃	C	fine
	Ankerite	CaFe(CO ₃) ₂	C	fine
	Quartz	SiO ₂	A	medium
	Baryte	BaSO ₄	R	fine
Efflorescences	Erythrite	Co(AsO ₄)·2H ₂ O	R	fine
Crusts	Posnjakite	Cu ₄ (SO ₄)(OH) ₆ ·H ₂ O	R	fine
	Atzurite	Cu ₃ (CO ₃) ₂ (OH) ₂	C	fine
	Malachite	Cu ₂ (CO ₃)(OH) ₂	RR	fine
	Brochantite	Cu ₄ SO ₄ (OH) ₆	A	fine

IMPORTANT: The visited outcrop is a protected site and therefore, the use of hammers is absolutely forbidden! Collection of samples is not recommended, taking into account the radioactive nature of these minerals.

6.3 Cierco lead and zinc mine

The Cierco mines are located in the Ribagorça region, in Aragón. The Cierco mines consist of Zn-Pb mineralizations which were exploited from early 20th century until the 1980s. The ore mined was sphalerite and galena, and was extracted from a complex set of galleries located at different height (Cudgy, 1977; Castroviejo and Moreno, 1983; Johnson et al., 1993, 1996). Some buildings of the former mine can be observed. The mineralisation is hosted in a skarn, and many minerals, all typical of skarns, are common in the mine dumps (Figs 6.5, 6.6 and 6.7). The main minerals described in the El Cierco mine can be found in Table 6.2.

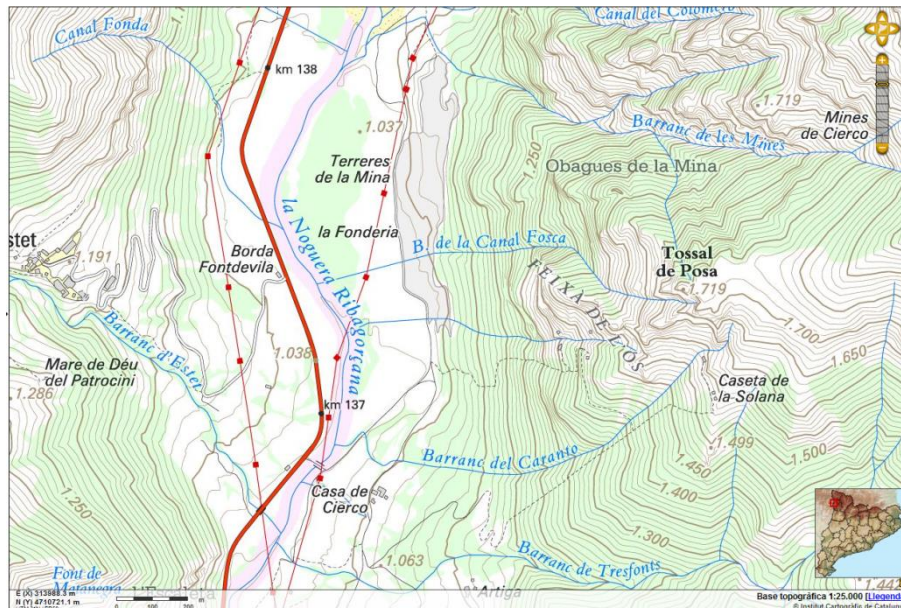


Figure 6.5. Topographic map showing the Cierco Mine. Adapted from ICGC - Catalan Cartographic and Geologic Institute Topographic Map, (<http://www.icgc.cat>)



Figure 6.6. Google Earth image of the Cierco mine (Google Earth ©)

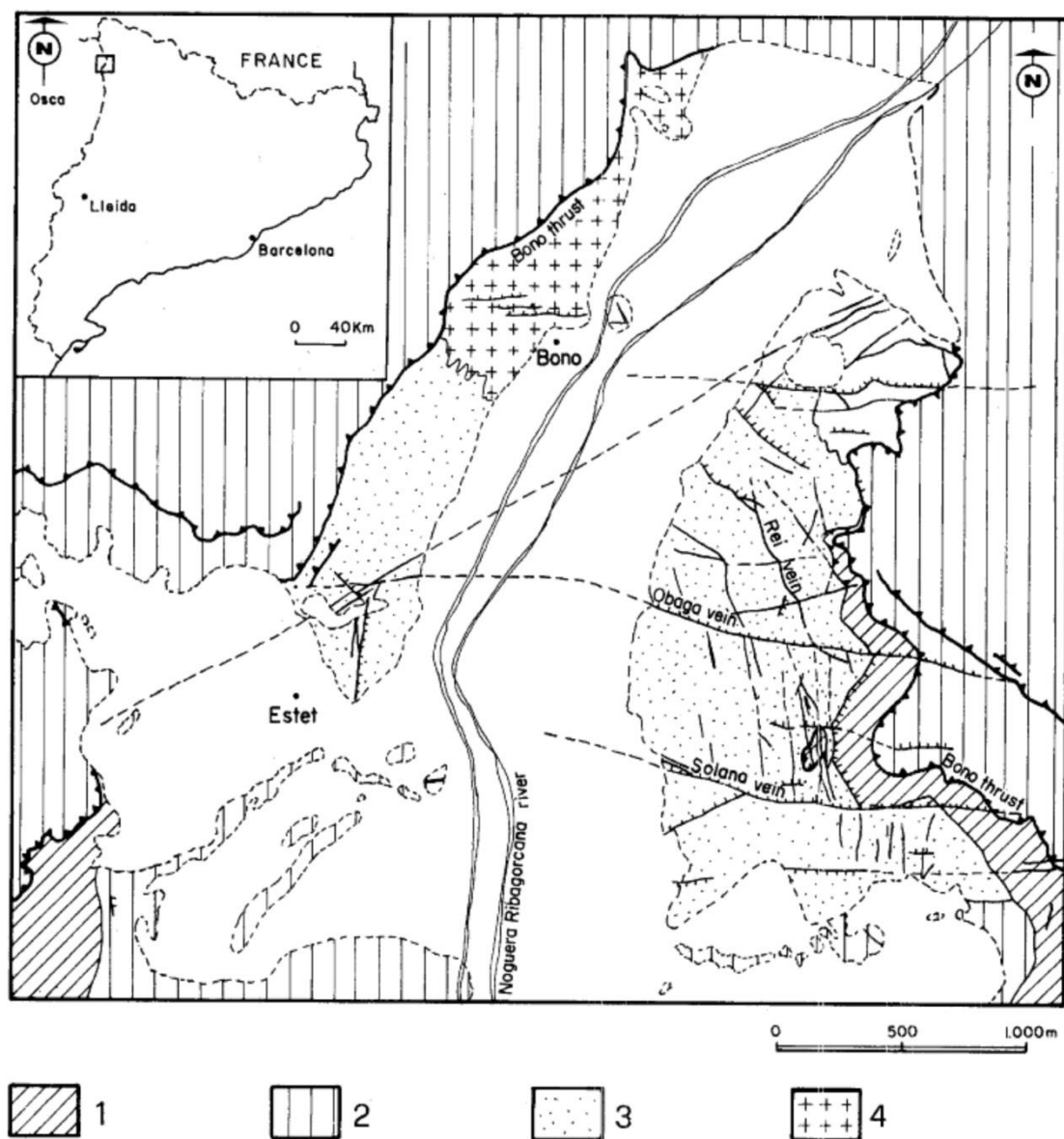


Figure 6.7 Geology of the Cierco mine (Castroviejo and Moreno, 1983). 1. Buntsandstein. 2. Paleozoic. 3. Metamorphic complex of Bono (Calc-silicate rocks). 4. Granodiorite.

Table 6.2 Main mineral species in the El Cierco mine.

Legend: AA: very abundant, A: abundant, C: common, R: rare, RR: very rare.

TIPOLOGY	MINERAL	FORMULA	%	Grain size
Porphyry	Quartz	SiO ₂	AA	medium
	Plagioclase	(Na,Ca)(Si,Al) ₄ O ₈	AA	medium
	Orthoclase	KAlSi ₃ O ₈	AA	medium
	Biotite	K(Mg,Fe) ₃ [AlSi ₃ O ₁₀ (OH,F) ₂	AA	medium
	Chlorite	(Mg, Fe) ₅ Al(Si ₃ Al)O ₁₀ (OH) ₈	AA	fine
	Epidote	Ca ₂ Fe ³⁺ Al ₂ O(SiO ₄)(Si ₂ O ₇)(OH)	A	fine
Skarn	Grossularite	Ca ₃ Al ₂ Si ₃ O ₁₂	AA	medium
	Andradite	Ca ₃ Fe ³⁺ ₂ Si ₃ O ₁₂	AA	medium
	Hedenbergite	CaFeSi ₂ O ₆	A	coarse
	Epidote	Ca ₂ Fe ³⁺ Al ₂ O(SiO ₄)(Si ₂ O ₇)(OH)	AA	coarse
	Quartz	SiO ₂	AA	coarse
	Chlorite	(Mg, Fe) ₅ Al(Si ₃ Al)O ₁₀ (OH) ₈	AA	fine
	Tremolite	Ca ₂ Mg ₅ Si ₈ O ₂₂ (OH) ₂	R	medium
	Magnetite	Fe ²⁺ Fe ³⁺ ₂ O ₄	A	coarse
	Hematite	Fe ₂ O ₃	A	coarse
	Pyrrhotite	Fe _{1-x} S	AA	coarse
	Pyrite	FeS ₂	A	coarse
	Chalcopyrite	FeCuS ₂	A	fine
	Calcite	CaCO ₃	AA	coarse
Vein	Quartz	SiO ₂	C	coarse
	Calcite	CaCO ₃	AA	coarse
	Barite	BaSO ₄	A	coarse
	Pyrite	FeS ₂	A	coarse
	Covellite	CuS	C	fine
	Bornite	Cu ₅ FeS ₄	C	fine
	Galena	PbS	AA	coarse
	Sphalerite	Zn,Fe)S	AA	coarse
	Chalcopyrite	(FeCuS ₂)	C	medium
Alterations	Azurite	Cu ₃ (CO ₃) ₂ (OH) ₂	C	fine
	Malachite	Cu ₂ (CO ₃)(OH) ₂	RR	fine
	Hidrozoicite	Zn ₅ (CO ₃) ₂ (OH) ₃	A	fine
	Cerussite	PbCO ₃	C	fine
	Greenockite	CdS	RR	fine

6.4 Victoria Mine

The Victoria mine benefited from Pb-Zn stratiform and non-related mineralization hosted in Silurian shales (Figs. 6.8, 6.9 and 6.10). The mine is composed by several galleries, some of them collapsed with time, some others are flooded, and only one gallery has been made suitable for touristic visits. For this reason, entering abandoned galleries is strictly forbidden, as well as using the hammer and taking samples in the touristic gallery. However, the ore minerals as well as the host rocks are very well represented in the mine dumps downhill (Table 6.3), and the visitors may find excellent specimens.

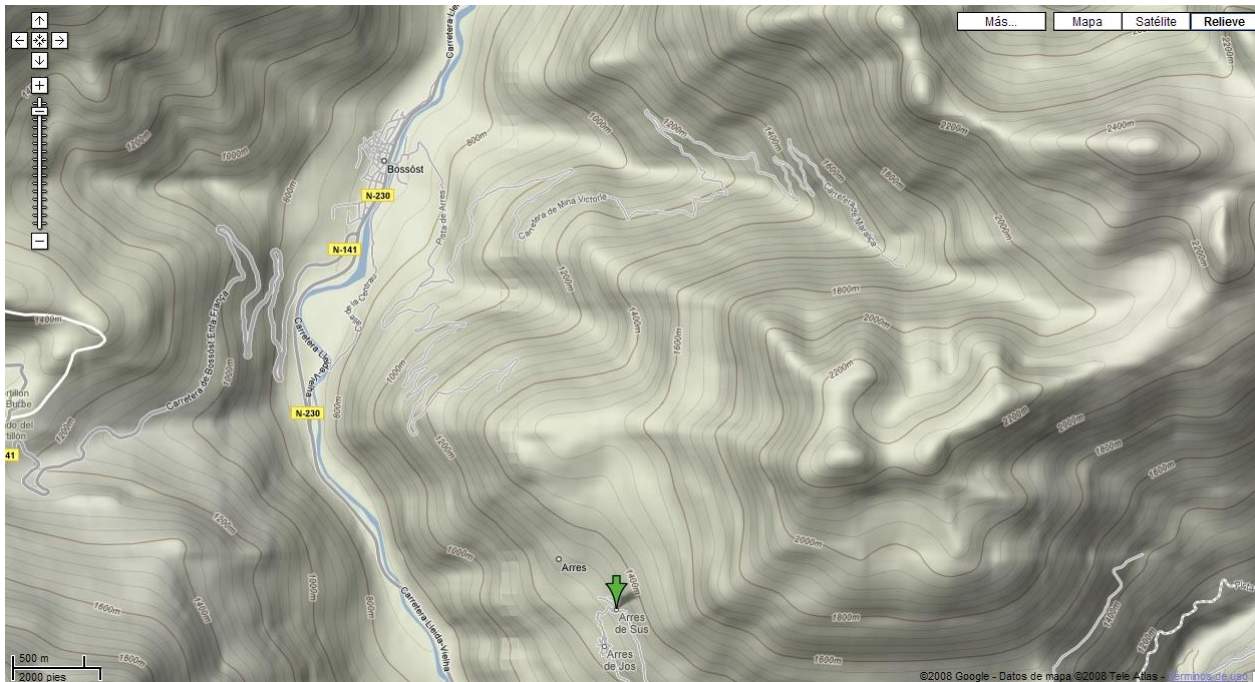


Figure 6.8. Topographic map of the area surrounding Arres de Sus area and the Victoria mine (<http://maps.google.es/>).

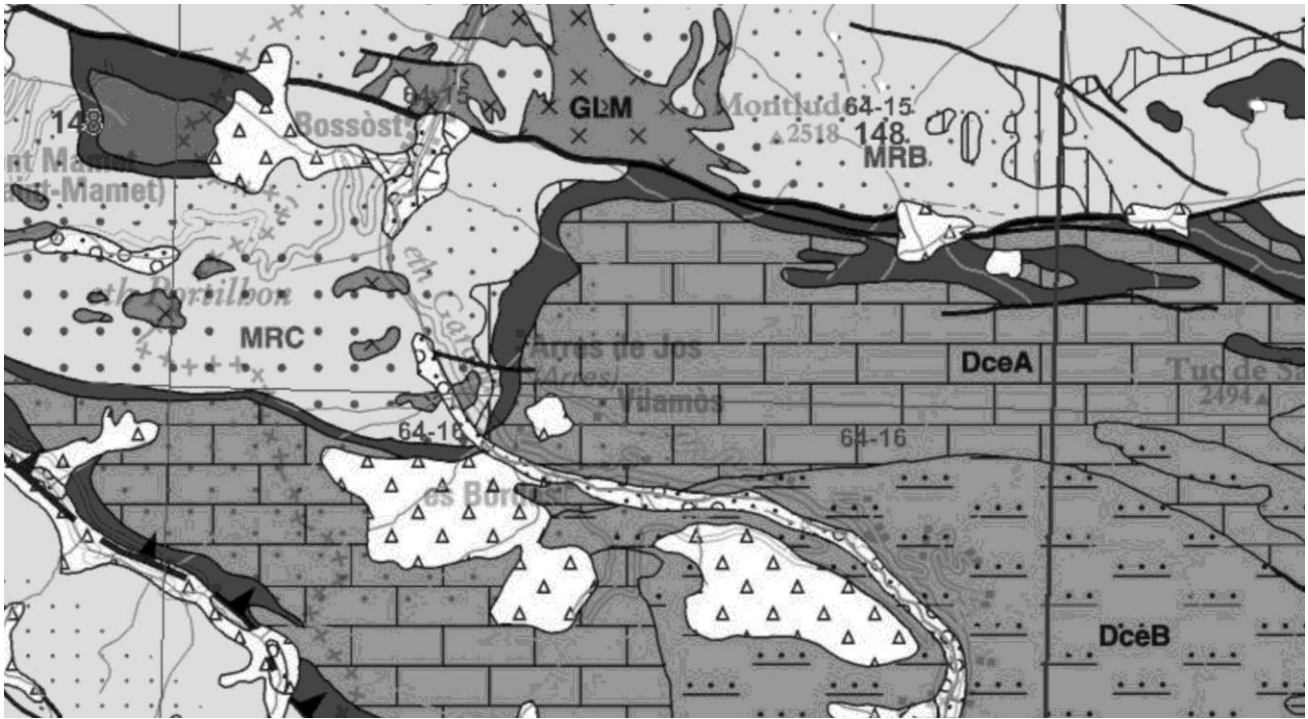


Figure 6.9. Geologic map of the Victoria mine (adapted from Sitter a Zwart, 1979 and the geologic map of Catalonia made by ICGC - Catalan Cartographic And Geologic Institute). Legend: MRB-MRC: Ordovician metapelites, dark gray: Silurian black shales; DceA: Devonian Calc-silicate rocks and limestones; DceB: Devonian marls and sandstones; Triangle pattern: Quaternary; Glm: Hercynian leucogranites and pegmaties.



Figure 6.10. Google Earth image of the Victoria mine (Google Earth ©)

Table 6.3. Main mineral species in the Victoria mine.

Legend: AA: very abundant, A: abundant, C: common, R: rare, RR: very rare.

TIPOLOGY	MINERAL	FORMULA	%	Grain size
Metamorphic Host rock	Quartz	SiO_2	AA	medium
	Muscovite	$\text{KAl}_2[\text{AlSi}_3\text{O}_{10}](\text{OH},\text{F})_2$	AA	medium
	Biotite	$\text{K}(\text{Mg},\text{Fe})_3[\text{AlSi}_3\text{O}_{10}](\text{OH},\text{F})_2$	AA	medium
	Chlorite	$(\text{Mg}, \text{Fe})_5\text{Al}(\text{Si}_3\text{Al})\text{O}_{10}(\text{OH})_8$	AA	medium
	Andalusite	Al_2SiO_5	AA	coarse
	Staurolite	$(\text{Fe}^{++},\text{Mg})_2\text{Al}_9(\text{Si},\text{Al})_4\text{O}_{20}(\text{O},\text{OH})_4$	AA	coarse
	Almandine	$\text{Fe}_3\text{Al}_2(\text{SiO}_4)_3$	AA	coarse
	Cordierite	$\text{Mg}_2\text{Al}_4\text{Si}_5\text{O}_{18}$	AA	coarse
	Diopside	$\text{CaMgSi}_2\text{O}_6$	RR	medium
	Pyrrhotite	Fe_{1-x}S	AA	fine
Veins	Sphalerite	$(\text{Zn},\text{Fe})\text{S}$	AA	coarse
	Galena	PbS	AA	medium
	Quartz	SiO_2	A	coarse
	Chlorite	$(\text{Mg}, \text{Fe})_5\text{Al}(\text{Si}_3\text{Al})\text{O}_{10}(\text{OH})_8$	AA	fine
	Gahnite	ZnAl_2O_4	R	coarse
	Covellite	CuS	C	fine
	Bornite	Cu_5FeS_4	C	fine
	Pyrrhotite	Fe_{1-x}S	A	coarse
	Pyrite	FeS_2	C	coarse
	Chalcopyrite	FeCuS_2	R	fine
Alterations	Azurite	$\text{Cu}_3(\text{CO}_3)_2(\text{OH})_2$	R	fine
	Malachite	$\text{Cu}_2(\text{CO}_3)(\text{OH})_2$	R	fine
	Hidrozoicite	$\text{Zn}_5(\text{CO}_3)_2(\text{OH})_3$	A	fine
	Cerussite	PbCO_3	C	fine
	Greenockite	CdS	R	fine

In the route from the town of Arres de Sus to the Victoria Mine (Fig. 6.11), some outcrops of the metamorphic host rocks can be observed, such as: 1) deformed Silurian black shales with disseminated pyrite mineralizations; with minor pegmatite mineralization 2) schists with staurolite and cordierite porphyroblasts in a biotite-muscovite foliated matrix.



Figure 6.11. Topographic map showing the route from Arres de Sus to the Victoria Mine zone (Google Earth ©)

In Figures 6.12, 6.13 and 6.14 it is shown the cartography of the touristic gallery in the Victoria Mine, and two geological sections respectively.

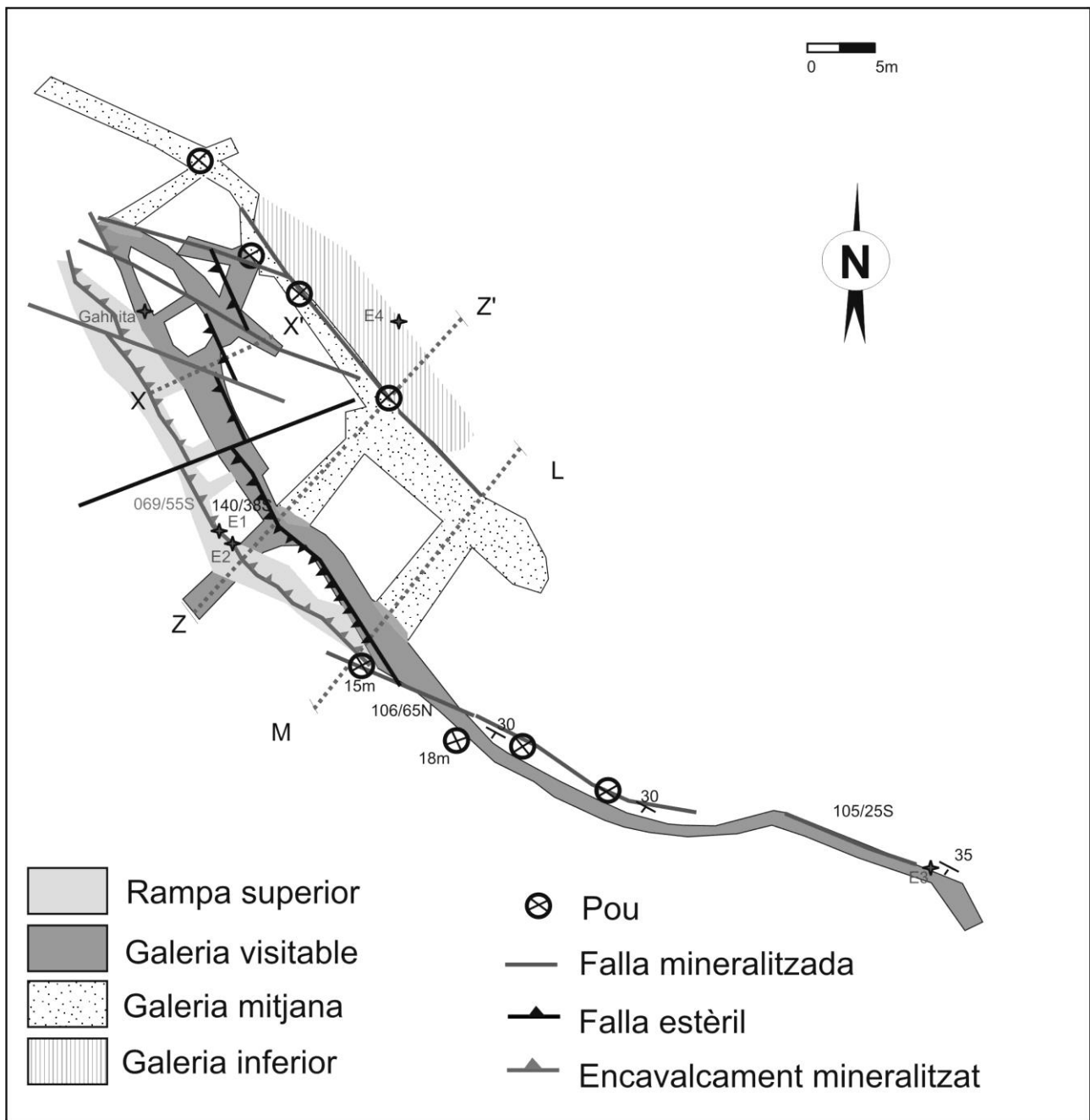


Figure 6.12 Geological cartography of the touristic gallery of the Victoria Mine (Bossòst, Val d'Aran, Northwestern Catalonia).

Legend:

“Rampa superior” = upper ramp/slope

“Galeria visitable” = touristic gallery

“Galeria mitjana” = intermediate gallery

“Galeria inferior” = lower gallery

“Pou” = pit

“Falla mineralitzada” = mineralized fault

“Falla estèril” = barren fault

“Encavalcament mineralitzat” = mineralized thrust

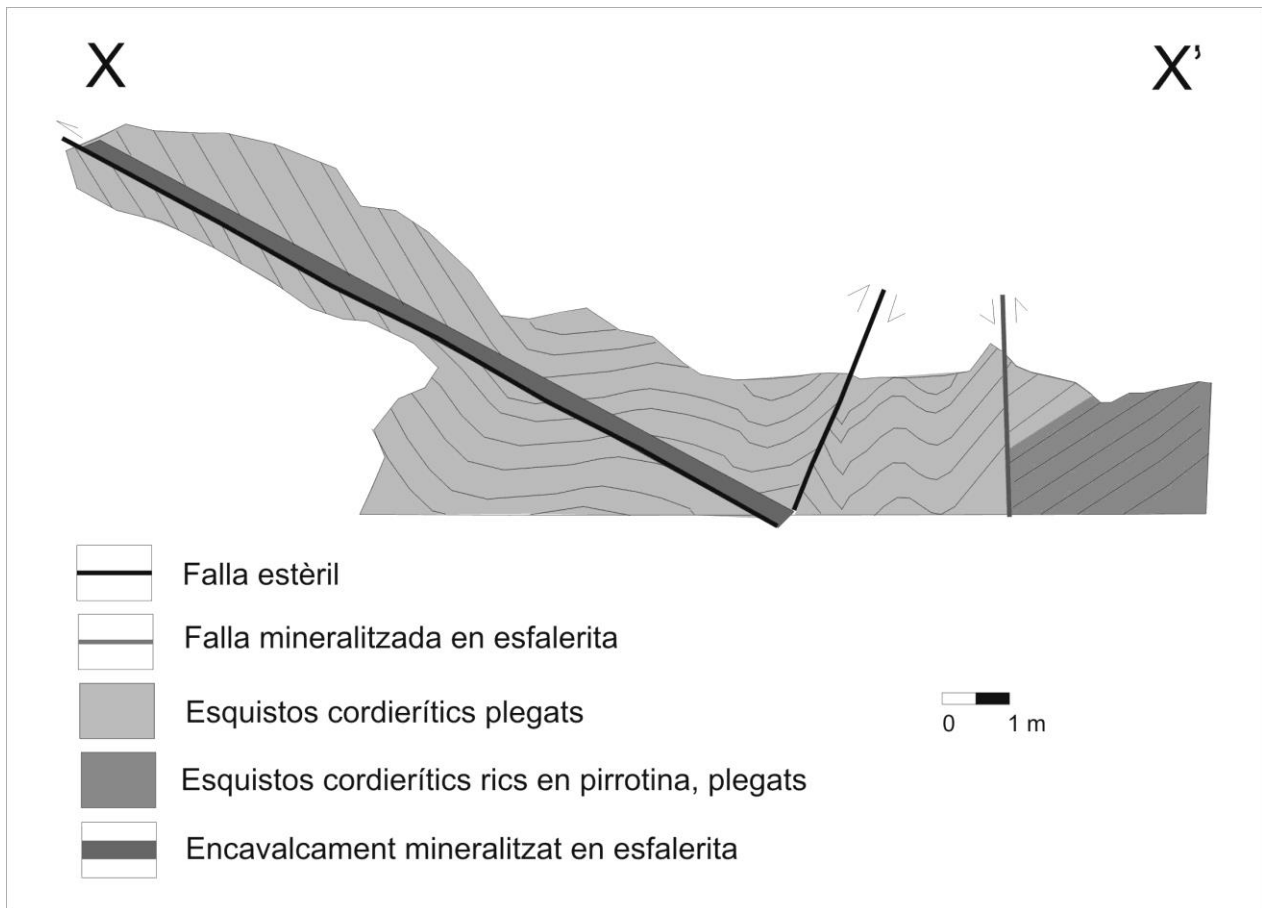


Figure 6.13 Geological sections X-X'. Situation is found in Figure 6.12.

Legend:

“Falla estèril” = Barren fault

“Falla mineralitzada en esfalerita” = Sphalerite vein

“Esquistos cordierítics plegats” = Folded cordieritic schists

“Esquistos cordierítics rics en pirrotina, plegats” = Pyrrhotite-rich folded cordieritic schists

“Encavalcament mineralitzat en esfalerita” = Sphalerite-bearing thrust

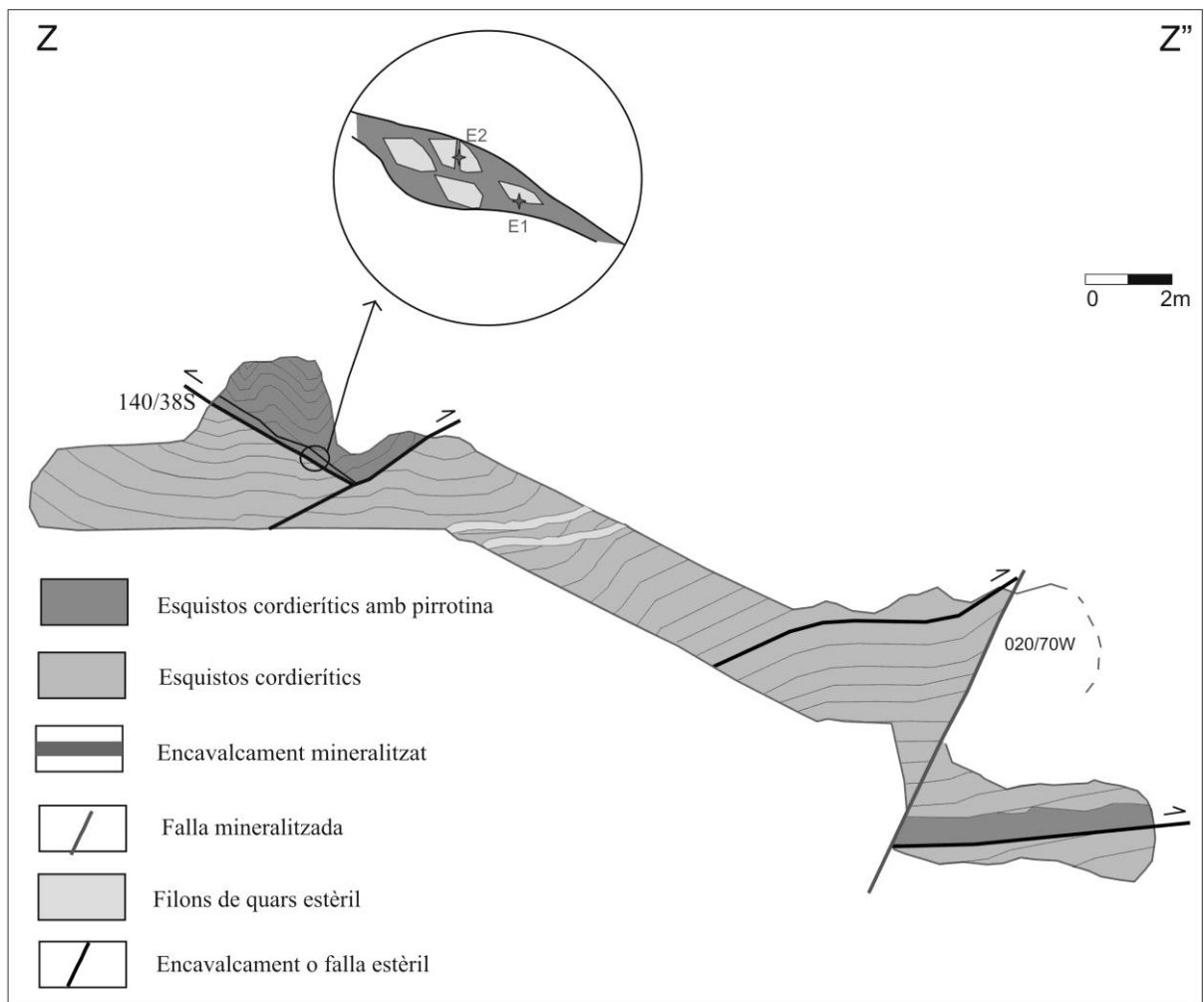


Figure 6.14 Geological section Z-Z'. Situation is found in Figure 6.12.

Legend:

“Esquistos cordierítics amb pirrotina” = Pyrrhotite-rich cordieritic schists

“Esquistos cordierítics” = Cordieritic schists

“Encavalcament mineralitzat” = Mineralized thrust

“Falla mineralitzada” = Mineralized fault

“Filons de quars estèril” = Barren quartz veins

“Encavalcament o falla estèril” = Barren thrust or fault

6.5 Silurian secondary minerals

Within the Silurian black shales, many secondary minerals have been developed due to the weathering of the primary mineralogy (Table 6.4).

Table 6.4 Mineral formed after the weathering of Silurian Shales near Arres Pound.

Legend: AA: very abundant, A: abundant, C: common, R: rare, RR: very rare.

Φ = Grain size

TIPOLOGY	MINERAL	STRUCTURAL FORMULA	%	GRAIN SIZE
Metamorphic Host rock	Quartz	SiO ₂	A	Medium
	Muscovite	KAl ₂ [AlSi ₃ O ₁₀](OH,F) ₂	AA	Medium
	Pyrite	FeS ₂	C	Fine
Secondary Minerals	Halotrichite	FeAl ₂ (SO ₄) ₄ *22H ₂ O	C	Fine
	Pickeringite	MgAl ₂ (SO ₄) ₄ *22H ₂ O	C	Fine
	Copiapite	Fe ²⁺ Fe ³⁺ ₄ (SO ₄) ₆ (OH) ₂ *20H ₂ O	C	Fine
	Alunogen	Al ₂ (SO ₄) ₃ *17H ₂ O	C	Fine

References

- ALMELA, A., RÍOS, J.M. (1947): *Explicación al mapa geológico de la provincia de Lérida*. Inst. Geol. Min. España. Madrid.
- ÁLVAREZ, A. (1974): *Estudio de los yacimientos de galena y esfalerita del área de Bossòst (Valle de Aran, Lérida)*. Tesis doctoral. Universitat de Barcelona, Inèdit. 195 pp.
- ARRIBAS, A. (1966): Mineralogía y metalogenia de los yacimientos españoles de uranio. Los indicios cuprouraníferos en el Trías de los Pirineos Catalanes. *Estudios Geológicos* **222**: 31-45.
- BARNOLAS, A., PUJALTE, V. (2004): La Cordillera Pirenaica. In: Vera, J.A. (Ed.): *Geología de España*. Instituto Geológico y Minero de España y Sociedad Geológica de España, Madrid, 234-241.
- CASTILLO, M., TORRÓ, L., CAMPENY, M., VILLANOVA, C., TAULER, E., MELGAREJO, J.C. (2009): Mineralogía del cepósito de uranio Eureka (Castell-estaó, Pirineo, Cataluña). *Macla* **11**, 53-54.
- CASTROVIEJO, R., MORENO, F. (1983): Estructura y metalogenia del campo filoniano de Cierco (Pb-Zn-Ag) en el Pirineo de Lérida. *Bol. Geol. Min.* **94,4**: 291-320.
- CUDEY, C. (1977): Sur quelques gîtes métallifères du revers méridional de la Maladetta (province de Lérida-Huesca, Espagne). *Bull. B.R.G.M.* **2,4** : 251-258.
- DE SITTER, L.U., ZWART, H.J. (1979, eds.): Geological map of the Central Pyrenees. Sheet 4. Valle de Aran, Spain. Scale 1:50.000. *Leidse Geologische Mededelingen* **50,1**: 1-74.
- JOHNSON, C.A., CARDELLACH, E., TRITLLA, J., HANAN, B.B. (1993): Origin of the Cierco Pb-Zn vein system (Central Pyrenees, Spain): evidence from stable isotopes, Sr isotopes and fluid inclusions. In: P.

Fenoll, J.I. Torres-Riz, Gervilla, F. (eds.): *Current Research in Geology Applied to Ore Deposits*. Publ. Univ. Granada, Granada: 135-138.

- JOHNSON, C.A., CARDELLACH, E., TRITLLA, J., HANAN, B.B. (1996): Cierco Pb-Zn-Ag vein deposits: isotopic and fluid inclusion evidence for formation during the Mesozoic extension in the Pyrenees of Spain. *Econ. Geol.* **91,3**: 497-506.
- POUIT, G. (1986): Les minéralisations Zn-Pb exhalatives sédimentaires de Bentaillou et de l'anticlinorium paléozoïque de Bossost (Pyrénées ariégeoises, France). *Chron. Rech. Min.* **48,5** : 3-16.



THE END

